Institut für Theoretische Physik I
Universität Stuttgart
Pfaffenwaldring 57
70550 Stuttgart

# Thermodynamic functionality of autonomous quantum networks

Von der Fakultät Mathematik und Physik der Universität Stuttgart zur Erlangung der Würde eines Doktors der Naturwissenschaften (Dr. rer. nat.) genehmigte Abhandlung

Vorgelegt von

Heiko Christian Schröder

aus Stuttgart

| | |
|---|---|
| Hauptberichter: | Prof. Dr. Günter Mahler |
| Mitberichter: | Prof. Dr. Ulrich Weiß |
| Tag der mündlichen Prüfung: | 21. Juli 2010 |

Institut für Theoretische Physik der Universität Stuttgart

2010

(Dissertation Universität Stuttgart)

# Danksagung

Natürlich ist das Gelingen einer Dissertation nicht denkbar ohne die Unterstützung, Ratschläge und Begleitung vieler Personen, denen ich hier meinen Dank aussprechen möchte.

Ich bedanke mich bei Prof. Dr. Günter Mahler für die Gelegenheit, meine Forschung in seiner Arbeitsgruppe durchzuführen. Besonderen Dank möchte ich ihm aussprechen für die gute Betreuung, die angenehme Arbeitsatmosphäre sowie die große Offenheit und das tiefe Interesse, welche er neuen Ideen und Konzepten entgegenbringt.

Danken möchte ich an dieser Stelle auch der Studienstiftung des deutschen Volkes, die diese Dissertation durch das mir gewährte Promotionsstipendium erst möglich gemacht hat. Über diesen finanziellen Aspekt hinaus bin ich dankbar für das entgegengebrachte Vertrauen sowie die vielfältigen Angebote und Veranstaltungen, besonders die Doktorandenforen.

Dank gilt auch Prof. Dr. Ulrich Weiß für die Übernahme des Mitberichts und die zügige Erstellung des Gutachtens, sowie Prof. Dr. Peter Michler für die Übernahme des Prüfungsvorsitzes.

Ich habe durch viele Diskussionen und immer offene Türen sehr von meinen (nun bereits teils ehemaligen) Kollegen aus der Arbeitsgruppe profitiert: Markus Henrich, Alexander Kettler, Suzanne Lanéry, Kilian Rambach, Pedro Vidal, Gerald Waldherr und Mohamed Youssef. Aus dieser Gruppe sind Thomas Jahnke, Florian Rempp, Jens Teifel und Hendrik Weimer besonders hervorzuheben, die mir in besonderem Maße als Kollegen und darüberhinaus Unterstützung waren.

Meinen Frühaufsteher-Frühstückskollegen Florian Rempp und Christoph Schimeczek möchte ich sehr für die regelmäßigen guten Starts in den Arbeitstag danken. Ferner danke ich allen Mitgliedern des 1. Instituts für Theoretische Physik für die gute Atmosphäre und manchen Anlass zum Lachen.

Über die Grenzen des Instituts hinaus gilt mein Dank meiner ganzen Familie für viel Geduld und Unterstützung, insbesondere meinen Eltern, die mir in vielfältiger Weise Studium und Promotion erleichtert haben. Ich danke auch den vielen Freunden, die mich während des Studiums begleitet haben und meine physikalischen Ausführungen und Abschweifungen immer mit großer Geduld und Gleichmut ertragen haben.

Mein größter Dank gilt aber Nathalie Papenfuß, die mich mit ihrer Liebe, Wärme und Fröhlichkeit während aller Phasen dieser Arbeit begleitet und getragen hat.

# Contents

# 1 Introduction

Thermodynamics is a theory of impressive success and a wide range of applicability. This is true despite its origin as a purely phenomenological theory in the late 16th and 17th century. It took about two hundred years until Boltzmann and Maxwell gave a foundation of thermodynamics in terms of statistical mechanics based on classical mechanics.

The typical view on how thermodynamics emerges from the microscopic equations of motion has been the following. Either the system itself is large or the system is small but weakly interacts with another system, that is large and thus can be considered thermodynamic (Brownian motion). Especially for the derivation of thermodynamic properties of processes, reservoirs play an important role that are perfect in the thermodynamical sense, which at least for heat baths means that they are infinitely large and always in equilibrium.

In the beginning 20th century, the invention of quantum mechanics has triggered various attempts to establish a theory of *quantum thermodynamics*, i.e., to explain and derive thermodynamics by quantum mechanics only. Starting with John von Neumann, those works first concentrated on proving the ergodic theorem for isolated quantum systems with a large number of degrees of freedom in the sense of the identity of time average and microcanonical ensemble average for certain (macroscopic) observables for a majority of the initial states (Neumann [1929], Bocchieri and Loinger [1959]). Later, Deutsch [1991] showed that the ergodic theorem holds for intensive and extensive observables under the presence of a random Hermitian perturbation, and Srednicki [1994] used results from quantum chaos to prove that thermalization occurs for a system of hard spheres in a box. Yet another view on the subject has been given recently by Reimann, arguing that limitations of control and measurement accuracy make statistical physics the appropriate description for typical large systems (Reimann [2007], Reimann [2008]).

In the recent years, another approach to quantum thermodynamics has received increased attention. This approach focuses on the role of the partitioning of the universe into "system" and "environment" and how the entanglement between those parts and the properties of typical environments lead to a thermal state in the system for almost any instant in time. In contrast to the previously mentioned works, this approach does not try to prove a (generalized) ergodic theorem and reaches its statements without invoking

time averages. This approach was first developed by Gemmer et al. (Gemmer et al. [2001], Borowski et al. [2003], Gemmer et al. [2004]), who established the emergence of thermodynamic behavior from quantum mechanics for a wide class of quantum systems and typical embeddings (see Tasaki [1998] for a similar but not as general result). Other recent papers have extended and clarified the results of the aforementioned authors (Goldstein et al. [2006], Linden et al. [2009a], Popescu et al. [2006]).

What is so fascinating about these findings is that it turns our understanding of thermodynamics upside down: No longer the presence of ideal thermodynamic reservoirs, which are by definition infinitely large and always in thermal equilibrium, makes a system thermodynamic but thermodynamic behavior of the system itself induced by an appropriate embedding becomes the crucial ingredient. Moreover, it turns out that not only macroscopic embeddings will induce thermal equilibrium but quantum networks as small as 10 spins may serve already as excellent thermal embeddings.

This opens the door to a number of interesting questions:

- Complementary to the emergence of relaxation (heat), how does mechanical control over a system (work) emerge in autonomous quantum systems? What types of embeddings allow for this form of control, and is there a lower limit to their size?
- If macroscopic size of embeddings is not necessary to induce heat and work effects, can we generalize the definitions of heat and work to encompass small quantum systems and their mutual effects as well?
- Small quantum systems allow for new types of control compared to classical thermodynamic systems. How does this affect thermodynamic functionality of quantum systems with respect to what we are used to from standard thermodynamics?

These questions guide us through the contents of this thesis. In Part I, we approach the question of emergence of work from quantum mechanics by making the connection between work, parametric control of a Hamiltonian, and classical driving with the help of the *factorization approximation (FA)*. We then use this link to propose the *LEMBAS method* to determine work and heat currents in arbitrary bipartite quantum systems, and discuss measures of how to assess the thermodynamic functionality of an arbitrary embedding. We then apply these concepts to a minimal model consisting of only a spin and a quantum harmonic oscillator (*spin-oscillator model, SOM*) to demonstrate that even a single oscillator may act as an ideal work reservoir. A slight variation of the model then illustrates the pros and cons of the proposed measures of thermodynamic functionality.

However, thermodynamics is first and foremost a theory of processes, and processes need both, thermal and mechanical control, heat and work. The first part only deals with work reservoir functionality, and treats heat effects as a contamination. To complete the picture, we discuss in Part II quantum thermodynamic machines implementing thermodynamic cycles. We first review some specialties of quantum thermodynamic processes in general and then present two models that implement cyclic thermodynamic nanomachines. In the last section of this part, we present our results of the *autonomous dynamical three spin machine (AD3SM)*, which in some sense is the synthesis of the presented models. It features a quantum work reservoir implemented by the SOM from Part I as its central element to achieve the machine functionality and is shown to operate as both, a heat engine and a heat pump.

The final part, Part III, is dedicated to a class of models that exhibit machine-like functionality without use of a thermodynamic cycle, which we therefore call *quantum thermodynamic pseudomachines*. The presented examples can all be understood as thermodynamic laser models with a varying degree of quantum modeling. In particular, we discuss the *extended dissipative Jaynes-Cummings model (ED JCM)* and the thermodynamic interpretation of its authors, that will be seen to contradict the results obtained by the LEMBAS method. We resolve this conflict by a careful analysis of the model itself and the thermodynamic concepts used by the authors. The resolution is seen to rely on the fact that the machine effect of all of these models depends on the transition-selective coupling of heat baths to a few-level quantum system.

Before we start with the main part, we give a quick overview of some important concepts used throughout the following the subsequent sections.

## 1.1 Thermodynamics and statistical physics

In this section, we quickly recapitulate notions from thermodynamics and statistical physics used throughout the following chapters. Parts of the presentation follow the lines of Schwabl [2006], Sec. 2.2 and Sec. 2.4.

The state of a thermodynamic system can be described by a set of macroscopic variables that decomposes into *intensive* and *extensive* variables: extensive variables grow proportionally to the size of the system, whereas intensive variables do not depend on the size. Important extensive variables are the internal energy $U$, the thermodynamic entropy $S^{\mathrm{td}}$, the volume $V$, and the particle number $N$. Absolute temperature $T$, pressure $p$, chemical potential $\mu$, etc., are to be mentioned as important examples of intensive variables. Additionally, there are the process quantities $Q$ and $W$, that designate the

heat and work absorbed during a transition of the system from one state to another, respectively.

The core of phenomenological thermodynamics is established by the 1st and 2nd law of thermodynamics. The *1st law*

$$\mathrm{d}U = đQ + đW \tag{1.1}$$

states the energy conservation and the equivalence of heat with other forms of energy. The total differential d distinguishes $U$ as a state variable in thermodynamic state space from the process variables $Q$, $W$, appearing as partial differentials denoted by đ in an infinitesimal state change.

The *2nd law* states what thermodynamic processes can take place and is related to irreversibility. A number of different formulations (Ramsey [1956]) of it exist. The *entropy formulation* is simply

$$\mathrm{d}S^{\mathrm{td}} \geq 0 \qquad \text{for any isolated system,} \tag{1.2}$$

where $S^{\mathrm{td}}$ is the thermodynamical entropy of the system. The equality holds for processes that involve only equilibrium states, that is for *quasistatic processes*.

In the *Clausius statement*, the 2nd law expresses the fact that it is impossible to construct a device operating in a closed cycle that will produce no other effect than the transfer of heat from a cooler to a hotter body. In the *Kelvin-Planck formulation*, the 2nd law says that it is impossible to construct a device that operates in a closed cycle and produces no effect other than extracting heat from a reservoir and performing an equivalent amount of work (in Sec. 9.4.2 it is seen that, if one allows for negative absolute temperature reservoirs, the Kelvin-Planck formulation has to be modified to keep its equivalence to the other formulations of the 2nd law).

For quasistatic processes, the *Gibbs fundamental relation* is given as

$$\mathrm{d}U = T\mathrm{d}S^{\mathrm{td}} - p\mathrm{d}V + \sum_j \mu_j \mathrm{d}N_j, \tag{1.3}$$

and work and heat are found to be

$$đQ = T\mathrm{d}S^{\mathrm{td}} \tag{1.4}$$

$$đW = -p\mathrm{d}V + \sum_j \mu_j \mathrm{d}N_j. \tag{1.5}$$

The work can contain additional work terms for example for magnetic systems $\vec{H}\mathrm{d}\vec{M}$ with the external magnetic field $\vec{H}$ and the magnetization $\vec{M}$.

For non-equilibrium processes, the *Clausius relation*

$$\mathrm{d}S^{\mathrm{td}} \geq \frac{\text{đ}Q_{\mathrm{rev}}}{T} \tag{1.6}$$

holds. $\text{đ}Q_{\mathrm{rev}}$ is the heat exchanged during the reversible substitute process for the irreversible process, and $T$ is the temperature of the ideal heat reservoir $\text{đ}Q_{\mathrm{rev}}$ is exchanged with.

Statistical physics establishes the connection of (phenomenological) thermodynamics with the microstates of a system, that is the classical or quantum state the system has on a microscopic level. The starting point of statistical mechanics is the famous *Boltzmann principle*

$$S^{\mathrm{td}} = \ln \Omega. \tag{1.7}$$

We have set $k_B = 1$ throughout this work, thus temperatures are given in units of the Boltzmann constant $k_B$. The Boltzmann principle relates the entropy $S^{\mathrm{td}}$ of an isolated system with the size of the state space $\Omega$, more precisely the number of microstates of the system that comply with the constraints determined by the macrostate. The macrostate in this case is characterized by *microcanonical conditions*, namely fixed volume $V$, fixed particle number $N$, and an internal energy from an infinitesimal interval $[U, U + \mathrm{d}U]$.

The Boltzmann principle assumes a priori equal probabilities for all the microstates, and thus, the probability distribution of the microstates is

$$\rho^{\mathrm{mic}} = \frac{\delta[U - H(q,p)]}{\Omega}, \tag{1.8}$$

where $H(q,p)$ is the Hamilton function of the classical system and $\Omega$ appears here as a normalization constant that can be associated with the volume of the energy shell defined by $[U, U + \mathrm{d}U]$. Likewise for a quantum system, the microcanonical density matrix is found to be

$$\hat{\rho}^{\mathrm{mic}} = \frac{1}{\Omega} \sum_n \delta(U - \epsilon_n) \, |\epsilon_n\rangle\langle\epsilon_n| \, . \tag{1.9}$$

Here, $\{|\epsilon_n\rangle\}$ is the energy eigenbasis of the Hamilton operator $\hat{H}$ of the system with a spectrum that in general is degenerate, in which case the index $n$ is to be understood as a vector $\vec{n}$ of quantum numbers uniquely labelling all states. Here, $\Omega = \sum_{\epsilon_n \in [U, U+\mathrm{d}U]} 1$ is the number of energy eigenstates in the energy shell. The von Neumann entropy of this density matrix is

$$S(\hat{\rho}^{\mathrm{mic}}) := -\mathrm{Tr}(\hat{\rho}^{\mathrm{mic}} \ln \hat{\rho}^{\mathrm{mic}}) = \ln \Omega = S^{\mathrm{td}}. \tag{1.10}$$

Now, let us consider a subsystem of this isolated system that is much smaller than the remainder of the system but still macroscopic. This subsystem interacts with the remainder of the total system such that energy is exchanged between the parts but the interaction energy is always negligible with respect to the parts' energy, and its density matrix is found to be

$$\hat{\rho}^{\mathrm{can}} = Z^{-1} \exp\left(-\frac{\hat{H}}{T}\right), \tag{1.11}$$

the *canonical density matrix* with the canonical partition function

$$Z = \mathrm{Tr}[\exp(-\hat{H}/T)] \tag{1.12}$$

and absolute temperature $T$. Again, the von Neumann entropy equals the thermodynamic entropy, and the subsystem is in thermal equilibrium with its environment.

Although statistical mechanics is extremely successful in describing thermodynamic systems and deriving thermodynamic properties from microscopic properties of the models, physicists have had a hard time justifying the a priori uniform probability distribution of the states in the microcanonical energy shell on rigorous grounds based on a microscopic derivation. Most notable attempts to this end are certainly the well-known $H$-theorem by Boltzmann [1872] and the ensemble concept together with quasiergodicity introduced by Gibbs [1960]. Both attempts are afflicted with a number of problems and objections, and/or could not be shown to hold in the generality one expects from the ubiquitous character of thermodynamics. In the following section, we present the results of an approach starting from quantum mechanics, which to our opinion represents a significant progress to the explanation of how thermodynamic behavior comes to life in a world governed by time-reversal invariant microscopic laws.

## 1.2 Quantum thermodynamics

In the following subsections, we do not present more than a short outline of the most important ideas and results of quantum thermodynamics along the lines of Tasaki [1998], Gemmer et al. [2001], Borowski et al. [2003], Gemmer et al. [2004], and Henrich et al. [2005]. Whenever we use the term "quantum thermodynamics" in the following, we mean this special approach from the field of quantum thermodynamics.

### 1.2.1 Embedding and partitioning

The basic concept of quantum thermodynamics is *embedding*: every quantum system has an environment with which it interacts. Therefore, any system is embedded in a (usually) much bigger environment. And any system interacts with its environment albeit only very weakly (even a particle in the vacuum interacts with the electromagnetic field). Due to this interaction, entanglement will typically arise. This embedding and the entanglement turn out to be crucial ingredients to the derivation of thermodynamics from quantum mechanics.

Based on these considerations, quantum thermodynamics starts always from bipartite systems in a pure state $|\Psi\rangle$ (total zero entropy), which consists of the system/gas "g" and the environment/container "c" and is described by a Hamiltonian

$$\hat{H} = \hat{\tilde{H}}_g + \hat{\tilde{H}}_{\text{int}} + \hat{H}_c \,. \tag{1.13}$$

$\hat{\tilde{H}}_{\text{int}}$ describes the interaction between the constituents of the environment with the constituents of the system. $\hat{\tilde{H}}_g$ and $\hat{\tilde{H}}_c$ are the local Hamilton operators of the gas system and the container, respectively. If one imagines a box filled with a gas, an important part of the interaction (and the interaction energy) is due to the confinement caused by the box (environment). This part of the interaction may be pulled out of the interaction by introducing an effective potential $\hat{V}$ representing that part,

$$\hat{H}_g = \hat{\tilde{H}}_g + \hat{V}, \qquad \hat{H}_{\text{int}} = \hat{\tilde{H}}_{\text{int}} - \hat{V},$$

and leading to

$$\hat{H} = \hat{H}_g + \hat{H}_{\text{int}} + \hat{H}_c \,. \tag{1.14}$$

What one now requires is that the remaining interaction $\hat{H}_{\text{int}}$ is small compared to the energies of the system and the environment:

$$\langle \hat{H}_{\text{int}} \rangle \ll \langle \hat{H}_g \rangle, \langle \hat{H}_c \rangle \quad \forall\, |\Psi\rangle \in \mathcal{H} \,. \tag{1.15}$$

The state vector of the total system describes a trajectory in the Hilbert space $\mathcal{H}$ with constant velocity $v = \sqrt{\langle\Psi(0)|\,\hat{H}^2\,|\Psi(0)\rangle - (\langle\Psi(0)|\,H\,|\Psi(0)\rangle)^2}$. Because of energy conservation (and therefore also conservation of all higher moments of $\hat{H}$), the system cannot reach any place in the Hilbert space but only any state in the *accessible region* which is defined as the set of states compliant with the initial state.

A particular consequence of irreversibility is that any system starting in whatever state will finally evolve to an equilibrium state which is characterized by maximum (von Neumann) entropy (which corresponds to minimal purity) under given constraints. This feature of irreversibility is reproduced by quantum thermodynamics, which we illustrate with the microcanonical coupling case in the next section.

### 1.2.2 Microcanonical coupling

In case of a microcanonical interaction, energy is conserved locally in both parts of the total system and therefore

$$\left[\hat{H}_g, \hat{H}\right] = 0, \qquad \left[\hat{H}_c, \hat{H}\right] = 0\,.$$

By consequence, not only the local energies $E_{c,g} = \langle \hat{H}_{c,g} \rangle$ but also the local energy distributions $p_c(E_c)$ and $p_g(E_g)$ are conserved. The minimum purity that is compatible with the above requirements then turns out to be

$$P_g^{\min} = \sum_{E_g} \frac{[p_g(E_g)]^2}{N_g(E_g)}, \tag{1.16}$$

where $N_{c,g}(E)$ are the degrees of degeneration of a state with energy $E$. By the Hilbert space average method (see, e.g., Gemmer et al. [2001] or Gemmer et al. [2004]) one can show that the average purity of the gas system for all states in the accessible region is given by

$$\overline{P_g} \approx \sum_{E_g} \frac{[p_g(E_g)]^2}{N_g(E_g)} + \sum_{E_c} \frac{[p_c(E_c)]^2}{N_c(E_c)} \tag{1.17}$$

if $N_c$ is big enough. Now, for $N_c(E_c) \gg N_g(E_g)$ or a significantly broader distribution $p_c(E_c)$ than that of the gas, Eq. (1.17) simply reduces to Eq. (1.16). Therefore, in this case, nearly every reachable state of the total system is linked to maximum entropy in the gas since minimum purity corresponds to maximum entropy.

If one considers that the state vector follows its trajectory in Hilbert space with constant velocity and that it is unlikely (although possible) for the system to stay near the initial state, it is clear that most of the time the system will be found in an equilibrium state. Therefore, irreversibility is explained by pure quantum mechanics. Moreover, the states with minimum purity provide the correct microcanonical distribution of the occupation numbers.

### 1.2.3 Conclusions

We refer here to Tasaki [1998], Gemmer et al. [2001], Borowski et al. [2003], Gemmer et al. [2004], Henrich et al. [2005], and related works for more details and investigations of how and when thermodynamic behavior emerges from quantum mechanics, and only summarize their results:

1. The reason for irreversibility is the embedding of a system in its environment and the entanglement caused by the interaction between the two.

2. For a bipartite quantum system that fulfills the requirements
   a) the coupling is microcanonical,
   b) $N_c(E_c) \gg N_g(E_g)$ or $p_c(E_c)$ is significantly broader than $p_g(E_g)$,

   one gets the result that the "gas part" is most likely found in the microcanonical equilibrium state corresponding to maximum entropy.

3. A quantum system with an environment that fulfills the requirements
   a) the coupling is weak,
   b) $N_c(E_c) \gg N_g(E_g)$ or $p_c(E_c)$ is significantly broader than $p_g(E_g)$,
   c) the degree of degeneracy of the environment increases exponentially with increasing energy,

   is most likely to be found in a state with maximum entropy and with a Boltzmann distribution for the occupation numbers of the energy eigenstates of the system.

4. All main features of thermodynamics and thermal equilibria can be explained from pure quantum mechanical considerations.

5. Even a single spin in an environment as small as ten spins may show thermodynamical behavior.

Quantum thermodynamics is thus able to explain thermodynamics from pure quantum mechanics without additional, physically questionable postulates. Thermodynamics emerges from quantum mechanics by the embedding in an environment or – stated the other way round – by an appropriate partitioning between system and environment even for pure total system states.

## 1.3 Open quantum systems

In this section, we present some basic concepts and properties of open quantum systems, namely the phenomenological Markovian quantum master equation (QME) in Sec. 1.3.1 and the derivation of the Markovian QME in Lindblad form from the microscopic Schrödinger dynamics in Sec. 1.3.2. The presentation of the subjects follow closely that of Breuer and Petruccione [2002] in Ch. 3.2 and Ch. 3.3.1.

### 1.3.1 Dynamical semigroup/Markov processes

Consider a total system consisting of system of interest $s$ and bath $b$. If the total system is closed, its state evolves according to the *Schrödinger equation*

$$i|\dot{\Psi(t)}\rangle = \hat{H}\,|\Psi(t)\rangle \tag{1.18}$$

or more generally according to the *Liouville-von Neumann equation*

$$\dot{\hat{\rho}}(t) = -i[\hat{H}, \hat{\rho}(t)] \tag{1.19}$$

for a mixed state $\hat{\rho}(t)$ if $\hat{H}$ is the Hamilton operator of the total system $s+b$. Note that we set $\hbar = 1$ throughout this work. Energies are thus given as angular frequencies in units of $\hbar$.

The total state at time $t$ is given with the help of the *time-evolution operator* $\hat{U}$ as $\hat{\rho}(t) = \hat{U}(t)\hat{\rho}(0)\hat{U}^{\dagger}(t)$. The *dynamical map* $\hat{V}(t)$ is defined as the transformation

$$\hat{\rho}_s(0) \mapsto \hat{\rho}_s(t) = \hat{V}(t)\hat{\rho}_s(0) = \mathrm{Tr}_b\{\hat{V}(t)[\hat{\rho}_s(0) \otimes \hat{\rho}_b]\hat{V}^{\dagger}(t)\}, \tag{1.20}$$

that maps the initial system state to the state at time $t$, where we have assumed that the total system has been initially prepared in a state factorizing state. The set $\{\hat{V}(t)|\forall t \geq 0\}$ contains the complete future of system $s$. If the correlations in the environment decay on a time-scale much shorter than the typical evolution of the system $s$, one may assume Markovian behavior of the dynamical map, expressed by the *semigroup property*

$$\hat{V}(t_1)\hat{V}(t_2) = \hat{V}(t_1 + t_2). \tag{1.21}$$

In many cases, a dynamical semigroup can be given in exponential form,

$$\hat{V}(t) = \exp(\mathcal{L}t), \tag{1.22}$$

where the generator $\mathcal{L}$ of the semigroup is a linear map. The dynamics of the system is then given as

$$\dot{\hat{\rho}}_s(t) = \mathcal{L}\hat{\rho}_s(t), \tag{1.23}$$

and the *Lindblad form* or *Lindblad master equation*

$$\begin{aligned}\mathcal{L}\hat{\rho}_s(t) = &- i\left[\hat{\tilde{H}}_s, \hat{\rho}_s(t)\right] \\ &+ \sum_k \gamma_k \left(\hat{A}_k \hat{\rho}_s(t) \hat{A}_k^\dagger - \frac{1}{2}\hat{A}_k^\dagger \hat{A}_k \hat{\rho}_s(t) - \frac{1}{2}\hat{\rho}_s(t)\hat{A}_k^\dagger \hat{A}_k\right)\end{aligned} \tag{1.24}$$

is the most general form of a generator of the dynamical semigroup of form Eq. (1.22). $\hat{A}_k$ are called the *Lindblad operators* and the second, incoherent part of the r.h.s. the *Lindblad dissipator*. The details of the derivation are found in Breuer and Petruccione [2002], Ch. 3.2.

### 1.3.2 Weak-coupling Markovian quantum master equation

Here, we summarize the steps taken to derive a Markovian QME in the weak-coupling limit from a microscopic model given by a Hamiltonian

$$\hat{H} = \hat{H}_s + \hat{H}_b + \hat{H}_{sb} \tag{1.25}$$

where $s$ refers to the system, $b$ to the bath, and $sb$ to the interaction. Throughout the following derivation we stay in the interaction picture and thus all quantities are now understood to be given in the interaction picture. Thus, $\hat{H} = \hat{H}_{sb}(t)$ and

$$\dot{\hat{\rho}}(t) = -i\left[\hat{H}_{sb}(t), \hat{\rho}(t)\right]. \tag{1.26}$$

Inserting the state $\hat{\rho}(t)$ in its integral form, taking the trace over the reservoir $b$ and assuming $\mathrm{Tr}_b[\hat{H}_{sb}(t), \hat{\rho}(0)] = 0$, one gets

$$\hat{\rho}_s(t) = -\int_0^t \mathrm{d}\tau\, \mathrm{Tr}_b\left[\hat{H}_{sb}(t), \left[\hat{H}_{sb}(\tau), \hat{\rho}(s)\right]\right]. \tag{1.27}$$

Now, to eliminate the total state $\hat{\rho}(t)$ from the r.h.s., the *Born approximation*

$$\hat{\rho}(t) = \hat{\rho}_s(t) \otimes \hat{\rho}_b \tag{1.28}$$

is introduced. The physical meaning of this approximation is that the reservoir $b$ is negligibly affected by the system $s$, and excitations of the reservoir decay

on a time-scale much shorter than the system dynamics time-scale. This leads to the equation

$$\dot{\hat{\rho}}_s(t) = -\int_0^t \mathrm{d}\tau \, \mathrm{Tr}_b \left[\hat{H}_{sb}(t), \left[\hat{H}_{sb}(\tau), \hat{\rho}_s(\tau) \otimes \hat{\rho}_b\right]\right]. \tag{1.29}$$

It follows the *Markov approximation* in two stages. First, Eq. (1.29) is made time-local by the replacement of $\hat{\rho}_s(\tau)$ with $\hat{\rho}_s(t)$. This yields the so-called *Redfield equation*

$$\dot{\hat{\rho}}_s(t) = -\int_0^t \mathrm{d}\tau \, \mathrm{Tr}_b \left[\hat{H}_{sb}(t), \left[\hat{H}_{sb}(\tau), \hat{\rho}_s(t) \otimes \hat{\rho}_b\right]\right], \tag{1.30}$$

which is still not Markovian. The second stage of the Markov approximation is the substitution of $\tau$ with $t - \tau$ plus moving the upper limit of the integral to infinity, and is permissible if the time scale $\tau_r$ over which the system state varies appreciably is large compared to $\tau_b$, the time scale on which the reservoir correlation functions decay.

To finally get a Markovian master equation, one must perform a third approximation, a *secular approximation* known as the *rotating wave approximation*. This approximation involves the averaging over the rapidly rotating terms in the master equation. Writing the Schrödinger picture interaction Hamiltonian without loss of generality as

$$\hat{H}_{sb} = \sum_j \hat{A}_j \otimes \hat{B}_j \tag{1.31}$$

with Hermitian operators $\hat{A}_j$ and $\hat{B}_j$, one can define eigenoperators of $\hat{H}_s$

$$\hat{A}_j(\omega) = \sum_{\omega = \epsilon' - \epsilon} |\epsilon\rangle\langle\epsilon| \, \hat{A}_j \, |\epsilon'\rangle\langle\epsilon'|, \tag{1.32}$$

where $\{|\epsilon\rangle\}$ is the energy eigenbasis of $\hat{H}_s$ with the energy eigenvalues $\{\epsilon\}$. If the interaction picture interaction Hamiltonian $\hat{H}_{sb}(t)$ is expressed in terms of the eigenoperators Eq. (1.32), Eq. (1.30) becomes

$$\dot{\hat{\rho}}_s(t) = \sum_{\omega,\omega'} \sum_{j,k} \mathrm{e}^{i(\omega' - \omega)t} \Gamma_{jk}(\omega) \Big( \hat{A}_k(\omega) \hat{\rho}_s(t) \hat{A}_j^\dagger(\omega') - \hat{A}_j^\dagger(\omega') \hat{A}_k(\omega) \hat{\rho}_s(t) \Big) + \mathrm{h.c.}, \tag{1.33}$$

and the secular approximation is then equivalent to omitting all terms on the r.h.s. for which $\omega' - \omega \neq 0$. The secular approximation is justified if the typical time scale of intrinsic evolution of $s$, $\tau_s$, is small compared to the relaxation time $\tau_r$.

Finally, this leads to the Markovian QME in the Schrödinger picture

$$\dot{\hat{\rho}}_s(t) = -i\left[\hat{\tilde{H}}_s, \hat{\rho}_s(t)\right] + \mathcal{L}\left[\hat{\rho}_s(t)\right] \tag{1.34}$$

with $\mathcal{L}\left[\hat{\rho}_s(t)\right]$ reading

$$\sum_{\omega}\sum_{j,k}\gamma_{jk}(\omega)\left(\hat{A}_k(\omega)\hat{\rho}_s(t)\hat{A}_j^{\dagger}(\omega) - \frac{1}{2}[\hat{A}_j^{\dagger}(\omega)\hat{A}_k(\omega), \hat{\rho}_s(t)]_+\right), \tag{1.35}$$

which is easily brought to Lindblad form by a diagonalization of the matrix of rates $\gamma_{jk}(\omega)$. The exact derivation of the rates $\gamma_{jk}(\omega)$ and of $\hat{\tilde{H}}_s = \hat{H}_s + \hat{H}_{\mathrm{LS}}$ is found in Breuer and Petruccione [2002], Sec. 3.3.1. Usually, the Lamb shift Hamiltonian $\hat{H}_{\mathrm{LS}}$ is negligible (Breuer and Petruccione [2002], Sec. 12.2.3.2).

# Part I

# Quantum work sources

# 2 Work and heat in quantum systems

The definition of work in quantum systems has been discussed in various papers (Alicki [1979], Kosloff and Ratner [1984], Talkner et al. [2007]) and has been applied successfully to quantum heat engines (Kieu [2004], Henrich et al. [2006], Henrich et al. [2007a], Henrich et al. [2007b], Allahverdyan et al. [2008]). Still, all those investigations typically deal with quantum systems that are subject to driving by means of a time-dependent Hamilton operator of the system. Thus, the identification and definition of work is determined *a priori* by relating it to the presence of classical driving, while no microscopic derivation of the concept is given. Here we deal with closed, finite quantum systems as suggested by quantum thermodynamics.

We are interested in the question under what conditions a quantum system coupled to another can exert the effect of a classical driver over the other system and thus be identified with a reversible work source. This is the complementary question to how relaxation and heat emerges from quantum mechanics answered by quantum thermodynamics. In addition, based on the factorization approximation presented in Sec. 2.1 and its relation to classical driving and work (Sec. 2.2), we propose and discuss a possible generalization of the definitions of work and heat in the context of quantum thermodynamics of finite isolated quantum systems with a given partitioning in Sec. 2.3 and Sec. 2.4. Finally, we address the problem of sensible definitions of work and heat source quality measures for non-ideal reservoirs in Sec. 2.5. The concepts and methods developed in this chapter make it possible to show in the following chapter that classical driving and therefore work is not a concept bound to macroscopic devices.

The contents of this and the following chapter are to large parts taken from my publications Weimer et al. [2008] and Schröder and Mahler [2010], but have been extended at some points.

## 2.1 Factorization approximation

The factorization approximation (FA) has been thoroughly discussed, e.g., by Gemmer and Mahler [2001] and Willis and Picard [1974]. We will therefore only summarize the basic statements and then give a generalization to the result of Gemmer and Mahler [2001].

In its form stated in Gemmer and Mahler [2001], the FA reads as follows. Let us consider a bipartite quantum system with Hamilton operator

$$\hat{H} = \hat{H}_1 + \hat{H}_{12} + \hat{H}_2 \tag{2.1}$$

acting on the joint Hilbert space $\mathcal{H}_{12} = \mathcal{H}_1 \otimes \mathcal{H}_2$. The operators $\hat{H}_1$ and $\hat{H}_2$ act on the respective local Hilbert spaces $\mathcal{H}_1$ and $\mathcal{H}_2$ only. Let the initial state factorize, i.e.,

$$|\Psi(0)\rangle = |\Psi_1(0)\rangle \otimes |\Psi_2(0)\rangle \ . \tag{2.2}$$

After some time $t$, the total state of the system either given by $|\Psi(t)\rangle$ or its density matrix $\hat{\rho}(t) = |\Psi(t)\rangle\langle\Psi(t)|$ gives rise to the reduced states of the two subsystems $\hat{\rho}_1(t) = \mathrm{Tr}_2(|\Psi(t)\rangle\langle\Psi(t)|)$ and $\hat{\rho}_2(t) = \mathrm{Tr}_1(|\Psi(t)\rangle\langle\Psi(t)|)$. Although the state was assumed to factorize initially, in general, the subsystem states no longer will be pure states due to entanglement introduced by the interaction between the subsystems. As the total state is pure, the subsystem purities $P[\hat{\rho}_1(t)] = \mathrm{Tr}\{[\hat{\rho}_1(t)]^2\}$ and $P[\hat{\rho}_2(t)] = \mathrm{Tr}\{[\hat{\rho}_2(t)]^2\}$ are equal at any instant $t$. Now, as long as the purity of the subsystems is close to 1, it can be shown that the dynamics of the system are, in good approximation, given by the reduced density matrices $\hat{\rho}_i = |\Psi_i(t)\rangle\langle\Psi_i(t)|$, $i = 1, 2$, where the $|\Psi_i(t)\rangle$ obey the coupled differential equations

$$i\,|\dot{\Psi}_1(t)\rangle = \left(\hat{H}_1 + \langle\Psi_2(t)|\,\hat{H}_{12}\,|\Psi_2(t)\rangle\right)|\Psi_1(t)\rangle \tag{2.3}$$

$$i\,|\dot{\Psi}_2(t)\rangle = \left(\hat{H}_2 + \langle\Psi_1(t)|\,\hat{H}_{12}\,|\Psi_1(t)\rangle\right)|\Psi_2(t)\rangle \tag{2.4}$$

up to an irrelevant relative phase (for a detailed derivation see Gemmer and Mahler [2001]). Obviously, the reduced states of the system evolve under the action of time-dependent effective Hamiltonians $\hat{H}_1 + \hat{H}_1^{\mathrm{eff}}(t)$ and $\hat{H}_2 + \hat{H}_2^{\mathrm{eff}}(t)$, respectively, with

$$\hat{H}_1^{\mathrm{eff}}(t) = \mathrm{Tr}_2\{\hat{H}_{12}[\hat{1} \otimes \hat{\rho}_2(t)]\} \tag{2.5}$$

$$\hat{H}_2^{\mathrm{eff}}(t) = \mathrm{Tr}_1\{\hat{H}_{12}[\hat{\rho}_1(t) \otimes \hat{1}]\} \tag{2.6}$$

and in the present case $\hat{\rho}_j(t) = |\Psi_j(t)\rangle\langle\Psi_j(t)|$, $j = 1, 2$.

The above statement can be generalized for the case of factorizing semi-mixed initial states, that is, states of the form

$$\hat{\rho}(0) = \hat{\rho}_1(0) \otimes |\Psi_2(0)\rangle\langle\Psi_2(0)| \; . \tag{2.7}$$

If the purity $P[\hat{\rho}_2(t)]$ of the initially pure system 2 remains close to unity, the dynamics of the system can be given approximately by the coupled differential equations

$$\dot{\hat{\rho}}_1(t) = -i\left[\hat{H}_1 + \hat{H}_1^{\rm eff}(t), \hat{\rho}_1(t)\right] \tag{2.8}$$

$$|\dot{\Psi}_2(t)\rangle = -i\left(\hat{H}_2 + \hat{H}_2^{\rm eff}(t)\right)|\Psi_2(t)\rangle \tag{2.9}$$

with $\hat{\rho}_2(t) = |\Psi_2(t)\rangle\langle\Psi_2(t)|$. Again, the effect of the subsystems on each other is to induce a time-dependent effective Hamiltonian that governs the time evolution of the subsystems.

The derivation of the generalized equations (2.8) and (2.9) is done as follows: Consider a tripartite system defined by the Hamiltonian

$$\hat{H} = \hat{H}_0 + \hat{H}_1 + \hat{H}_{12} + \hat{H}_2 \, . \tag{2.10}$$

Let us assume that system 0 has interacted with system 1 in the past but is now decoupled from system 1. System 2, however, is supposed to have been uncoupled in the past and is now being coupled to system 1 alone. Finally, we assume that the combined system 01 and system 2 are initially in a pure state. We are then left with an initial state for the whole system of the form

$$\hat{\rho}(0) = \hat{\rho}_{01}(0) \otimes \hat{\rho}_2(0) \tag{2.11}$$

with $\hat{\rho}_{01}(0) = |\Psi_{01}(0)\rangle\langle\Psi_{01}(0)|$ and $\hat{\rho}_2(0) = |\Psi_2(0)\rangle\langle\Psi_2(0)|$.

We now consider the dynamics of this system with respect to the given initial state. In the case that $\mathrm{Tr}[\hat{\rho}_2^2(t)] \approx 1$ holds, the FA is applicable to the whole system yielding the two coupled equations

$$i\,|\dot{\Psi}_{01}(t)\rangle = [\hat{H}_0 + \hat{H}_1 + \langle\Psi_2(t)|\,\hat{H}_{12}\,|\Psi_2(t)\rangle]\,|\Psi_{01}(t)\rangle \tag{2.12}$$

$$i\,|\dot{\Psi}_2(t)\rangle = [\hat{H}_2 + \langle\Psi_{01}(t)|\,\hat{H}_{12}\,|\Psi_{01}(t)\rangle]\,|\Psi_2(t)\rangle \, . \tag{2.13}$$

By restating Eq. (2.12) in the form

$$i\dot{\hat{\rho}}_{01}(t) = \left[\hat{H}_0 + \hat{H}_1 + \langle\Psi_2(t)|\,\hat{H}_{12}\,|\Psi_2(t)\rangle\,, \hat{\rho}_{01}(t)\right] \tag{2.14}$$

and taking the trace of the Hilbert space of the ancillary system 0, we arrive at the result

$$i\dot{\hat{\rho}}_1(t) = \left[\hat{H}_1 + \langle\Psi_2(t)|\,\hat{H}_{12}\,|\Psi_2(t)\rangle\,, \hat{\rho}_1(t)\right] . \tag{2.15}$$

To get this result, we have made use of the two partial trace relations

$$\mathrm{Tr}_0\left[\hat{A}\otimes\hat{1}_1,\hat{B}\right] = 0 \tag{2.16}$$

$$\mathrm{Tr}_0\left[\hat{1}_0\otimes\hat{A},\hat{B}\right] = \left[\hat{A},\mathrm{Tr}_0\hat{B}\right] \tag{2.17}$$

(for the derivation, see App. B). Note that in contrast to the case of the FA for a bipartite system, the criterion for the applicability of the FA is the purity dynamics of system 2 alone.

Here, we would like to stress the fact that, as long as the prerequisites for the FA are met, Eqs. (2.8, 2.9) present an alternative description of the system dynamics: The subsystems can be considered classical drivers for each other. It is remarkable that this feature is reciprocal and based on (approximate) constancy of the subsystem purities (entropies).

## 2.2 Classical driving and work

The energy exchanged this way can aptly be called "work": Classically one would define the work $W$ imparted over time $t_S$ on a Hamiltonian system $H(\lambda)$ with $\lambda$ denoting the time-dependent control parameter as given by Jarzynski [1997]

$$W = \int_0^{t_S} \mathrm{d}t \frac{\mathrm{d}\lambda}{\mathrm{d}t}\frac{\partial H}{\partial\lambda}[\vec{z}(t)], \tag{2.18}$$

where $\vec{z}(t)$ denotes the system's state trajectory in phase space. One notes, however, that in the quantum case the energy exchange will, in general, be contaminated by contributions violating the constancy of local purity. This contamination is a characteristic feature of the underlying total (unitary) dynamics. Close to thermal equilibrium such a contribution would be called heat, đ$Q$: Work and heat in open quantum systems are usually defined as

$$\mathrm{d}U = \mathrm{d}\langle\hat{H}\rangle = \underbrace{\mathrm{Tr}(\hat{\rho}\mathrm{d}\hat{H})}_{đW} + \underbrace{\mathrm{Tr}(\hat{H}\mathrm{d}\hat{\rho})}_{đQ} \tag{2.19}$$

(Alicki [1979], Kosloff and Ratner [1984], Kieu [2004], Henrich et al. [2006], Henrich et al. [2007a]) again recognizing the energy exchange in the FA scenario as work.

We emphasize here, that explicitly time-dependent Hamiltonians are usually not considered fundamental. Therefore, there is no way how they could come

about save by an effective description of a system like the FA. If one denied any physical significance of such an effective description and hence considered it only a mathematical simplification without physical meaning, one obviously would have to deny the physical existence of classical drivers altogether. This is not a reasonable option.

## 2.3 Definition of LEMBAS

The effective dynamics according to Eqs. (2.8, 2.9) allows for an intuitive approach to the concept of work: In general, however, this applies only approximately; the deviations remain unquantified. In this section, we develop generalized definitions of work and heat based on the fundamental idea that the part of the dynamics of a system that is induced by a effectively time-dependent Hamiltonian like in Eqs. (2.8) and (2.9) is associated with work as outlined in the previous section. Then, the deviations of Eqs. (2.8, 2.9) can be related to heat.

We again consider an autonomous bipartite system as in (2.1). We now focus on the local properties of subsystem 1 only, however our scheme would work also for subsystem 2. The problem of local addressability has been discussed intensively in quantum computing (Nielsen and Chuang [2000]). Nevertheless, we need first to clarify how a local measurement of heat and work for a part of a bigger total system might work. Such a local measurement of work or heat will have to be based on a coupling to a heat bath or work reservoir, respectively. The energy exchanged with a bath must be heat, that with a classical driver must be work. In both cases the coupling will be realized by an interaction Hamiltonian $\hat{H}_{AM}$ of the type

$$\hat{H}_{AM} = \sum_i \hat{A}_i \otimes \hat{M}_i, \tag{2.20}$$

where the operators $\hat{A}_i$ act only on subsystem 1, and the $\hat{M}_i$ only on the measuring device $M$. Choosing the operators $\hat{A}_i$ may seem rather arbitrary but can have important consequences on the observed values. For example, let us consider a system with an effective local Hamiltonian

$$\hat{H}_1 + \hat{H}_1^{\text{eff}} = \frac{\Delta E}{2}\hat{\sigma}_z. \tag{2.21}$$

We now consider four cases: first, the system will be coupled to a work reservoir, which can always be modeled by a classical driver as the work reservoir must always have zero entropy, by definition. We use $\hat{A}_i = \hat{A} = g\sin(\omega t)\hat{\sigma}_x$

| | work reservoir | heat bath |
|---|---|---|
| $\hat{\sigma}_x$ | $\mathrm{d}U = đW = 0$ | $\mathrm{d}U = đQ \neq 0$ |
| $\hat{\sigma}_z$ | $\mathrm{d}U = đW \neq 0$ | $\mathrm{d}U = đQ = 0$ |

**Table 2.1:** Dependency of measured heat and work on the interaction operator by which a heat bath or work reservoir is coupled to the system (2.21).

and $\hat{A} = g\sin(\omega t)\hat{\sigma}_z$, respectively. For simplicity, we assume that the driving frequency is off-resonant with respect to the eigenfrequency of $\hat{H}_+\hat{H}_1^{\mathrm{eff}}$. Therefore, in the $\hat{\sigma}_x$ case there will be no transfer of energy, while in the $\hat{\sigma}_z$ case $\mathrm{d}U$ is non-zero, and all energy is transferred as work. We then repeat the process when coupling the system to a heat bath. Here, we have $\hat{A} = \lambda\hat{\sigma}_x$ and $\hat{A} = \lambda\hat{\sigma}_z$, respectively. In the $\hat{\sigma}_x$ case, this results in the system relaxing to the canonical state $\hat{\rho} = Z^{-1}\exp[-\beta(\hat{H}_1 + \hat{H}_1^{\mathrm{eff}})]$, with $\beta$ being the inverse temperature. However, the $\hat{\sigma}_z$ coupling results in a pure dephasing of the system, i.e, $\mathrm{d}U = đQ = 0$. A summary of the possible combinations is shown in Table 2.3.

The concrete physical realization of the local measurement thus defines a local effective measurement basis (LEMBAS), which provides a reference for all measurements of work or heat. Which choice of basis is the correct one cannot be decided by the LEMBAS principle. However, there are only few choices which are reasonable and which we will discuss in the following and show to be consistent.

In the following, we do not consider the effect of the actual measurement on the dynamics of the system. We only assume that some fixed basis has been chosen as required by the LEMBAS principle, and then compute work and heat with respect to this basis. Note that this procedure is similar to a hypothetic von Neumann measurement – the probability for each outcome can be calculated without including the measurement device in the dynamics.

We now define the infinitesimal work $đW_1$ performed on system 1 as the change in its internal energy $\mathrm{d}U_1$ that does not change its local von Neumann entropy, i.e.

$$\mathrm{d}S_1 = 0 \Leftrightarrow đW_1 = \mathrm{d}U_1. \tag{2.22}$$

The remainder is defined as the infinitesimal heat $đQ$. It is important to note that work and heat will then turn out to be basis-dependent quantities as they depend on the choice of the measurement basis.

The dynamics of the subsystem 1 is given by the Liouville-von Neumann equation

$$\dot{\hat{\rho}}_1(t) = -i\left[\hat{H}_1 + \hat{H}_1^{\text{eff}}(t), \hat{\rho}_1(t)\right] + \mathcal{L}_1^{\text{eff}}[\hat{\rho}(t)], \tag{2.23}$$

where $\hat{\rho}_1(t)$ is the reduced density operator of the subsystem, $\hat{H}_1^{\text{eff}}(t)$ is an effective Hamiltonian describing the unitary dynamics induced by subsystem 2 on subsystem 1, and $\mathcal{L}_1^{\text{eff}}$ is a superoperator describing incoherent processes, which may derive from the environment of the total bipartite system (if present), but here, in particular, from the influence of subsystem 2 on subsystem 1. Since $\mathcal{L}_1^{\text{eff}}$ is, in general, a function of the density operator of the full system $\hat{\rho}(t)$, Eq. (2.23) is typically not a closed differential equation for $\hat{\rho}_1(t)$.

In the following we choose the energy basis of subsystem 1 as the measurement basis, so that only the parts of the total effective Hamiltonian $\hat{H}_1^{\text{eff}}(t)$ that commute with $\hat{H}_1$ contribute to the described type of experiment. To find this part $\hat{H}_{1,a}^{\text{eff}}(t)$, we expand $\hat{H}_1^{\text{eff}}(t)$ in the transition operator basis defined by the energy eigenstates $\{|j\rangle\}$ of $\hat{H}_1 = \sum_j \epsilon_j |j\rangle\langle j|$:

$$\hat{H}_1^{\text{eff}}(t) = \sum_{jk} [\hat{H}_1^{\text{eff}}(t)]_{jk} |j\rangle\langle k| \tag{2.24}$$

For this operator basis, we have

$$[|j\rangle\langle k|, \hat{H}_1] = \omega_{kj} |j\rangle\langle k|, \tag{2.25}$$

where $\omega_{kj}$ is the difference between the energy eigenvalues of the states $|k\rangle$ and $|j\rangle$, and therefore $\omega_{jj} = 0$ for non-degenerate energy eigenvalues. Now, we define

$$\hat{H}_{1,a}^{\text{eff}}(t) = \sum_j [\hat{H}_{1,a}^{\text{eff}}(t)]_{jj} |j\rangle\langle j| \tag{2.26}$$

which is the diagonal part of $\hat{H}_1^{\text{eff}}(t)$. From Eq. (2.25), we see that no non-zero linear combination of transition operators with $j \neq k$ can ever commute with $\hat{H}_1$ and therefore, neither $\hat{H}_{1,b}^{\text{eff}}(t) = \hat{H}_1^{\text{eff}}(t) - \hat{H}_{1,a}^{\text{eff}}(t)$, nor any part of it commutes with $\hat{H}_1$. Hence, $\hat{H}_{1,a}^{\text{eff}}(t)$ is the part contributing to the measurement as required, and we have

$$[\hat{H}_{1,a}^{\text{eff}}(t), \hat{H}_1] = 0, \quad [\hat{H}_{1,b}^{\text{eff}}(t), \hat{H}_1] \neq 0. \tag{2.27}$$

The latter inequality holds except for the case where $\hat{H}_{1,b}^{\text{eff}}(t) = 0$. An analogous result can be achieved in the case of degenerate eigenvalues of $\hat{H}_1$, and is given in App. A.1.

If a measurement of the local energy is performed in the energy eigenbasis of $\hat{H}_1$, the corresponding local energy operator is

$$\hat{H}_1'(t) = \hat{H}_1 + \hat{H}_{1,a}^{\text{eff}}(t). \tag{2.28}$$

Therefore, the change in internal energy within subsystem 1 is given by

$$\mathrm{d}U_1 = \frac{\mathrm{d}}{\mathrm{d}t}\mathrm{Tr}[\hat{H}_1'(t)\hat{\rho}_1(t)]\mathrm{d}t = \mathrm{Tr}\left(\dot{\hat{H}}_1'(t)\hat{\rho}_1(t) + \hat{H}_1'(t)\dot{\hat{\rho}}_1(t)\right)\mathrm{d}t. \tag{2.29}$$

Using (2.23) and assuming $\hat{H}_1$ to be time-independent leads to

$$\begin{aligned}\mathrm{d}U_1 = \mathrm{Tr}\Big(&\dot{\hat{H}}_{1,a}^{\text{eff}}(t)\hat{\rho}_1(t) \\ &-i[\hat{H}_1'(t), \hat{H}_{1,b}^{\text{eff}}(t)]\hat{\rho}_1(t) + \hat{H}_1'(t)\mathcal{L}_1^{\text{eff}}[\hat{\rho}(t)]\Big)\,\mathrm{d}t,\end{aligned} \tag{2.30}$$

where the cyclicity of the trace has been used. Observing that the dynamics induced by the first two terms is unitary, we arrive at

$$\text{đ}W_1 = \mathrm{Tr}\left(\dot{\hat{H}}_{1,a}^{\text{eff}}(t)\hat{\rho}_1(t) - i\left[\hat{H}_1'(t), \hat{H}_{1,b}^{\text{eff}}(t)\right]\hat{\rho}_1(t)\right)\mathrm{d}t \tag{2.31}$$

$$\text{đ}Q_1 = \mathrm{Tr}\{\hat{H}_1'(t)\mathcal{L}_1^{\text{eff}}[\hat{\rho}(t)]\}\mathrm{d}t. \tag{2.32}$$

In this sense, it is possible to define heat and work for any quantum mechanical process, regardless of the type of dynamics or the states involved.

In order to actually compute đ$W$ and đ$Q$, the effective Hamiltonian $\hat{H}_1^{\text{eff}}(t)$ is required. By starting with the Liouville-von Neumann equation for the full system

$$\dot{\hat{\rho}}(t) = -i[\hat{H}, \hat{\rho}(t)] \tag{2.33}$$

and taking the partial trace over subsystem 2 yields

$$\dot{\hat{\rho}}_1(t) = -i\mathrm{Tr}_2[\hat{H}_1 + \hat{H}_2 + \hat{H}_{12}, \hat{\rho}(t)]. \tag{2.34}$$

Using some theorems on partial traces (see App. B) shows that terms involving $\hat{H}_2$ vanish and $\hat{H}_1$ generates the local dynamics in subsystem 1. For dealing with the terms involving $\hat{H}_{12}$ we first split the density operator as

$$\hat{\rho}(t) = \hat{\rho}_1(t) \otimes \hat{\rho}_2(t) + \hat{C}_{12}(t), \tag{2.35}$$

where $\hat{\rho}_{1,2}(t)$ are the reduced density operators for $A$ and $B$, respectively, and $\hat{C}_{12}(t)$ is the operator describing the correlations between both subsystems. Since the factorization approximation is exact for the first term, we can write (cf. Gemmer and Mahler [2001])

$$\mathrm{Tr}_2[\hat{H}_{12}, \hat{\rho}_1(t) \otimes \hat{\rho}_2(t)] = [\hat{H}_1^{\mathrm{eff}}(t), \hat{\rho}_1(t)], \tag{2.36}$$

where $\hat{H}_1^{\mathrm{eff}}(t)$ is given by

$$\hat{H}_1^{\mathrm{eff}}(t) = \mathrm{Tr}_2\{\hat{H}_{12}[\hat{1}_1 \otimes \hat{\rho}_2(t)]\}. \tag{2.37}$$

Now we show that the processes generated by $[\hat{H}_{12}, \hat{C}_{12}(t)]$ cannot result in unitary dynamics but will always change the local von Neumann entropy $S_1$. In order to proof this, we convince ourselves that its time derivative is non-zero, i.e,

$$\dot{S}_1 = -\mathrm{Tr}\{[\hat{H}_{12}, \hat{C}_{12}(t)] \log \hat{\rho}_1(t) \otimes \hat{1}_2\} \neq 0. \tag{2.38}$$

Therefore, any dynamics generated by this term results in a contribution to $\mathcal{L}_1^{\mathrm{eff}}$. If the dynamics of the full system was unitary, we would thus simply have

$$\mathcal{L}_1^{\mathrm{eff}}[\hat{\rho}(t)] = -i\mathrm{Tr}_2[\hat{H}_{12}, \hat{C}_{12}(t)]. \tag{2.39}$$

as the total incoherent term.

## 2.4 Properties of LEMBAS

### 2.4.1 Clausius relation

In Weimer et al. [2008], we have shown that for $\hat{H}_1'(t) = \hat{H}_1 + \hat{H}_{1,a}^{\mathrm{eff}}(t)$ and $\hat{H}_{1,b}^{\mathrm{eff}}(t) = 0$, the LEMBAS heat and work fulfill the standard thermodynamic Clausius relation if the process under consideration is quasistatic, that is, if system 1 is in a canonical equilibrium state with respect to the internal energy operator $\hat{H}_1'(t)$ determined by the LEMBAS principle,

$$\hat{\rho}_1(t) = \frac{1}{Z(t)} \exp\left[-\frac{1}{T_1}\hat{H}_1(t)'\right] \tag{2.40}$$

with $Z(t) = \mathrm{Tr}\{\exp[-\hat{H}_1(t)'/T_1]\}$ during the whole process.

To show this, we first introduce a formally defined local temperature $T_1^*$ according to the Clausius relation for a system in equilibrium,

$$\mathrm{d}S_1 = \frac{1}{T_1^*}\text{đ}Q_1 = \frac{1}{T_1^*}\mathrm{Tr}\{\hat{H}_1'\mathcal{L}_1^{\mathrm{eff}}[\hat{\rho}(t)]\}\mathrm{d}t, \tag{2.41}$$

where $\mathrm{d}S_1$ is the infinitesimal change of the von-Neumann entropy of system 1. The equality sign is due to the fact that the process is considered quasistatic. We can, however, give another representation of $\mathrm{d}S_1$ because of

$$\mathrm{d}S_1 = \mathrm{dTr}[-\hat{\rho}_1(t)\log\hat{\rho}_1(t)]. \tag{2.42}$$

After carrying out the differentiation, the insertion of Eq. (2.23) and Eq. (2.39) for the incurred differentials of $\hat{\rho}_1(t)$ and some algebra, we end up with

$$\mathrm{d}S_1 = -\mathrm{Tr}\{\mathcal{L}_1^{\mathrm{eff}}[\hat{\rho}(t)]\log\hat{\rho}_1(t)\}\mathrm{d}t. \tag{2.43}$$

Equating Eq. (2.41) and Eq. (2.43) then yields

$$T_1^* = -\frac{\mathrm{Tr}\{\hat{H}_1'\mathcal{L}_1^{\mathrm{eff}}[\hat{\rho}(t)]\}}{\mathrm{Tr}\{\mathcal{L}_1^{\mathrm{eff}}[\hat{\rho}(t)]\log\hat{\rho}_1(t)\}} \tag{2.44}$$

for the formal definition of local temperature $T_1^*$.

Since we deal with a process in thermal equilibrium, the Gibbs relation

$$\mathrm{d}U_1 = T_1^*\mathrm{d}S_1 + \sum_n p_n\mathrm{d}\epsilon_n \tag{2.45}$$

is expected to hold for a system with microstates $n$ with energy $\epsilon_n$. $p_n$ are the occupation numbers of the states and fulfill the Boltzmann distribution. Also, the microstates of a quantum system with internal energy operator $\hat{H}_1'(t)$ are given by its eigenstates and the energies are the energy eigenvalues, so

$$\sum_n p_n\mathrm{d}\epsilon_n(t) = \mathrm{Tr}[\hat{\rho}_1(t)\mathrm{d}\hat{H}_1(t)] = \mathrm{Tr}[\hat{\rho}_1(t)\mathrm{d}\hat{H}_{1,a}^{\mathrm{eff}}(t)] \tag{2.46}$$

is the work term. The directly calculated internal energy change of subsystem 1 is

$$\begin{aligned}\mathrm{d}U_1 &= \mathrm{d}\langle\hat{H}_1'\rangle \\ &= \mathrm{Tr}\left(\dot{\hat{H}}_{1,a}^{\mathrm{eff}}(t)\hat{\rho}_1(t) - i\left[\hat{H}_1'(t), \hat{H}_{1,b}^{\mathrm{eff}}(t)\right]\hat{\rho}_1(t)\right. \\ &\qquad\left. + \hat{H}_1'(t)\mathcal{L}_1^{\mathrm{eff}}[\hat{\rho}(t)]\right)\mathrm{d}t.\end{aligned} \tag{2.47}$$

Note that the commutator on the r.h.s. is 0 [because of $\hat{H}^{\rm eff}_{1,b}(t) = 0$]. The last part of Eq. (2.47) equals $T_1^* {\rm d}S_1$ per definition (2.41), and is the only term of ${\rm d}U_1$ that is associated with a change of entropy (cf. Sec. 2.3). We thus obtain

$$T_1^* = T_1 = \frac{\partial U_1}{\partial S_1}. \tag{2.48}$$

The formal local temperature defined in Eq. (2.44) thus coincides with the standard thermodynamic definition of temperature $T_1$ of the system in equilibrium, and the heat and work derived by the LEMBAS principle is consistent with the Clausius relation in equilibrium with respect to the chosen $\hat{H}'_1$. However, the local temperature $T_1^*$ is not necessarily equal to the global temperature $T$ of the compound system 1+2 due to the interaction between the individual subsystems inducing correlations (cf. Hartmann et al. [2004a,b]).

We note in passing that the same arguments hold for $\hat{H}'_1(t) = \hat{H}_1 + \hat{H}^{\rm eff}_1(t)$ as in this case, the commutator in Eq. (2.47) vanishes due to $[\hat{H}'_1(t), \hat{\rho}_1(t)] = 0$, because the equilibrium state (2.40) is defined with respect to the internal energy $\hat{H}'_1(t)$ and we can make use of the trace relation

$${\rm Tr}\{[\hat{A}, \hat{B}]\hat{C}\} = {\rm Tr}\{[\hat{C}, \hat{A}]\hat{B}\} \tag{2.49}$$

following from the invariance of the trace under cyclic permutations.

We conclude that the LEMBAS definitions of work and heat lead to a formal local temperature definition that can be identified with the standard thermodynamic temperature in equilibrium and the Clausius equation holds. This statement has been shown to be true for two specific choices of the local measurement basis, namely

$$\hat{H}'_1 = \hat{H}_1 + \hat{H}^{\rm eff}_{1,a}(t) \tag{2.50}$$

and

$$\hat{H}''_1 = \hat{H}_1 + \hat{H}^{\rm eff}_1(t) \tag{2.51}$$

. Note that by consequence, both choices of the local measurement basis in principle are compatible with standard thermodynamics.

### 2.4.2 Example: Spin driven by a laser

Using the LEMBAS principle, it is now possible to investigate work and heat also in non-standard physical scenarios. First we consider a two-level atom with a local Hamiltonian $\hat{H}_1$ interacting with a laser field (subsystem 2). In the

semiclassical treatment of the radiation field emitted by a laser the respective Hamiltonian is given by

$$\hat{H} = \hat{H}_1 + \hat{H}_1^{\text{eff}}(t) = \frac{\omega_0}{2}\hat{\sigma}_z + g\sin(\omega t)\hat{\sigma}_x, \tag{2.52}$$

where $g$ is the coupling strength and $\omega$ the laser frequency. In the rotating wave approximation the Hamiltonian can be made time-independent. We investigate the situation where the atom is initially in a thermal state described by the density operator

$$\hat{\rho}(0) = Z^{-1}(\beta)\exp(-\beta\hat{H}_1), \tag{2.53}$$

with $Z$ being the partition function and $\beta$ the inverse temperature. The time-evolution of the density operator $\hat{\rho}(t)$ can be obtained by switching to the rotating frame and diagonalizing the Hamiltonian.

Since (2.52) is already an effective description for system 1, we can directly compute $đW_1$ and $đQ_1$ once we know $\hat{\rho}(t)$, resulting in

$$đW_1(\delta, g) = \frac{\omega_0 g^2}{2\Omega}\tanh\frac{\beta\omega_0}{2}\sin\Omega t \tag{2.54}$$

$$đQ_1 = 0, \tag{2.55}$$

where $\Omega = \sqrt{g^2+\delta^2}$ is the Rabi frequency and $\delta = \omega - \omega_0$ is the detuning from the resonance frequency. $đW_1$ is the energy stored in subsystem 1 that could be retrieved after the preparing field has been switched off at time $\Omega t = \pi/2$. For comparison, with the previously used definition for the work [Eq. (2.19)] one was led to

$$đW_1(\delta, g) = \frac{(\omega_0+\delta)g^2}{2\Omega}\tanh\frac{\beta\omega_0}{2}\sin\Omega t. \tag{2.56}$$

Comparison of the two results shows that in the latter case the maximum is not at the resonance frequency ($\delta = 0$), i.e., only our generalized approach is able to produce the correct physical result.

### 2.4.3 Measurability

$đW, đQ$ are no observables, and neither are the integrated heat and work $W$ and $Q$ along a path in quantum state space. This is a crucial feature of heat and work being *process quantities* in contrast to state variables like internal energy and all other physical quantities that can be given as an observable $\hat{O}$ and whose expectation value is found as $\text{Tr}(\hat{O}\hat{\rho})$. Thus, our definitions of heat and work fulfill an important property as also noted in Talkner et al. [2007].

Although heat and work are no observables and thus not directly measurable, they are measurable in the sense of an inferred quantity, either by a measurement as proposed in Sec. 2.3 and by recording changes of energy in attached work and heat reservoirs, or – in principle – by measuring all quantities appearing in the defining Eqs. (2.31, 2.32), including and most important the total system state $\hat{\rho}(t)$ to infer the quantities $\hat{H}_1^{\text{eff}}(t)$ and $\mathcal{L}_1^{\text{eff}}(t)$.

Some preliminary considerations of how the measurement scheme proposed in Sec. 2.3 works in detail and how the measurement basis might be inferred from that are given in App. A.2.

### 2.4.4 Relation to thermodynamic heat and work

How do these generalized definitions connect to their thermodynamic analogues? In the thermodynamic limit, that is, close to the thermodynamic equilibrium and for infinitely sized subsystems with weak couplings, the von Neumann entropy of the respective subsystem and its thermodynamic entropy coincide and the LEMBAS definitions of work and heat blend in with their thermodynamic counterparts (cf. the result for the Clausius relation in Sec. 2.4.1).

But also in far from equilibrium situations, the LEMBAS definitions can be associated with work and heat in the following sense: We know from the results of quantum thermodynamics (Gemmer et al. [2001], Borowski et al. [2003], Gemmer et al. [2004]) that thermodynamic behavior of a system can be seen to result from an embedding in an environment which by itself needs not to be and usually is not thermodynamic (in equilibrium, infinite, weak coupling). Thus, validity of thermodynamic concepts is not a property of the total system but has to do with whether or not the system of interest is influenced by its environment in such a way that thermodynamic properties emerge, which is a purely local consideration. The LEMBAS definitions take this concept to the extreme in the sense that they state that "what locally has a work effect $\hat{H}_1^{\text{eff}}(t)$, is work" and "what locally has a heat effect $\mathcal{L}_1^{\text{eff}}[\hat{\rho}(t)]$, is heat" even for non-thermodynamic (in the classical sense), far from equilibrium situations. Making the distinction in this way is justified by the fact that classical driving can be unambiguously identified as work even in the thermodynamic sense and, therefore, any effect $\mathcal{L}_1^{\text{eff}}[\hat{\rho}(t)]$ not related to work is identified as heat.

Finally, we note that the LEMBAS definitions retain the properties that

1. work is energy exchange due to changing parameters of the Hamilton operator that describes the system;

2. heat is energy exchange associated with change of entropy, although here a generalized definition of entropy is to be used.

### 2.4.5 Open questions

Although the basic idea of LEMBAS is fairly clear and plausible, there are still some not yet satisfactorily answered questions. The first of them applies to the uniqueness of the decomposition of the effective Hamiltonian $\hat{H}_1^{\text{eff}}(t)$: Given its expansion in the transition operator basis as described in Sec. 2.3, the decomposition is well-defined [Eq. (2.26)]. However, it can be shown that choosing another operator basis will lead to another part of the effective Hamiltonian to be recognized as the commuting part (see Sec. A.1). One possible solution of this problem could be that conditions can be found for a given measurement situation that single out a certain operator basis on which to expand $\hat{H}_1^{\text{eff}}(t)$. If this is not the case, it could be necessary to perform a maximization of đ$W$ with respect to all possible operator bases, since the work is expected to have a maximum that in general is different from d$U$. For the heat on the contrary it is expected that one can always find an operator basis, where all change of the internal energy is found to be heat, in some sense the worst choice of a basis.

The second question is related to the preceding one and to the exact mechanism by which the LEMBAS measurement scheme singles out a certain measurement basis and – as noted above – possibly the decomposition operator basis. This has proven to be not an easily solved problem for general situations and we defer the presentation of some considerations to this questions to App. A.2.

The last question is concerned with the effects local projective energy measurements have on the system, namely alteration of the environment of the measured system due to entanglement and co-jumps. This has mainly two consequences: First, not only the measured system's state has changed but due to the co-jump effect, the effective Hamiltonian acting on the system is also no longer the same. It is not clear how this effect should possibly taken into account by the LEMBAS measurement scheme. A detailed derivation of the co-jump effects and some preliminary considerations of the problems are given in Sec. A.3.

## 2.5 Work source quality measures

In order to complete the exposition of concepts used in the following chapter to demonstrate that single quantum systems can act as work reservoirs under certain conditions, we discuss how to define work reservoir functionality under non-ideal circumstances in this section.

An ideal work reservoir can be defined as a system exchanging energy only in the form of work. It is obvious that this definition is too restrictive for the classification of realistic models, that is, models involving finite size, finite interaction and limited control. No realistic model can comply to the idea of such an ideal work source as even arbitrary small but finite deviations from this idealized concept would lead to a rejection of a model as a work source. Additional complications arise due to the fact that we have to consider processes, the properties of which may change with time.

Thus, there is need for a more differentiated measure of work reservoir functionality. In a non-ideal world, special attention is to be paid to the definition and quantification of the quality of a work reservoir to be able to compare and to draw conclusions on justified grounds.

Basically, one can distinguish two types of measures depending on whether they refer to a single point in time or to a (finite or infinitely large) interval of time. We like to refer to them as *instantaneous* and *integral* measures and our main interest lies on the integral ones, defined with respect to some finite time interval (again because under realistic condition it is not expected that a system can be a work source for all times).

In the following section, we present two different approaches to the problem based on two distinct physical reasonings.

### 2.5.1 Purity based

Comparing Eq. (2.23), the exact local dynamics of subsystem 1

$$\dot{\hat{\rho}}_1(t) = -i\left[\hat{H}_1 + \hat{H}_1^{\text{eff}}(t), \hat{\rho}_1(t)\right] + \mathcal{L}_1^{\text{eff}}[\hat{\rho}(t)],$$

to Eq. (2.8), the result for the generalized form of the FA

$$\dot{\hat{\rho}}_1(t) = -i\left[\hat{H}_1 + \hat{H}_1^{\text{eff}}(t), \hat{\rho}_1(t)\right],$$

one realizes immediately that the applicability of the FA is equivalent to the vanishing of $\mathcal{L}_1^{\text{eff}}$. Thus, if the total system was initially in a semi-mixed state, $\mathcal{L}_1^{\text{eff}}$ is negligible if $P[\hat{\rho}_2(t)] \approx 1$. In this sense, $P[\hat{\rho}_2(t)]$ is a measure of work reservoir functionality. The closer it is to 1, the smaller $\mathcal{L}_1^{\text{eff}}$ has to be and the less energy may be exchanged as heat instead of work. Note that acting as a work reservoir is a reciprocal property, i.e., each subsystem acts on its partner in an analogous way. This is in perfect agreement with what we know from thermodynamics. If we have two systems undergoing a process during which only work is exchanged between them, both systems obviously act as work reservoirs for each other although we may imagine one system to be the

gas filling a box and the other system to be the piston capping the box and being connected to a spring.

At first glance, the purity therefore seems to be a good candidate for assessing work source quality: It is an easy quantity to compute – even analytically – and by its connection to the FA, the physical reasoning is clear.

However, as clear as the ideal situation with $P[\hat{\rho}_2(t)] = 1$ is, it is unclear to give a quantitative interpretation for purities lower than unity because there is neither an obvious relation between $P[\hat{\rho}_2(t)]$ and $\mathcal{L}_1^{\text{eff}}$ nor between $\mathcal{L}_1^{\text{eff}}$ and the quality of the work reservoir functionality. Moreover, one should expect that the same purity decrease for different systems, especially of different size, has to be weighted differently. Thus, any concrete choice of a minimum purity beyond which a system will be accepted as a work reservoir will remain somewhat arbitrary and difficult to compare with other systems' purity behavior. If such a purity threshold was given, the respective system could be considered as a work source for any time interval during which the purity stays above the given threshold.

As will become evident in Sec. 3.3, there is another problem besides the arbitrary definition of the threshold when using this measure: The decrease in purity is linked to the size of $\mathcal{L}_1^{\text{eff}}$ only. Thus, the purity does not contain any information about the relative effects of $\hat{H}_1^{\text{eff}}(t)$ and $\mathcal{L}_1^{\text{eff}}$. Since the former is related to work and the latter to heat, a comparison of both in terms of their effect on the energy of the system is in general expected to be an important part of the assessment of work source quality.

### 2.5.2 Work and heat based

We introduce the ratio

$$r(t) := \frac{|\dot{W}(t)|}{|\dot{W}(t)| + |\dot{Q}(t)|} \tag{2.57}$$

which has the following convenient properties:

- $r(t) \in [0, 1]$
- $r(t) = 1 \Leftrightarrow \dot{W}(t) \neq 0$ and $\dot{Q}(t) = 0$: ideal work source
- $r(t) = 0 \Leftrightarrow \dot{W}(t) = 0$ and $\dot{Q}(t) \neq 0$: ideal heat source

Provided there is energy exchange at all (i.e. not both, $\dot{W}$ and $\dot{Q}$ are zero), $r$ is well behaved. As we took separate moduli in the denominator, there can be no compensation due to opposite sign.

Based on this instantaneous measure, we can develop an integral measure for finite time intervals $[t_0, t_1]$. Directly integrating over $r(t)$ is not an option for this would completely ignore the time-dependence of the total of the absolute fluxes and therefore the necessary weighting of $r$. It is straightforward to apply the necessary weight, integrate and then normalize to get

$$\begin{aligned} R(t_1, t_0) &:= \frac{\int_{t_0}^{t_1} r(t) \left( |\dot{W}(t)| + |\dot{Q}(t)| \right) \mathrm{d}t}{\int_{t_0}^{t_1} |\dot{W}(t)| + |\dot{Q}(t)| \, \mathrm{d}t} \\ &= \frac{\int_{t_0}^{t_1} |\dot{W}(t)| \mathrm{d}t}{\int_{t_0}^{t_1} |\dot{W}(t)| + |\dot{Q}(t)| \, \mathrm{d}t}. \end{aligned} \tag{2.58}$$

Defining the quantities

$$\mathcal{W}(t_1, t_0) := \int_{t_0}^{t_1} |\dot{W}(t)| \, \mathrm{d}t, \quad \mathcal{Q}(t_1, t_0) := \int_{t_0}^{t_1} |\dot{Q}(t)| \, \mathrm{d}t \tag{2.59}$$

we can rewrite Eq. (2.58) in the form of Eq. (2.57) as

$$R(t_1, t_0) := \frac{\mathcal{W}(t_1, t_0)}{\mathcal{W}(t_1, t_0) + \mathcal{Q}(t_1, t_0)}. \tag{2.60}$$

This integral measure has the same special limits like the instantaneous measure with the following interpretations:

- $R(t_1, t_0) = 1 \Leftrightarrow \dot{Q}(t) = 0$ for all $t \in [t_0, t_1]$ and $\dot{W}(t) \neq 0$ for some $t \in [t_0, t_1]$: ideal work source

- $R(t_1, t_0) = 0 \Leftrightarrow \dot{W}(t) = 0$ for all $t \in [t_0, t_1]$ and $\dot{Q}(t) \neq 0$ for some $t \in [t_0, t_1]$: ideal heat source

It also shares the definition range $R(t_1, t_0) \in [0, 1]$ with the instantaneous measure.

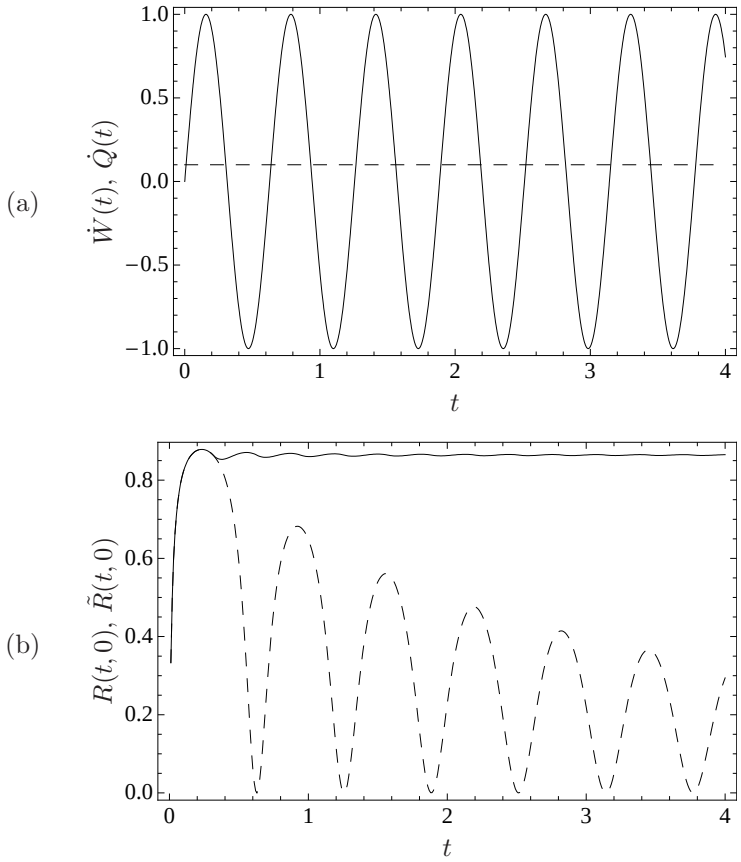


**Figure 2.1:** Heat, work and alternative work reservoir quality measures for an oscillating piston performing work on a gas volume. The piston is thought of being massive and hotter than the gas thus leading to a small heat leakage into the gas system. (a) solid: work flux, dashed: heat flux, (b) solid: the proposed work source quality measure $R(t,0)$ [cf. Eq. (2.60)], dashed: the alternative measure $\tilde{R}(t,0)$ based on the integrated work and heat [Eq. (2.63)].

We emphasize here that a measure based directly on the integrated work and heat,

$$W(t_1, t_0) = \int_{t_0}^{t_1} \dot{W}(t)\mathrm{d}t \tag{2.61}$$

$$Q(t_1, t_0) = \int_{t_0}^{t_1} \dot{Q}(t)\mathrm{d}t, \tag{2.62}$$

is not able to accomplish such precise assessment of the work source quality: For oscillating fluxes, e.g., $W(t_1, t_0)$ might reach 0 for some interval, although during the time interval there might have flown vast amounts of work. Compared with the integrated heat $Q(t_1, t_0)$ for this interval, the system would thus appear as a pure heat bath on the given interval – obviously not a sensible result.

We illustrate this with the help of a model consisting of a gas being periodically compressed and expanded by a piston. The piston itself is supposed to be massive and of higher temperature than the gas, thus not only acting as a work source but also as a heat bath for the gas. The work and heat flux applied to the gas by the piston in this situation are depicted in Fig. 2.1(a). We now consider the alternative quality measure

$$\tilde{R}(t_1, t_0) = \frac{W(t_1, t_0)}{W(t_1, t_0) + Q(t_1, t_0)} \tag{2.63}$$

that depends directly on the integrated work and heat, and apply it to this model. Clearly, the work integrated over any integer number of periods of the piston's oscillation is zero, while the integrated heat is positive on all intervals. Thus, on each interval of a length that is an integer multiple of the period time the piston would be classified as a pure heat source consistent with $\tilde{R}(t_1, t_0) = 0$. In Fig. 2.1(b), the dashed line represents $\tilde{R}(t, 0)$ and we readily see that it vanishes whenever the piston has completed one period. Looking at the fluxes in Fig. 2.1(a) again, we see however clearly that the piston has a work effect much more prominent than the small heat leakage and thus should be identified as a rather good work source on all intervals where more than a single cycle is performed. In no way it would be expected that a system providing work at a much higher rate than heat at almost all times of the dynamics could be repeatingly classified as a perfect heat bath, as is the case for $\tilde{R}(t, 0)$ periodically reaching zero. The solid line in Fig. 2.1(b) corresponds nicely with this argument and shows the result for the quality

measure $R(t,0)$ if applied to the model. As expected, after already a single cycle, the piston's functionality is clearly assessed as a rather good work source with an approximately constant work source quality above 0.8 for longer times.

We conclude that a quality measure based on the integrated heat and work is not suitable to assess the functionality of an environment. By employing the integrals of the absolute fluxes in the chosen definition, we achieve a much stronger statement about the quality of the functionality. Finally, let us note that there is also a drawback to this measure, namely the difficulty of calculating it because of the integration over the absolute values of the fluxes.

# 3 Spin-oscillator model

In the previous chapter, we have discussed how coupled quantum systems may exert classical driving on each other, and how this feature is connected to the thermodynamical concept of work.

Equipped with the methods developed there, namely the factorization approximation (FA) (Sec. 2.1), the definition of heat and work according to the LEMBAS approach (Sec. 2.3), and the work source quality measures (Sec. 2.5), we go on to present and discuss the spin-oscillator model (SOM) with respect to work reservoir functionality. We introduce two versions of the SOM and their fundamental dynamical properties in view of the applicability of the FA in Sec. 3.1. In Sec. 3.2, we demonstrate under what conditions the model can act as an ideal work source in the thermodynamic sense despite its quantumness. We show how this perfect work reservoir functionality is deteriorated by a small additional term in the interaction in the subsequent Sec. 3.3, and how useful the two types of work reservoir quality measures are for the assessment of the functionality of the parts.

## 3.1 System and dynamics

We turn now to the description of the model we will use to demonstrate the existence of small quantum systems that may act as work sources. We illustrate the features of the FA and the various work measures we have discussed above and discuss the model and its properties with special focus on the dynamics of the purity.

The model is a single spin interacting with a harmonic oscillator (*spin-oscillator model, SOM*). On the one hand, the SOM serves as an allusion to a classical steam engine with a gas of some temperature (spin) and a piston periodically compressing and expanding the gas (oscillator). On the other hand, the SOM has been used in previous related works as a central element of quantum thermodynamic machines (Henrich et al. [2006, 2007a], Tonner and Mahler [2006]). Also, the simplicity and therefore partially possible analytical treatment of the model has further motivated the choice.

The SOM is defined by the Hamiltonian

$$\hat{H} = \frac{\omega_s}{2}\hat{\sigma}_z + \hat{H}_{\rm int} + \omega_o\left(\hat{a}^\dagger\hat{a} + \frac{1}{2}\right). \tag{3.1}$$

We denote the spin and oscillator local Hamilton operators as $\hat{H}_s$ and $\hat{H}_o$, respectively. The eigenstates of $\hat{H}_s$ are $|0\rangle$ and $|1\rangle$ with the respective eigenvalues $\mp\omega_s/2$. The eigenstates of $\hat{H}_o$ are defined as $\{|k\rangle\}$ with eigenvalues $\omega_o(k+1/2)$, where $k = 0, 1, 2, \ldots$.

Alternatively, we will consider the $z$- and the $xz$-interaction,

$$\hat{H}_{\rm int} = \{\hat{H}_z, \hat{H}_{xz}\}, \tag{3.2}$$

where

$$\hat{H}_z = \lambda\hat{\sigma}_z\hat{x} \tag{3.3}$$

$$\hat{H}_{xz} = \lambda(\hat{\sigma}_z + \kappa\hat{\sigma}_x)\hat{x}. \tag{3.4}$$

For the initial state of the total system, we assume that the spin has interacted in the past with some heat bath in order to establish a thermal state but now is decoupled from said bath (or the bath coupling is so weak that its influence may be neglected during the period of evolution one is interested in). The oscillator is prepared in a coherent state $|\alpha\rangle$. Thus, the total initial state is

$$\hat{\rho}(0) = \begin{pmatrix} c & 0 \\ 0 & 1-c \end{pmatrix} \otimes |\alpha\rangle\langle\alpha| \tag{3.5}$$

where the spin's state is given in its energy eigenbasis. The self-generated process imposed on the spin via coupling to the oscillator might thus be called "adiabatic"; however, due to quantum mechanical interactions the local entropy (purity) will, in general, not be constant, see below.

### 3.1.1 $z$-SOM dynamics

Representing the Hamiltonian (3.1) in the eigenbasis of the spin, one finds that it has a block-diagonal structure:

$$\begin{aligned} \hat{H} &= \begin{pmatrix} \hat{H}_o - \lambda\hat{x} - \frac{\omega_S}{2} & \\ & \hat{H}_o + \lambda\hat{x} + \frac{\omega_S}{2} \end{pmatrix} \\ &=: \begin{pmatrix} \hat{H}_- & \\ & \hat{H}_+ \end{pmatrix} \end{aligned} \tag{3.6}$$

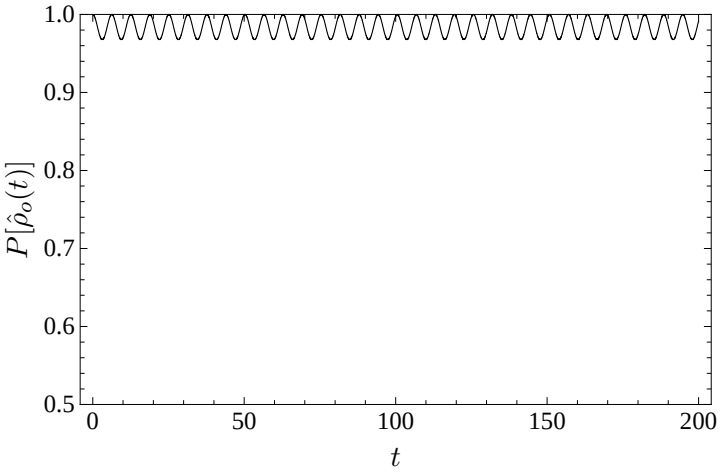


**Figure 3.1:** Purity dynamics of the oscillator in the $z$-SOM for the special parameters $\lambda = 0.1, c = 0.7, \alpha = 0, m = \omega_s = \omega_o = 1$.

The same obviously holds for the time-evolution operator

$$\hat{U}(t_1, t_0) = \exp[-i\hat{H}(t_1 - t_0)] \tag{3.7}$$

and – by the block-diagonal structure of the initial state – also for the propagated state $\hat{\rho}(t)$ of the total system:

$$\hat{\rho}(t) = \begin{pmatrix} c\,|\alpha_-(t)\rangle\langle\alpha_-(t)| & \\ & (1-c)\,|\alpha_+(t)\rangle\langle\alpha_+(t)| \end{pmatrix} \tag{3.8}$$

Here, we have used the definitions $|\alpha_\pm(t)\rangle := \hat{U}_\pm(t,0)\,|\alpha\rangle$ and $\hat{U}_\pm(t_1,t_0) = \exp\left[-i\hat{H}_\pm(t_1 - t_0)\right]$. Note that the dynamics of the system are periodic because both Hamilton operators $\hat{H}_\pm$ describe (displaced) harmonic oscillators with the same frequency $\omega_o$. Thus, we have $\hat{U}(t_1 + 2\pi m\omega_o^{-1}, t_0 + 2\pi n\omega_o^{-1}) = \hat{U}(t_1, t_0)$ for integer numbers $n, m$.

Because of the simple structure of the time-evolution of the system, the purity of the oscillator can be derived analytically from Eq. (3.8) by considering the oscillator's reduced state

$$\hat{\rho}_o(t) = c\,|\alpha_-(t)\rangle\langle\alpha_-(t)| + (1-c)\,|\alpha_+(t)\rangle\langle\alpha_+(t)|\,. \tag{3.9}$$

Taking the square and the trace of this expression, we get

$$P[\hat{\rho}_o(t)] = c^2 + (1-c)^2 + 2c(1-c)\,|\langle\alpha_-(t)|\alpha_+(t)\rangle|^2\,. \tag{3.10}$$

for the purity of the oscillator. For the time-dependent term we find

$$\begin{aligned} |\langle\alpha_-(t)|\alpha_+(t)\rangle|^2 &= \left|\langle\alpha|\,\hat{U}_-^\dagger(t,0)\hat{U}_+(t,0)\,|\alpha\rangle\right|^2 \\ &= \left|\langle\alpha|\exp(i\hat{H}_-t)\exp(-i\hat{H}_+t)\,|\alpha\rangle\right|^2 . \end{aligned} \tag{3.11}$$

Making use of the displacement operator $\hat{D}(\alpha) = \exp(\alpha\hat{a}^\dagger - \alpha^*\hat{a})$ and its properties

$$\hat{D}(-\alpha)\hat{x}\hat{D}(\alpha) = \hat{x} + \sqrt{\frac{2}{m\omega_o}}\,\mathrm{Re}(\alpha) \tag{3.12}$$

$$\hat{D}(-\alpha)\hat{p}\hat{D}(\alpha) = \hat{p} + \sqrt{2m\omega_o}\,\mathrm{Im}(\alpha), \tag{3.13}$$

we can express $\hat{H}_\pm$ as

$$\hat{H}_\pm = \hat{D}(-\beta_\pm)\hat{H}_o\hat{D}(\beta_\pm) + C \tag{3.14}$$

and therefore have

$$\hat{U}_\pm(t,0) = \mathrm{e}^{-iCt}\hat{D}(-\beta_\pm)\exp(-i\hat{H}_ot)\hat{D}(\beta_\pm) \tag{3.15}$$

with $\beta_\pm = \mp\lambda/\sqrt{2m\omega_o^3}$ up to constant factors or a phase, respectively, which are irrelevant for the computation of the modulus in Eq. (3.11). With the help of the relations

$$\hat{D}(\alpha)\hat{D}(\beta) = \exp[i\,\mathrm{Im}(\alpha\beta^*)]\hat{D}(\alpha+\beta) \tag{3.16}$$

$$\exp(-i\hat{H}_ot)\,|\alpha\rangle = \exp(-i\omega_ot/2)\,|\alpha\exp(-i\omega_ot)\rangle \tag{3.17}$$

(for the first one, see Vogel and Welsch [2006], Ch. 3, for the second, see App. C) we arrive at

$$|\alpha_\pm(t)\rangle = \exp[i\phi_\pm(t)]\,|(\alpha+\beta_\pm)\exp(-i\omega_ot) - \beta_\pm\rangle\,. \tag{3.18}$$

Finally making use of the relation $|\langle\alpha|\alpha'\rangle|^2 = \exp(-|\alpha-\alpha'|^2)$ (see Vogel and Welsch [2006], Ch. 3), Eq. (3.18) yields the result

$$|\langle\alpha_-(t)|\alpha_+(t)\rangle|^2 = \exp\left[-8\frac{\lambda^2}{m\omega_o^3}\sin^2\left(\frac{1}{2}\omega_ot\right)\right] \tag{3.19}$$

for the time-dependent part of Eq. (3.10) ($m$ is the oscillator mass). For pure initial spin states ($c = 0, 1$) we have $P[\hat{\rho}_o(t)] = 1$. An example for $P[\hat{\rho}_o(t)]$ for a mixed initial spin state is given in Fig. 3.1.

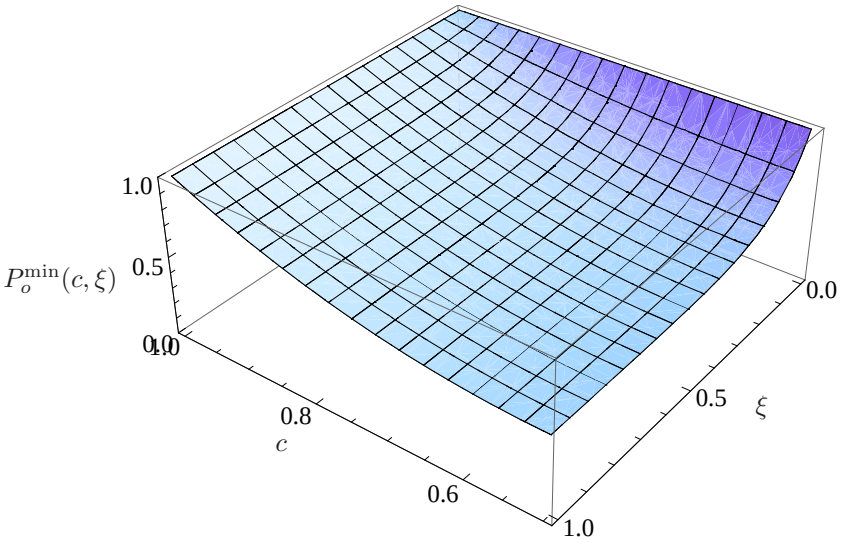


**Figure 3.2:** Minimum oscillator purity landscape of the $z$-SOM as a function of $c$ and $\xi$.

It is easy to see from Eqs. (3.10, 3.19) that the minimum purity with respect to $t$ and $c$ is

$$P_o^{\min} = \frac{1}{2}\left[1 + \exp\left(-8\xi\right)\right], \tag{3.20}$$

where

$$\xi = \frac{\lambda^2}{m\omega_o^3}. \tag{3.21}$$

Fig. 3.2 shows the minimum oscillator purity landscape depending on the parameters $c$ and $\xi$. Obviously, one has to choose $\xi \to 0$ to ensure the applicability of the FA for arbitrary $c$, which corresponds to arbitrary temperatures of the spin, and thus

$$1 - P_o^{\min} \ll 1. \tag{3.22}$$

We can distinguish two different ways to enforce the limit $\xi \to 0$:

$$m \to \infty,\ \omega_o = \text{const.},\ \lambda = \text{const.} \tag{3.23}$$

$$\omega_o \to \infty,\ m = \text{const.},\ \lambda^2/\omega_o = \text{const.} \tag{3.24}$$

Their relevance will become clear in Sec. 3.2. If one accepts the resulting finite $P_o^{\min}$ for some finite $\xi$, the local coherence time may be called infinite.

### 3.1.2 $xz$-SOM dynamics

We discuss now the more complicated case of an interaction of form Eq. (3.4). This interaction is motivated by the following considerations. First, the above case is very special in that the minimum purity reached can be controlled completely by the system parameters. The more general $xz$-interaction case will show that this property is dependent on the interaction. Second, the chosen interaction allows us to study the effect of imperfect control over the exact form of the interaction as it might be the case for a more realistic experimental situation. Finally, the $xz$-interaction exhibits a remarkable diversity of dynamics which serves to illustrate the pros and cons of the proposed work reservoir quality measures as well as the possibility to realize quantum work sources within the given model.

First, we show that a Hamiltonian

$$\hat{H} = \frac{\omega_s}{2}\hat{\sigma}_z + \lambda \hat{s}\hat{x} + \omega_o \left(\hat{a}^\dagger \hat{a} + \frac{1}{2}\right) \tag{3.25}$$

with an arbitrary operator $\hat{s}$ acting on the spin's Hilbert space is equivalent to the $xz$-SOM. This is seen from the expansion of $\hat{s}$ in the operator basis $\{\hat{Q}_k | k = 0, 1, 2, 3\} = \frac{1}{\sqrt{2}}\{\hat{1}, \hat{\sigma}_x, \hat{\sigma}_y, \hat{\sigma}_z\}$, which reads

$$\hat{s} = \sum_{k=0}^{3} \mathrm{Tr}(\hat{Q}_k^\dagger \hat{s})\hat{Q}_k \tag{3.26}$$

(for details refer to Mahler and Weberruß [1998], pp. 34–49). The $\hat{1}$ term is local to the oscillator and can be absorbed in $\hat{H}_o$, while the $\hat{\sigma}_k$ terms can always be transformed to the form $\hat{s} = \lambda(\hat{\sigma}_z + \kappa\hat{\sigma}_x)$ by the local transformation $\exp(-i\phi\hat{\sigma}_z)$ with appropriately chosen real $\phi$. This corresponds to a rotation around the $z$-axis of the spin. The $xz$-SOM discussed here is therefore representative for the whole class of Hamiltonians of the form (3.25).

Now, we want to look into the behavior of the system for $|\kappa| \lesssim 1$. To get insight into the dynamics, we invoke a rotating wave approximation (RWA). For that purpose, we first write the $xz$-SOM interaction Hamiltonian $\hat{H}_{xz}$ in

the interaction picture

$$\begin{aligned}\hat{\tilde{H}}_{xz} \propto\, & \hat{\sigma}_z\hat{a}\exp\left(i\frac{\Omega-\Delta}{2}t\right) + \hat{\sigma}_z\hat{a}^\dagger\exp\left(-i\frac{\Omega-\Delta}{2}t\right) \\ & + \kappa[\hat{\sigma}_+\hat{a}\exp(-i\Delta t) + \hat{\sigma}_-\hat{a}\exp(i\Omega t) \\ & + \hat{\sigma}_+\hat{a}^\dagger\exp(-i\Omega t) + \hat{\sigma}_-\hat{a}^\dagger\exp(i\Delta t)],\end{aligned} \tag{3.27}$$

where we have defined $\Omega := \omega_s + \omega_o$ and $\Delta := \omega_s - \omega_o$. By restricting ourselves to the resonant case $\Delta = 0$ and omitting all terms rotating with frequencies $\Omega$ and $\Omega/2$, the $xz$-SOM Hamiltonian in RWA turns out to be

$$\hat{H}_{xz}^{\mathrm{RWA}} = \frac{\omega}{2}\hat{\sigma}_z + g(\hat{\sigma}_+\hat{a} + \hat{\sigma}_-\hat{a}^\dagger) + \omega\left(\hat{a}^\dagger\hat{a} + \frac{1}{2}\right) \tag{3.28}$$

in the Schrödinger picture. This is just the Hamiltonian $\hat{H}_{\mathrm{JC}}$ of the Jaynes-Cummings model (JCM) (Jaynes and Cummings [1963], Shore and Knight [1993]) with

$$g = \frac{\lambda\kappa}{\sqrt{2m\omega}} \tag{3.29}$$

and $\omega = \omega_s = \omega_o$. According to Shirley [1965] and Larson [2007], the RWA is accurate as long as $g/\Omega \ll 1$. This condition is met for all relevant cases, since we consider in the following a situation where the parameters $m$, $\omega$, and $\lambda$ have been chosen such that for $\kappa = 0$ ($z$-SOM) the FA holds for all times.

Now let us turn to the interpretation of the result. First, we note that by performing the RWA, in particular, the $\hat{\sigma}_z$ term of the interaction Hamiltonian is removed. Therefore, the $xz$-SOM in RWA captures the effect of the $\hat{\sigma}_x$ interaction alone and, in turn, this means that the main dynamics are governed by the $\hat{\sigma}_x$ part of the interaction alone.

Second, the dynamics of the JCM (and therefore of the $xz$-SOM in RWA) scale in time with $g^{-1}$. This is most clear from the exact time-evolution operator for the JCM (Scully and Zubairy [1997], p. 205) in the case of exact resonance

$$\hat{U}_{\mathrm{JC}}(t) = \begin{pmatrix} \cos(gt\hat{B}) & -i\hat{a}^\dagger\sin(gt\hat{A})\hat{A}^{-1} \\ -i\sin(gt\hat{A})\hat{A}^{-1}\hat{a} & \cos(gt\hat{A}) \end{pmatrix} \tag{3.30}$$

with $\hat{A} = \sqrt{\hat{a}^\dagger\hat{a} + 1}$ and $\hat{B} = \sqrt{\hat{a}^\dagger\hat{a}}$.

The numerical results of the dynamics of the purity of the oscillator are given in Fig. 3.3 for the case of a coherent initial state with one photon in the cavity on average ($\alpha = 1$). The deviations of the numerical results for the

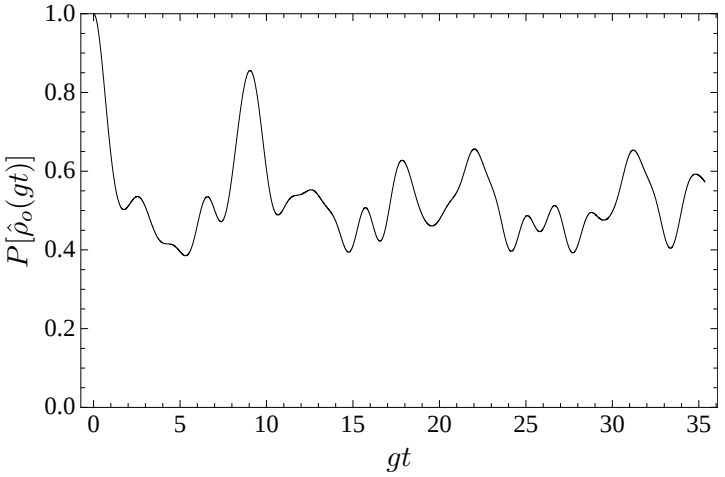


**Figure 3.3:** Purity of the oscillator for numerically exact dynamics of the $xz$-SOM in RWA for arbitrary $g$. The parameters are: $m = 1$, $\lambda = 0.01$, $\alpha = \omega_o = \omega_s = 1$, $c = 0.7$.

$xz$-SOM with and without RWA for three different orders of magnitude of $g$ [and thus $\kappa$ by virtue of Eq. (3.29)] are given in Fig. 3.4. One sees from that figure that the RWA yields good results (less then 10% relative deviation) up to $\kappa \approx 10$. This shows again that the RWA gives an accurate description of the $xz$-SOM dynamics in agreement with the expectation given above.

It is obvious from Figs. 3.1, and 3.3 that the purity behavior of the $xz$-SOM is fundamentally different from the $z$-case. The decrease of the purity due to the additional $\hat{\sigma}_x$ interaction term is several orders of magnitude stronger than what is expected from the $\hat{\sigma}_z$ term alone and due to the approximate scaling behavior of the $xz$-SOM, the minimum does not depend on $\kappa$, as long as $\kappa$ is not zero. We conclude from that, that in the presence of an arbitrarily small but non-vanishing $\hat{\sigma}_x$ term the FA and with it the work reservoir quality of the oscillator will break down in finite time. Reduction of $\kappa$ can only delay the breakdown and, thus, if $\lambda, \kappa \neq 0$ no choice of the other model parameters can prevent the breakdown. This result is in agreement with the finding of Gemmer and Mahler [2001] that the coherence time for the JCM depends on the interaction strength such that weaker interaction leads to longer coherence time.

In the above sense, the work reservoir functionality in the given quantum scenario is quite sensitive to the quality of control of the interaction between

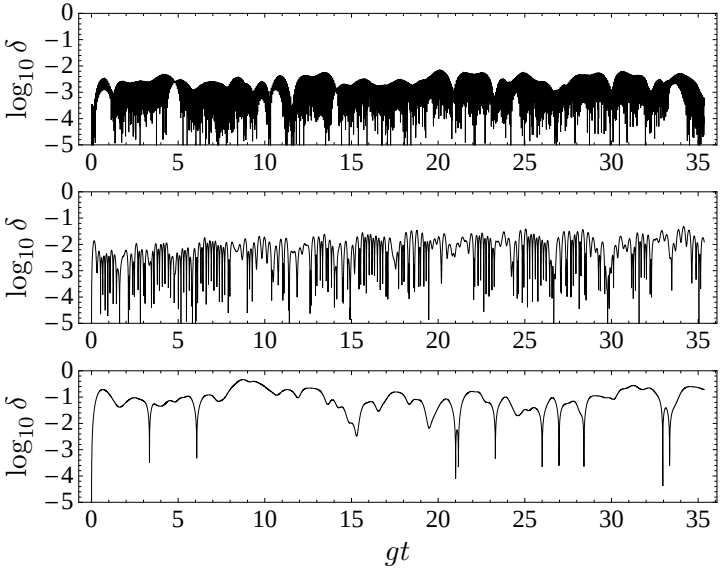


**Figure 3.4:** Common logarithm of the absolute deviation $\delta$ of the (numerically exact) purity dynamics with and without RWA for (top to bottom) $g = -0.01, -0.1, -1$ corresponding to $\kappa = \sqrt{2}, 10\sqrt{2}, 100\sqrt{2}$ according to Eq. (3.29) with the parameters $\lambda = -0.01$, $m = 1$, $\alpha = \omega_o = \omega_s = 1$, $c = 0.7$.

spin and oscillator.

## 3.2 Quantum work source

Focusing here on the $z$-SOM, let us assume that one has chosen the parameters of the system such that Eq. (3.22) is fulfilled. We can then apply the FA not only to describe the dynamics of the system up to any desired accuracy but moreover, we get a new level of description combined with new physical insight in the properties and characteristics of the system. This will be outlined below.

Applying the FA to this SOM, we find according to Eqs. (2.8) and (2.9) the following effective coupled equations

$$\dot{\hat{\rho}}_s = -i\left[\left(\frac{\omega_s}{2} + \lambda\langle\hat{x}\rangle(t)\right)\hat{\sigma}_z, \hat{\rho}_s\right] \tag{3.31}$$

$$|\dot{\Psi}(t)\rangle = -i[\hat{H}_o + \lambda(1-2c)\hat{x}]\,|\Psi(t)\rangle\,, \tag{3.32}$$

where we have defined $\langle\hat{x}\rangle(t) := \langle\Psi(t)|\,\hat{x}\,|\Psi(t)\rangle$. Hence, the spin is driven by the oscillator displacement which acts like an additional time-dependent magnetic field modulating the spin's Zeeman splitting. On the other hand, the spin dynamics lead to a constant displacement of the oscillator potential. In this sense there is asymmetry between the two subsystems: The effective Hamiltonian for the oscillator is modified but not time-dependent.

Clearly, this result is in agreement with the result which one would obtain from applying the integral measure based on $\mathcal{W}$ and $\mathcal{Q}$: The latter is zero, since according to Sec. 3.1.1 and Eq. (3.31), the spin's state does not change and the oscillator only exerts classical driving on the spin. The local effective energy change of the spin resulting from the driving is 100% work. Hence, the oscillator acts as an ideal work source at least in the limits discussed in Sec. 3.1.1, Eqs. (3.23, 3.24).

However, it has to be noted that the peak-to-peak amplitude $\Delta\omega_s^{\text{eff}} = \lambda\left(\langle\hat{x}\rangle_{\max} - \langle\hat{x}\rangle_{\min}\right)$ of the effective spin splitting is dependent on the system parameters in the following way. The effective Hamiltonian of the oscillator $\hat{H}_o^{\text{eff}} = [\hat{H}_o + \lambda(1-2c)\hat{x}]$ [Eq. (3.32)] may be rewritten in the form

$$\hat{H}_o^{\text{eff}} = \frac{1}{2}\omega_o\left(\hat{\tilde{X}}^2 + \hat{\tilde{P}}^2\right) + \text{const.} \tag{3.33}$$

with the dimensionless position and momentum operators

$$\hat{\tilde{X}} = \hat{X} + \sqrt{\frac{\lambda^2}{m\omega_o}}(1-2c) \tag{3.34}$$

$$\hat{\tilde{P}} = \hat{P}, \tag{3.35}$$

where $\hat{X} = \sqrt{m\omega_o}\hat{x}$, $\hat{P} = \hat{p}/\sqrt{m\omega_o}$. Making use of the properties of the displacement operator $\hat{D}(\alpha)$ [Eqs. (3.12, 3.13)], one finds that

$$\hat{H}_o^{\text{eff}} = \hat{D}(-\gamma)\hat{H}_o\hat{D}(\gamma) \tag{3.36}$$

with

$$\gamma = \sqrt{\frac{\lambda^2}{2m\omega_o^3}}(1-2c) = \sqrt{\frac{\xi}{2}}(1-2c). \tag{3.37}$$

In order to compute the peak-to-peak amplitude of the effective spin splitting

$$\Delta\omega_s^{\text{eff}} = \lambda\left(\langle\hat{x}\rangle_{\max} - \langle\hat{x}\rangle_{\min}\right) \tag{3.38}$$

we need to evaluate

$$\begin{aligned}\langle\hat{x}\rangle(t) &= \langle\alpha(t)|\,\hat{x}\,|\alpha(t)\rangle &(3.39)\\ &= \langle\alpha|\exp(i\hat{H}_o^{\text{eff}}t)\hat{x}\exp(-i\hat{H}_o^{\text{eff}}t)\,|\alpha\rangle\\ &= \langle\alpha|\,\hat{D}(-\gamma)\exp(i\hat{H}_o t)\hat{D}(\gamma)\hat{x}\hat{D}(-\gamma)\exp(-i\hat{H}_o t)\hat{D}(\gamma)\,|\alpha\rangle\\ &= \langle\alpha+\gamma|\exp(i\hat{H}_o t)\hat{x}\exp(-i\hat{H}_o t)\,|\alpha+\gamma\rangle + \tilde{\gamma}, &(3.40)\end{aligned}$$

where we have used Eqs. (3.12, 3.16, 3.36) assuming $\alpha \in \mathbb{R}$ and defining $\tilde{\gamma} = \sqrt{2/(m\omega_o)}\gamma$. Now, we can see that the first term is just the time evolution of the expectation value of the position of the original oscillator described by $\hat{H}_o$ for a coherent initial state $|\alpha+\gamma\rangle$. With the help of Eq. (3.17) it is straightforward to show that $\langle\hat{X}\rangle_{\max} - \langle\hat{X}\rangle_{\min} = 2\sqrt{2}|\alpha+\gamma|$ and therefore

$$\Delta\omega_s^{\text{eff}} = 2\lambda\sqrt{\frac{2}{m\omega_o}}|\alpha+\gamma|. \tag{3.41}$$

Note that this result is only exact if the Hamiltonian governing the oscillator's dynamics is $\hat{H}_o^{\text{eff}}$ and $\mathcal{L}_o^{\text{eff}}[\hat{\rho}(t)] = 0$, that is if the FA is exact. Still, if the FA holds in good approximation, Eq. (3.41) is a good approximation as well.

For the first limit proposed in Eq. (3.23) in which the FA becomes exact, we therefore find that both $\gamma \to 0$ and $\Delta\omega_s^{\text{eff}} \to 0$, if all parameters besides $m$ are kept constant. Thus, the work effect induced by the oscillator diminishes more and more for increasingly better fulfilled FA. This can be avoided, though, by additionally imposing $\alpha \to \infty$, such that $|\alpha|^2/m$ remains constant, which then defines the splitting's amplitude. This is a classical limit in that the mass and average excitation number of the oscillator go to infinity.

There is also a true quantum limit, though, which is found to be realized exploiting the second limit given in Eq. (3.24). Here, by letting $\omega_o \to \infty$, we

enforce that $\xi \to 0$ so that the factorization approximation becomes exact. However, by requiring $\lambda^2/\omega_o = \text{const.}$, the prefactor of $\Delta\omega_s^{\text{eff}}$ in Eq. (3.41), $2\sqrt{2\lambda^2/(m\omega_o)}$, becomes constant. Thus, although $\gamma \to 0$, $\Delta\omega_s^{\text{eff}}$ retains a finite value

$$\Delta\omega_s^{\text{eff}} \to 2\lambda\sqrt{\frac{2}{m\omega_o}}|\alpha| = \text{const.} \tag{3.42}$$

for arbitrary (small but finite) $m$ and $\alpha$ in the limit of exact FA.

By the preceding reasoning, we conclude that the oscillator is, indeed, a work reservoir for the spin, periodically changing the spin splitting and therefore transferring work to/from it. What is special about that finding is the fact that a true quantum system (the oscillator in the quantum limit of the $z$-SOM) can be set up as an ideal work source and, thus, the work concept is not tied to classical devices. Moreover, as long as we fulfill Eq. (3.22) the oscillator behaves as a work reservoir for any time-period.

## 3.3 Imperfect work source

In this section, we present and discuss our results for the work reservoir behavior in the more general $xz$-SOM presented in Sec. 3.1.2 with focus on the suitability of the work source quality measures proposed in Sec. 2.5.

The numerical results used herein have been produced with the *Mathematica* package using the following techniques: We have computed the time evolution of the system by direct diagonalization of the Hamilton operator (with a cut-off chosen such that only states with occupation probability higher than $10^{-6}$ are included). Integration of quantities – where necessary – has been performed using the rectangle rule and the error of integration has been controlled by crosschecking with results for the trapezoidal rule and/or for smaller time steps.

### 3.3.1 Purity based approach

We first need to define a lower bound for the purity of the oscillator. The $\hat{\sigma}_z$ coupling alone already leading to some limited purity loss in the oscillator can be considered as sort of a "natural" purity drop, which has to be accepted for any system that interacts at all and that is present even if the FA is good and the work source quality high.

The work source functionality is considered to fail when the purity decrease of the RWA dynamics (caused by the $\hat{\sigma}_x$ interaction term) reaches the maximum purity drop $P_o^{\min}$ of the $\hat{\sigma}_z$ dynamics alone found for the given system

parameters $(\lambda, \omega_s, \omega_o, m)$. This allows us to define a breakdown time $t^*$ by $P[\hat{\rho}_o(t^*)] = P_o^{\min}$.

The close connection of the $xz$-SOM dynamics to the JCM dynamics seems to suggest an analytical approach based on the standard approximations made to solve the JCM (see, e.g., Basdevant and Dalibard [2000], Ch. 6): approximation of the occupation probability of the coherent state with a Gaussian and linearization of the spectrum of the JCM around its peak. With those approximations a fairly accurate description of the JCM's typical collapse and revival behavior of the spin polarization for high initial photon numbers ($|\alpha| \gg 1$) is possible. After the initial collapse of polarization, the spin reaches its minimum purity (Shore and Knight [1993]) and the oscillator purity will as well have dropped significantly.

Unfortunately, even in the high photon number limit the accuracy of this analytical approach in the relevant time interval up to this point of the evolution is insufficient: Typical values of the purity drop due to the $\hat{\sigma}_z$ interaction are of the order of $10^{-2}$, while the error of the mentioned approximations is of around the same order during the collapse. This renders the application of those approximations futile and since a full analytical analysis is much too involved, we will only exemplify some results based on numerics.

To this end, we choose the following parameters for the $xz$-SOM: $\omega_o = \omega_s = 1$ (resonant case), $m = 1$, $\lambda = \kappa = 0.1$. In the following, we consider the results of two special cases:

(a) $\alpha = 0$, $c = 0.5$

(b) $\alpha = 2$, $c = 1$

These two examples are drawn from a set of results for initial states with parameters $\alpha \in [0, 4]$ and $c \in [0.5, 1.0]$ and have been chosen for they represent in some sense extremal cases, that will be seen to nicely illustrate the features of the different work source quality measures. A short overview about the more general behavior of the $xz$-SOM is given in Sec. 3.3.3.

The purity behavior of the examples is shown in Fig. 3.5. The time after which the FA is estimated to fail is roughly $t^*_{(a)} \approx 28$ and $t^*_{(b)} \approx 73$. Although this means that the second case is expected to exhibit work reservoir functionality about three times longer than the first case, one would conclude from the curves that for both cases, the oscillator's work source functionality degrades quickly after the initial high purity phase and is virtually absent at least for $t > 100$.

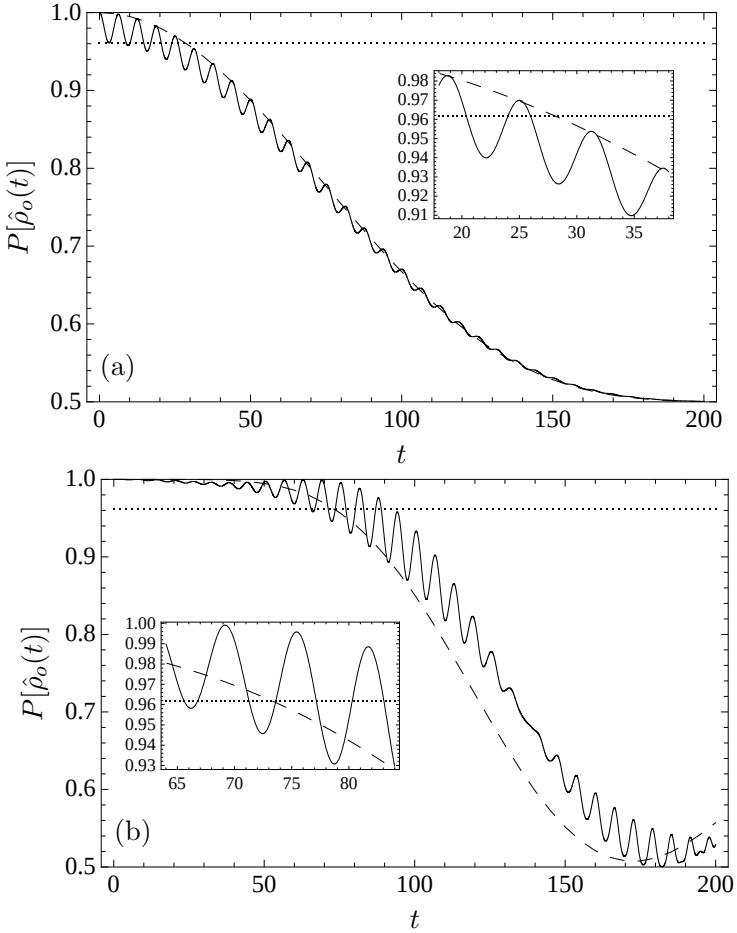


**Figure 3.5:** Oscillator purity behavior of two special cases [(a) $\alpha = 0$, $c = 0.5$ and (b) $\alpha = 2$, $c = 1$] of $xz$-SOM and comparison with minimum purity of $z$-SOM for the given system parameters: Numerical exact result (solid line), numerical result with RWA (dashed), minimum $z$-SOM purity (dotted), which – according to Eq. (3.20) – is $[1+\exp(-2/25)]/2 \approx 0.962$. The insets show the crossings of RWA-purity with minimum $z$-SOM purity.

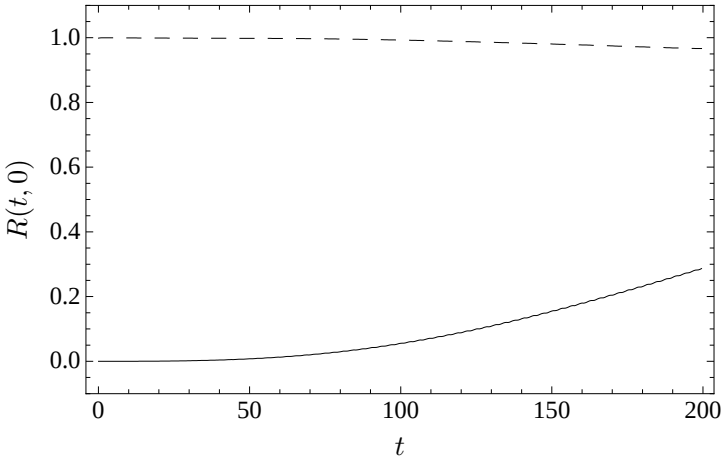


**Figure 3.6:** Integral work reservoir quality measure $R(t,0)$ as defined in Eq. (2.60) for the examples as of Fig. 3.5: (a) $\alpha = 0, c = 0.5$ (solid line), (b) $\alpha = 2, c = 1$ (dashed)

### 3.3.2 Work/heat based approach

Taking now a look at the result for the integral quality measure $R$ shown in Fig. 3.6 one comes to a completely different conclusion: In case (a) the oscillator starts as a perfect heat source rather than a perfect work source and only in the course of time a work source effect arises, whereas in case (b) the oscillator is recognized as a nearly ideal work source during the whole interval. It is astonishing to see that the purity based measure gives such a different picture since the reasoning based on the FA is still valid: During the initial phase, $\mathcal{L}_s^{\text{eff}}$ is close to 0.

The reason for this seemingly contradictory characterization becomes evident when examining the results for the integrated work and heat, $W(t)$ and $Q(t)$ (see Fig. 3.7). In both presented cases, the total heat flow in the beginning of the dynamics is small as expected from the FA argument. Also, the heat becomes significant not before $t^*_{(a)}$ and $t^*_{(b)}$, respectively, which again demonstrates the strong connection between heat and purity.

However, the work exhibits a completely different behavior for the two cases: In the first case, the work remains almost constant at zero until oscillations set in at around $t \approx 100$ [see the inset of Fig. 3.7(a)]. Those oscillations lead to the slow increase in work source quality in the second half of the considered time interval. Although the oscillations have only small amplitude, their work

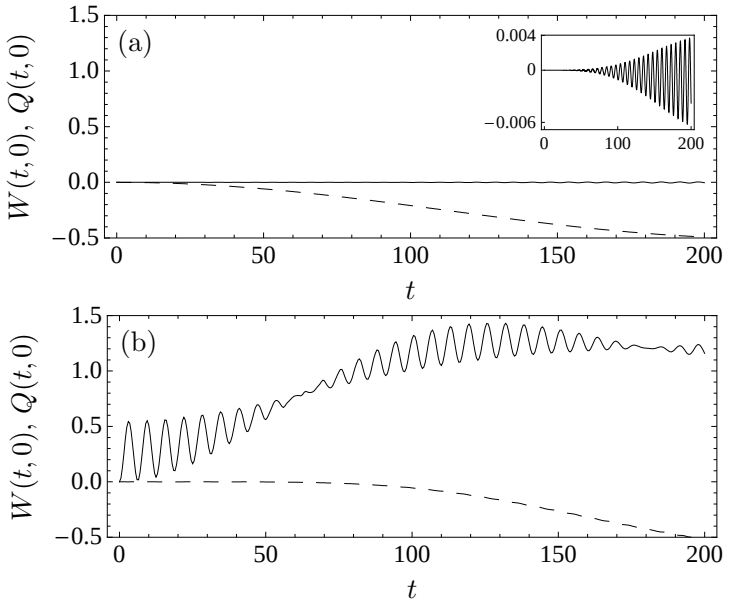


**Figure 3.7:** Integrated work $W(t,0)$ (solid line) and heat $Q(t,0)$ (dashed) for the two chosen examples as of Fig. 3.6. The inset of case (a) shows $W(t,0)$ alone.

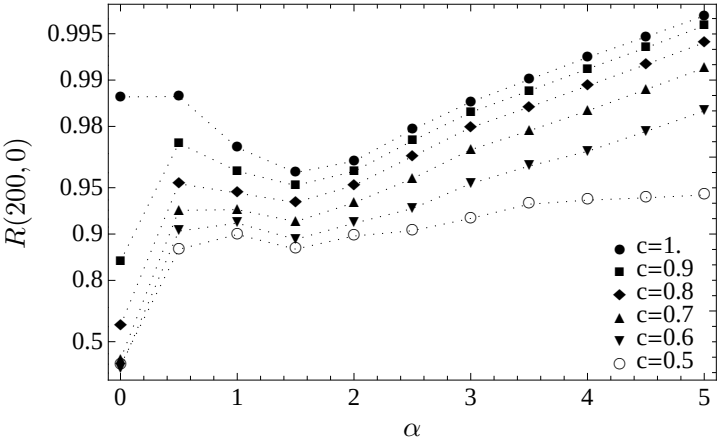


**Figure 3.8:** Log-scale plot of the overall work source quality $R$ for the time interval $[0, 200]$. The behavior of $R(200, 0)$ is shown depending on the initial state determined by the parameters $\alpha$ and $c$. $R$ is defined in Eq. (2.60), $\alpha$ and $c$ in Eq. (3.5).

source effect becomes significant due to their frequency, which is high when compared to the time scale of heat dynamics.

In case (b), $W(t, 0)$ shows strong oscillations of an amplitude orders of magnitude larger than in case (a) from the very beginning of the dynamics. Thus, the reason for the contradiction to the purity measure result can be traced back to the problem already touched on in Sec. 2.5.1: Although the purity can be used as a measure for the size of the incoherent part of the effective dynamics of the spin, $\mathcal{L}_s^{\text{eff}}$, which is associated with the heat flow, it is completely insensitive to the size and effects of the coherent part $\hat{H}_s^{\text{eff}}$ and thus the actual work source effect!

From this result, we can draw the conclusion that due to the fact that the purity measure is linked to $\mathcal{L}_s^{\text{eff}}$ alone, it can only be used as an indicator for the absence of a significant heat flux. In order to get the full picture, a more detailed analysis of the work and heat fluxes via the measure $R$ is mandatory.

### 3.3.3 Work source quality as function of $c$ and $\alpha$

Computing $R$ as defined in Eq. (2.60) for a low photon number parameter window ($\alpha \in [0, 4]$) and initial spin temperatures ranging from 0 to $\infty$ ($c \in [0.5, 1]$), we find the following trends (cf. Fig. 3.8):

For $\alpha = 0$, the overall work source quality of the considered interval $t \in [0, 200]$ is generally significantly lower than for the corresponding (with respect to $c$) cases for $\alpha > 0$, and $R(200, 0)$ ranges from roughly 0.8 to 0.2 with decreasing $c$, except for the particular initial state $c = 1$, $\alpha = 0$. Initial states with $\alpha = 0$ lead to a significant work effect despite their lack of initial excitation of the oscillator. This is easily explained in view of Eq. (3.32): For $c \neq 0.5$, the oscillator is subject to an effective displacement of its potential. Expanded in the set of the eigenstates of this effective Hamiltonian, the initial state $|0\rangle$ is a coherent superposition state again.

For $\alpha > 0$, $R(200, 0)$ takes on values close to or above 0.9, with a slow increase for higher $\alpha$ and $c$. The first increase can be related to the higher excitation of the oscillator and the resulting bigger amplitude of the position expectation. The second trend has to do with a special property of the initial states $|0\rangle|\alpha\rangle$ and $|1\rangle|\alpha\rangle$ of which the initial state of the $xz$-SOM is a statistical mixture.

In order to explain the trend for increasing $c$, we invoke the first order perturbation theory for the extremal initial states $|0\rangle|\alpha\rangle$ and $|1\rangle|\alpha\rangle$ which is applicable to the beginning of the dynamics, as long as $gt^* \ll 1$ holds with $g = 10^{-2}/\sqrt{2}$. It is convenient to apply the perturbation theory in the interaction picture. All interaction picture quantities are denoted by a superscript "$I$". The expansion of the time-evolution of the state is given by

$$|\Psi^I(t)\rangle = |\Psi(0)\rangle + \hat{U}_1^I(t)\,|\Psi(0)\rangle + \mathcal{O}(g^2) \tag{3.43}$$

and the first order contribution to the time-evolution operator $\hat{U}_1^I(t)$ is given by (see, e.g., Messiah [1990], p. 207ff)

$$\hat{U}_1^I(t) = -i \int_0^t \mathrm{d}\tau \hat{V}^I(\tau) \tag{3.44}$$

and

$$\begin{aligned} \hat{V}^I(t) &= \hat{U}_0^\dagger(t)\hat{V}\hat{U}_0(t) \\ &= g \exp[i(\hat{H}_s + \hat{H}_o)t](\hat{\sigma}_+\hat{a} + \hat{\sigma}_-\hat{a}^\dagger) \exp[-i(\hat{H}_s + \hat{H}_o)t] \\ &= g(\hat{\sigma}_+\hat{a} + \hat{\sigma}_-\hat{a}^\dagger) \end{aligned} \tag{3.45}$$

is the interaction operator in the interaction picture. According to the RWA, only terms of the interaction are kept which are time-independent in the interaction picture, thus the last equality. From Eqs. (3.45) and (3.44), it follows that

$$\hat{U}_1^I(t) = -igt(\hat{\sigma}_+\hat{a} + \hat{\sigma}_-\hat{a}^\dagger). \tag{3.46}$$

The time evolution of a state in the JCM is therefore given in first order perturbation by

$$|\Psi^I(t)\rangle = [\hat{1} - igt(\hat{\sigma}_+\hat{a} + \hat{\sigma}_-\hat{a}^\dagger)]\,|\Psi(0)\rangle + \mathcal{O}(g^2). \tag{3.47}$$

Here, we consider $|0\rangle|\alpha\rangle$ and $|1\rangle|\alpha\rangle$ as initial states. Together with

$$\hat{a}^\dagger\,|\alpha\rangle = \left(\frac{\partial}{\partial\alpha^*} + \frac{\alpha*}{2}\right)|\alpha\rangle \tag{3.48}$$

(see, e.g., Vogel and Welsch [2006]) we find for those states

$$\hat{U}^I(t)\,|0\rangle|\alpha\rangle = (|0\rangle - i\alpha gt\,|1\rangle)\,|\alpha\rangle + \mathcal{O}(g^2) \tag{3.49}$$

$$\hat{U}^I(t)\,|1\rangle|\alpha\rangle = \left(|1\rangle - i\frac{\alpha^*}{2}gt\,|0\rangle\right)|\alpha\rangle - igt\,|0\rangle\,\frac{\partial}{\partial\alpha^*}\,|\alpha\rangle + \mathcal{O}(g^2) \tag{3.50}$$

where

$$\frac{\partial}{\partial\alpha^*}\,|\alpha\rangle := \frac{\partial}{\partial\alpha^*}\left[\exp\left(-\frac{|\alpha|^2}{2}\right)\sum_{n=0}^{\infty}\frac{\alpha^n}{\sqrt{n!}}\,|n\rangle\right] \tag{3.51}$$

($\alpha^*$ is the complex conjugate of $\alpha$). From this form of the state $\partial_{\alpha^*}\,|\alpha\rangle$, we easily see that in first order $\hat{U}^I(t)\,|0\rangle|\alpha\rangle$ factorizes contrary to $\hat{U}^I(t)\,|1\rangle|\alpha\rangle$. The purity behavior of the initial state $\rho(0) = [c\,|0\rangle\langle 0| + (1-c)\,|1\rangle\langle 1|] \otimes |\alpha\rangle\langle\alpha|$ continuously changes from the $|0\rangle|\alpha\rangle$ case to the $|1\rangle|\alpha\rangle$ case. As the $|1\rangle|\alpha\rangle$ state becomes more and more mixed into the initial state with decreasing $c$, a significant purity drop happens at earlier times of the evolution. The same is true for the heat flow, which is tied to the purity drop. With this increased heat flow at the early stage of the evolution, $\mathcal{Q}(200, 0)$ reaches higher values for decreasing $c$.

Moreover, the size of work flux for the same change of effective splitting of the spin decreases with decreasing $c$ until it reaches 0 for $c = 0.5$. Thus, in the beginning and as long as the spin's state is close to its initial occupation, the work source effect of the oscillator is reduced or suppressed additionally. Clearly, this reduces the work source quality and explains the trend seen in the numerical results.

## 3.4 Influence of different measurement basis

We finally compare the results for the two extremal cases discussed in Sec. 3.3.2 with results obtained for a different choice of measurement basis, namely

$$\hat{H}_s''(t) := \hat{H}_s + \hat{H}_s^{\text{eff}}(t) \tag{3.52}$$

[cf. Eq. (2.51)]. This basis relates to the complete effective Hamiltonian governing the local dynamics of the spin [cf. Eq. (2.23)] in the $xz$-SOM. In Sec. 2.4.1 we demonstrated that this choice of the measurement basis also leads to a consistent Clausius relation in equilibrium, and in Sec. 2.3 we mentioned, that the choice of $\hat{H}_1''(t)$ instead of $\hat{H}_1'(t)$ could be sensible depending on the physical situation of the measurement setup.

Choosing the measurement basis according to Eq. (3.52), we end up with the following definitions of work and heat:

$$\dot{W}_s(t) = \mathrm{Tr}[\dot{\hat{H}}_s^{\mathrm{eff}}(t)\hat{\rho}_s(t)] \tag{3.53}$$

$$\dot{Q}_s(t) = \mathrm{Tr}\{[\hat{H}_s + \hat{H}_s^{\mathrm{eff}}(t)]\mathcal{L}_s^{\mathrm{eff}}[\hat{\rho}(t)]\}. \tag{3.54}$$

The derivation according to Sec. 2.3 starts with the time derivative of the internal energy defined with use of the new measurement basis Eq. (3.52),

$$\dot{U}_s(t) = \frac{\mathrm{d}}{\mathrm{d}t}\langle \hat{H}_s'(t)\rangle = \mathrm{Tr}\left(\dot{\hat{H}}_s^{\mathrm{eff}}(t)\hat{\rho}_s + \hat{H}_s'(t)\dot{\hat{\rho}}_s(t)\right). \tag{3.55}$$

Plugging in the local dynamics $\dot{\hat{\rho}}_s(t) = -i[\hat{H}_s''(t), \hat{\rho}_s(t)] + \mathcal{L}_s^{\mathrm{eff}}[\hat{\rho}(t)]$ then yields the result above by noticing that the trace over the commutator expression $[\hat{H}_s''(t), \hat{\rho}_s(t)]\hat{H}_s''(t)$ vanishes due to the invariance of the trace under cyclic permutations.

In Fig. 3.9 and Fig. 3.10, the results for the heat and work fluxes for the two definitions and the two examples used throughout the previous section are shown. The results for the fluxes lie right on top of each other with deviations at least two orders of magnitudes smaller than the absolute values. Clearly, the almost perfect agreement of the fluxes is reflected by almost matching results for the integral quality measure $R(t, 0)$ as well, as seen in Fig. 3.11. Again, the deviations are at least about three orders of magnitudes lower than the absolute values of $R(t, 0)$.

We conclude that in the presented cases the choice of the measurement basis is irrelevant to the findings of the previous section and seems to have little effect on the typical results for the discussed model.

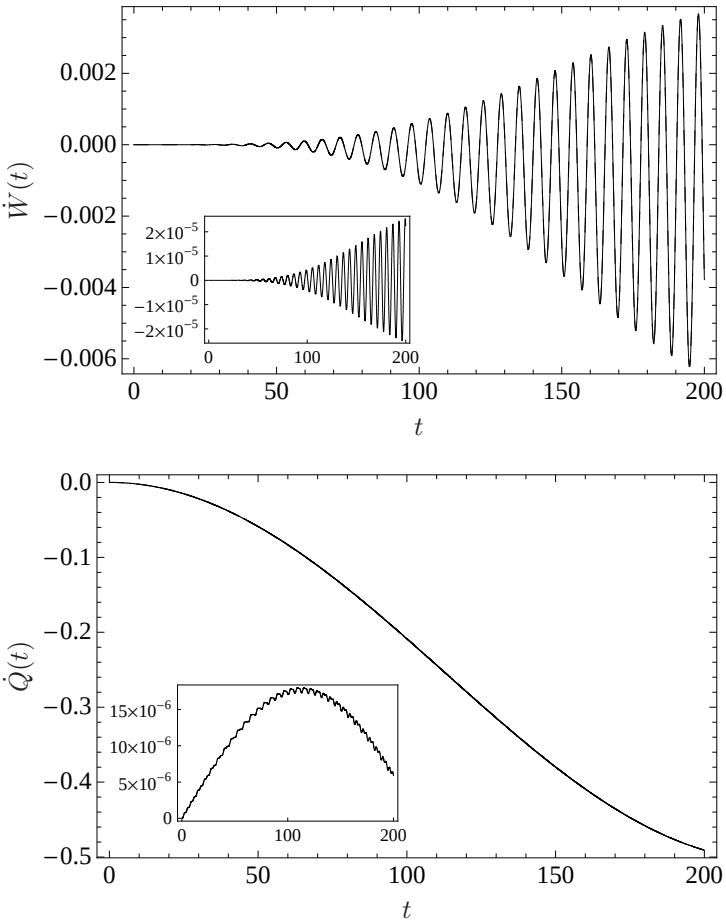


**Figure 3.9:** Heat and work fluxes for $\hat{H}_s'(t)$ (solid, definition from Sec. 3.3) and $\hat{H}_s''(t)$ [dashed, definition from Eq. (3.52)] for the case $\alpha = 0$, $c = 0.5$. The insets show the deviations for the two definitions.

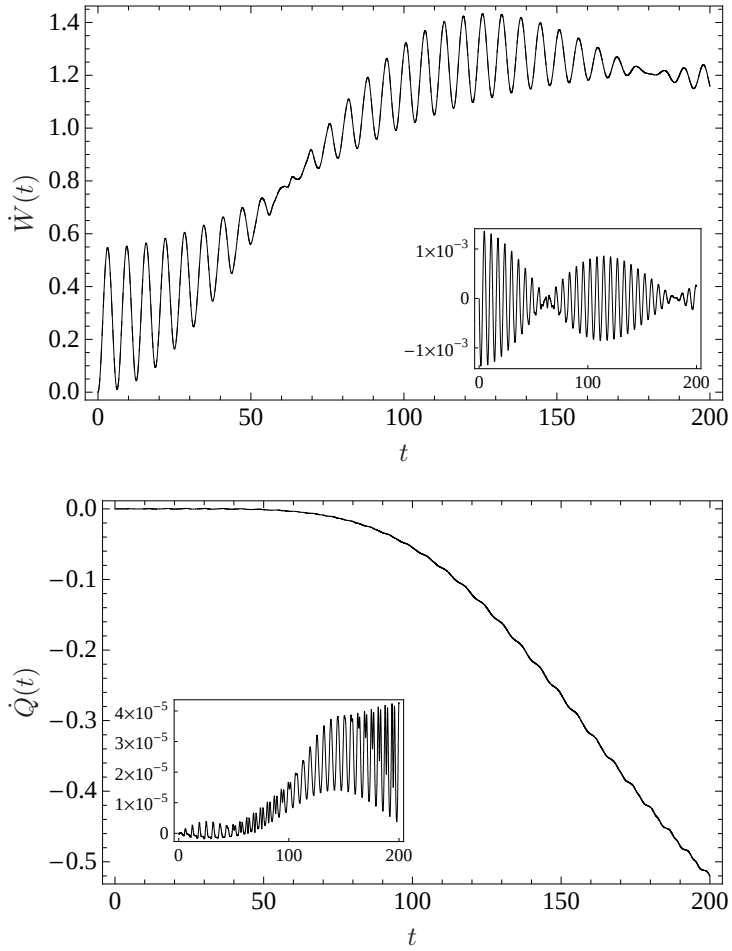


**Figure 3.10:** Heat and work fluxes as of Fig. 3.9 but for $\alpha = 2$, $c = 1.0$. The insets show the deviations for the two definitions.

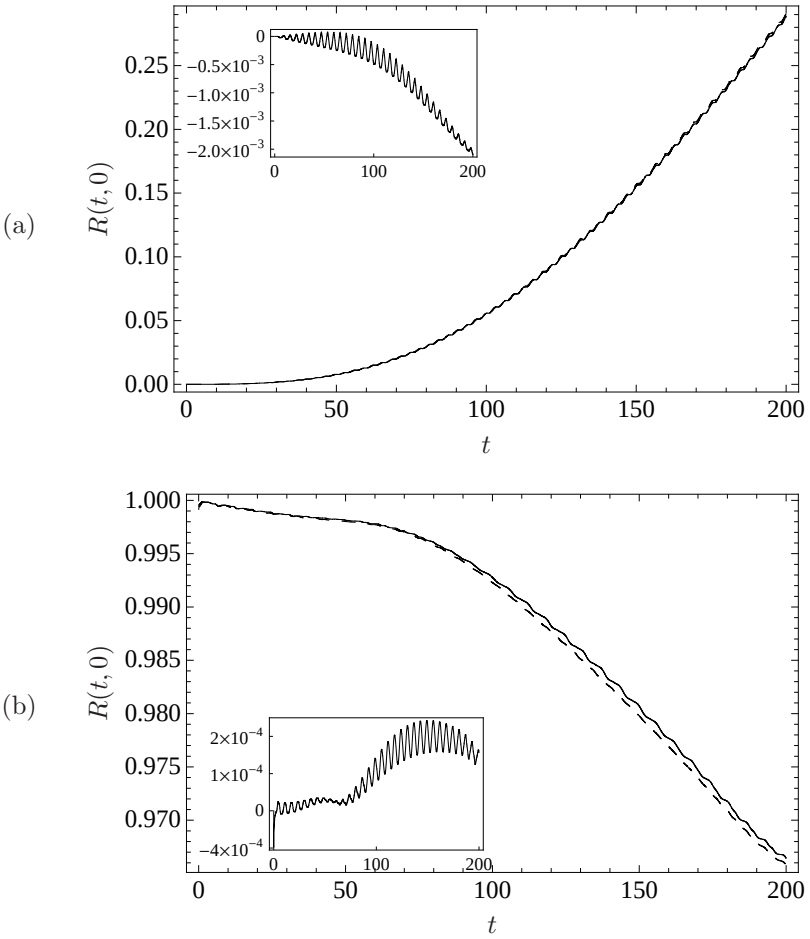


**Figure 3.11:** Integral work reservoir quality measure $R(t,0)$ for $\hat{H}'_s(t)$ (solid, definition from Sec. 3.3) and $\hat{H}''_s(t)$ [dashed, definition from Eq. (3.52)] for the cases (a) $\alpha = 0$, $c = 0.5$ (upper figure) and (b) $\alpha = 2$, $c = 1.0$ (lower figure). The insets show the deviations for the two definitions.

# 4 Interim summary

Work and heat are related to thermodynamic processes, which seem to require external control. In this part, we have argued that work functionality may show up even in closed bipartite quantum systems and down to the nanoscale. We have shown under what general conditions the respective subsystem dynamics may be described by time-dependent effective Hamiltonians (factorization approximation) and in this sense act as classical drivers for each other. We have then brought forward the argument that energy exchanged under such conditions has to be considered work from the viewpoint of thermodynamics.

We then went on to generalize the definitions of thermodynamic heat and work to closed bipartite quantum systems based on the reasoning that local effective classical driving is related to work, whereas the incoherent remainder of the local effective dynamics accounts for the heat. The considerations of how such generalized heat and work would be measured lead us to the definition of LEMBAS. The LEMBAS work and heat definitions are consistent with the 2nd law in form of the Clausius relation for two intuitive choices of the measurement and the application of the LEMBAS definitions to the example model of a two-level system driven by a laser yields the expected result (maximum work transfer at resonance).

In order to be able to assess the overall quality of thermodynamic functionality of arbitrary environments, we have introduced the local and global measures $r(t)$ and $R(t_1, t_0)$ of heat and work source quality and established that these measures have all the qualities necessary to give a precise classification of environments under scrutiny. We have demonstrated that due to the lack of sensitivity to the effects of the local time-dependent effective Hamiltonian a measure based on the purity alone is only an indicator for the absence of a significant heat flux, in general.

To give an example for a quantum work source and to illustrate the properties of the given work source quality measures, we have applied these concepts to the $z$-SOM confirming that a system as small and simple as a single harmonic oscillator coupled to a spin can act as a work reservoir for the latter. Additionally, we examined the more general case of the $xz$-SOM and confirmed that for an exact assessment of heat and work source quality, the measure based on the absolute heat and work fluxes, $R(t_1, t_0)$, has to be pre-

ferred over the purity. To complete our considerations, we determined that the influence of the choice of measurement basis on the results of this chapter is negligible.

Finally, with regard to quantum thermodynamic machines, we note that the implementation of a full thermodynamic process within a closed quantum system will require driving as well as thermalizing embeddings, contrary to the focus on driving environments in this part. A model providing both and thus being able to exhibit machine-like behavior is the topic of the following part.

# Part II

# Cyclic thermodynamic nanomachines

# 5 Overview

Thermodynamics developed as a theory of thermodynamic machines and processes, and it is therefore not surprising that the description of such machines and processes is at the core of thermodynamics. The description encompasses the heat and work exchanged during the steps of a process as well as the overall achievable efficiencies. The most fundamental thermodynamic process is by far the Carnot process by virtue of its direct connection to the second law of thermodynamics and thus to the concept of irreversibility.

The level of description provided by thermodynamics is phenomenological and in the limit of infinite systems, quasistatic (i.e., infinitely slow) processes and infinitely small interactions strength between systems and the reservoirs they are coupled to. Every part of the model is thought to be in equilibrium. All those idealizations have made it possible to derive rather simple laws for the considered processes, which – despite their simplicity – are fundamental as they provide upper bounds for the efficiency of any thermodynamic process by the well-known Clausius inequality

$$\mathrm{d}S \geq \frac{đQ_{\mathrm{rev}}}{T} \tag{5.1}$$

and, moreover, determine which process can be performed in reality and which not.

Typically, thermodynamic processes consist of several steps during which they are coupled either to a heat bath (e.g. isotherm) or a work source (adiabate) or both (e.g. isochore). It is to note here that these processes represent the full set of possible controls that an experimenter has over a thermodynamic system: parametric control of the Hamiltonian via work sources and thermal control over the state via heat baths.

Quantum thermodynamic processes differ in a number of points from their classical counterparts and by including more and more elements of a thermodynamic machine into the quantum modeling, the differences increase. However, one moves away from the thermodynamic setting by doing so. Increasing the explicitly modeled part, however, will also increase the appropriateness of the discussed models, and is necessary in order to be able to discuss thermodynamics in the regime of finite strength interactions, finite (quantum) systems and/or non-equilibrium.

## 5.1 Peculiarities of quantum thermodynamic processes

### 5.1.1 Single and finite systems

Classical statistical mechanics always deals with the statistical properties of ensembles of systems by the identification of the time average of a single system with the ensemble average via the quasiergodic hypothesis (Gibbs [1960]). It is the thermodynamic limit of infinitely large numbers or times that makes it possible to exactly derive the laws of thermodynamics, and it is therefore expected that those laws only hold with good accuracy for large enough systems.

In contrast to the situation in classical statistical mechanics, in quantum thermodynamics we can speak of a single system being in a thermal state not only in the sense of a time average and ergodic behavior, but for any instant in time, indeed. This is possible because the density matrix $\hat{\rho}$ of a system can not only be understood as an ensemble of quantum systems each in a well-defined but statistically distributed pure state. In this case, the density matrix description is necessary due to a subjective lack of knowledge.

In the case of entanglement, however, the local state of a subsystem is indefinite and the reduced density matrix becomes the state of that single system by an objective lack of knowledge in the same way $|\Psi\rangle$ is understood to be a pure state of a single system: Even the universe does not yet "know" what state the subsystem is in. Note that this distinction is not fictitious: Although the statistical mixture and the entangled subsystem behave exactly the same with respect to local measurements since we always need to measure an ensemble of quantum systems, it is possible to distinguish the two cases by measurement. Namely, if we were able to measure the total state of the subsystem and the environment it is entangled with, we would find that the total state would be pure and, indeed, the local states would not yet be determined. On the contrary, in the case of a true statistical mixture, the total system would behave as a statistical mixture as well.

Taking the results of quantum thermodynamics into account, we find the following: Quantum thermodynamics predicts the canonical density matrix as the state of quantum systems embedded in fairly typical environments (weak coupling, limit of infinitely large environment, energy exchanging interaction) if the total system is in a pure state (see Sec. 1.2). In this case, the density matrix description of the embedded system is a direct consequence of the entanglement with its environment. Thus, in the sense elaborated above, the single system subject to a thermodynamic embedding is truly in a thermal

state.

If we are able to assign a thermal state even to some small part of a system, we can for example think of a single spin or some other simple and single system as the work medium of a quantum thermodynamic machine. This is indeed what has been considered by a number of authors in Scully [2002], Kieu [2004], Tonner and Mahler [2005], Janzing [2006], Henrich et al. [2007a], Allahverdyan et al. [2008] (for a comprehensive survey of thermodynamic processes realizable this way and their properties, see Quan et al. [2007], Quan [2009]). In all of these cases, although we have been talking about single systems, we still imagined them being subject to an embedding that would lead in good approximation to a thermal state in the system at all instants of the process. So far, nothing really new happens since due to the statistical nature of quantum measurements – in the end – this single system just maps the well known canonical ensemble. However, with single systems comes finiteness of systems. Finiteness can come into play in different forms: a finite number of particles, a finite interaction strength, a finite reservoir. In the case of finite interaction strength, even a system in contact with an otherwise ideal embedding no longer behaves as expected from standard thermodynamics.

A good example for this is given by the equilibrium properties of a damped quantum harmonic oscillator coupled to an infinite heat bath with finite interaction strength (Hänggi and Ingold [2005]). Namely, the equilibrium state of the oscillator no longer is the thermodynamically expected canonical state for temperatures $T \approx \omega$, where $\omega$ is the oscillator angular frequency. This implies that for a zero temperature bath, in particular, the oscillator's equilibrium state is not the ground state but instead a slightly excited mixed state. This has two important consequences: First, the definition of the correct thermodynamical free energy is no longer obvious at all (cf. Hänggi et al. [2008]) and second, one could conceive that it was possible to extract work from a zero temperature bath by the use of the excitation generated in equilibrium when the system has first been in its ground state and then been brought in contact with the zero temperature bath. However, Kim and Mahler [2006] have demonstrated that for all physical reasonable spectral densities of baths, the excess energy of the equilibrium state is less than the work needed to establish the coupling between bath and oscillator to begin with. Thus, the second law is not violated.

Another aspect of finiteness encountered in more and more quantum models are finite and autonomous reservoirs and reservoirs that no longer are ideal. In the previous part, we discussed such finite and autonomous reservoirs in detail with a focus on the work effect, and we demonstrated that such reservoirs can still be characterized by their thermodynamic functionality within the LEMBAS approach. We put forth the argument that from the view of quan-

tum thermodynamics, not the thermodynamic properties of the environment are essential (embeddings that itself are not thermodynamical may still lead to thermodynamics in systems they affect), but what thermodynamic effects emerge in a system due to the presence of its environment is important.

Taken to the extreme, this means that for any closed model and any partitioning of this model into system and environment, the effective local dynamics of the system [cf. Sec. 2.3, Eq. (2.23)] may be considered a (usually nonequilibrium) quantum thermodynamic process emergent from the partitioning and the dynamics of the total system. This emergent process is understood in terms of heat, work, internal energy and entropy due to the fact that these quantities can be defined for any step of such a process. This is a rather pragmatic point of view, though, which puts aside the fact that the underlying processes have little in common with what an engineer encounters in his field.

What they have in common, though, is that almost any real process encountered in engineering is so far from the ideal world of equilibrium thermodynamics that it definitely comes as a surprise that they are still assessable in terms of thermodynamic notions as work, heat, internal energy, efficiency, and so on, and that this assessment nevertheless gives useful information about such a process. We take this as a hint that a sufficient set of thermodynamic concepts may survive the transition from equilibrium thermodynamics to real and emergent processes despite the finiteness of systems and interactions and the possibly strong nonequilibrium character of the processes, and appear as traces or fingerprints of standard thermodynamics in the form of generalized concepts in quite general situations like, e.g., the LEMBAS definition of work and heat. However, whether these generalized concepts are universal, robust, useful and unique is yet to be explored in detail.

### 5.1.2 Discrete and finite state spaces

Most quantum systems of interest for our purpose come with a discrete spectrum. Moreover, systems with a Hilbert space consisting of only two or a few levels are especially important not only due to their simplicity of description, but also because of their simplicity of control and their prevalence in quantum information theory. It makes them perfect candidates for inclusion in models as there is quite a number of possible realizations from the field of quantum computation, which again makes it probable that the models can be tested. Examples for successful realizations of few-level quantum systems that are controllable to a high degree are ions in optical traps (Leibfried et al. [2003]), Rydberg atoms (Saffman et al. [2010]), quantum circuit QED (Blais et al. [2007], DiCarlo et al. [2009]), and the NV-center in diamond (Neumann et al. [2008], Neumann et al. [2010]).

Along with finite Hilbert spaces comes the capability of controlling the properties of small groups of states and single states, in particular the eigenenergies of those states. With a simple example, we will show here that this enhanced control of quantum systems can lead to a quite paradoxical effect, when dealing with quasistatic processes.

Let us first consider a common example from statistical mechanics to illustrate the problem: the canonical ensemble of distinguishable non-interacting particles in a one-dimensional box (along the lines of Baus and Tejero [2008], Ch. 5). The partition sum of this system is simply the product of all the single particle partition sums:

$$Z(\beta, L, N) = [Z(\beta, L, 1)]^N \tag{5.2}$$

and the single particle partition sum is given by

$$Z(\beta, L, 1) = \sum_n \exp[-\beta \epsilon_n(L)], \tag{5.3}$$

where $\beta$ is the inverse temperature, $L$ the length of the box and $\epsilon_n(L)$ the energy of the $n$th eigenstate (microstate) of the system. The dependence of the eigenenergies $\epsilon_n(L)$ on the length of the box is

$$\epsilon_n(L) = \frac{n^2 \hbar^2 \pi^2}{2mL^2} \tag{5.4}$$

with the particle mass $m$, and the occupation numbers of the microstates are readily found to be

$$p_n(L) = \frac{\exp[-\beta \epsilon_n(L)]}{Z(\beta, L, 1)}. \tag{5.5}$$

One can perform work on the system by changing the length of the box. If this is done quasistatically and adiabatically, the occupation numbers are preserved. As a function of the new length $L'$ they can be expressed as

$$p'_n(L') = \frac{\exp[-\beta' \epsilon_n(L')]}{Z(\beta', L', 1)} \tag{5.6}$$

with the help of the new temperature $\beta' = \beta L'^2/L^2$ because of

$$\begin{aligned} &\exp\left(-\frac{n^2\hbar^2\pi^2}{2m}\frac{\beta}{L^2}\right) \\ &= \exp\left(-\frac{n^2\hbar^2\pi^2}{2m}\frac{\beta L'^2}{L^2}\frac{1}{L'^2}\right) \\ &= \exp\left(-\frac{n^2\hbar^2\pi^2}{2m}\frac{\beta'}{L'^2}\right). \end{aligned} \tag{5.7}$$

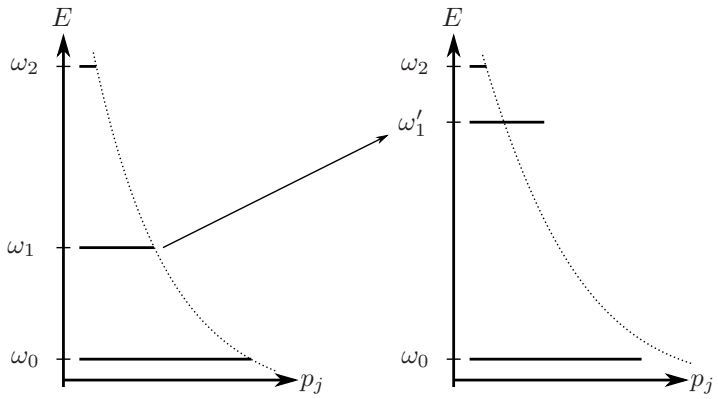


**Figure 5.1:** Process with a three-level quantum model. The system is in thermal equilibrium at the beginning (left-hand side), the lengths of the levels indicate the occupation numbers $p_j$ and coincide with the equilibrium distribution (dotted). After performing an infinitely slow process during which only one of the states changes its energy and all occupation numbers are conserved, the distribution is no longer thermal (right-hand side).

Thus, the new state is just a canonical state again, although with changed inverse temperature $\beta'$ as expected for a quasistatical process.

Let us now turn to the quantum model of Fig. 5.1, that is characterized by a finite Hilbert space of dimension 3 (for sake of simplicity) and by the ability to control the eigenenergy of one of the three states by an external parameter (for sake of the argument). The Hamiltonian of the system is

$$\hat{H}(\omega_1) = \sum_{j=0}^{2} \omega_j \, |j\rangle\langle j| \,, \tag{5.8}$$

and by making $\omega_1$ an argument of the Hamiltonian we have indicated that it is subject to external parametric control. In this model, $\omega_1$ takes a similar role as the length $L$ of the previous model, although on a more fine-grained level.

We consider now a process, where the system initially is in a thermal state with the occupation numbers $p_j = \exp(-\beta\omega_j)/Z(\beta;\omega_j)$. The process itself is thought to be an infinitely slow variation of the parameter $\omega_1$ to a new value $\omega_1'$ without coupling to a bath whatsoever. By the quantum adiabatic theorem (Ehrenfest [1916], Born and Fock [1928]) we know, that the final state

of the system is identical to the initial state, $\hat{\rho}_\mathrm{f} = \hat{\rho}_\mathrm{i}$. The state is no longer thermal, however, since the energy of $|1\rangle$ has changed, and so has $Z(\beta;\omega_1)$. Thus, although the process has been performed infinitely slow and without contact to a heat bath, the process is not quasistatic: The system is not in equilibrium all the time. This is a peculiarity of quantum thermodynamic systems resulting from the detailed control that can be exerted over quantum systems, and the effect is always to be taken into account when there is control over the spectrum that is nonuniform.

Another specialty of quantum systems with finite state space is the existence of negative absolute temperature states, i.e. inversion of the occupation numbers with a canonical distribution,

$$\hat{\rho}^\mathrm{can} = \frac{1}{Z(\beta)} \exp(-\beta \hat{H}) \tag{5.9}$$

with inverse temperature $\beta < 0$. In works from Ramsey [1956] and Landsberg [1977], the thermodynamic implications of negative absolute temperatures are discussed. The most important result is that negative temperature baths can release heat while decreasing the overall entropy. This requires a reformulation of the Kelvin-Planck form of the 2nd law such that for negative temperature reservoirs, there is no longer an upper limit on the work that can be performed with the heat extracted from the bath, but a lower limit that has to be performed at minimum. We will see that this feature becomes relevant for the ED JCM discussed in the following part and defer a more detailed discussion of the consequences of negative absolute temperatures to Sec. 9.4.2.

### 5.1.3 Role of quantum coherence

Another aspect of quantum systems that may happen to be of importance for quantum thermodynamical processes is the role of quantum coherence, a concept completely absent from classical physics. All classical ensembles correspond to quantum states that are diagonal in the energy eigenbasis. However, a quantum system starting in such a diagonal state subject to some unitary dynamics can develop off-diagonal terms in the density matrix. These coherences are connected to thermodynamic considerations via the von Neumann entropy $S = -\mathrm{Tr}(\hat{\rho}\log\hat{\rho})$, which plays an important role in the derivation of quantum thermodynamics (cf. Sec. 1.2, Gemmer et al. [2004]). Also, in the LEMBAS approach they become relevant for the work flux $\dot{W}(t)$ due to the term depending on $\hat{H}^\mathrm{eff}_{1,b}(t)$ [cf. Eq. (2.31)].

The existence of quantum coherence allows for processes unconceivable in the realm of statistical physics. As an example we consider a quantum system subject to an environment that only destroys coherences without changing

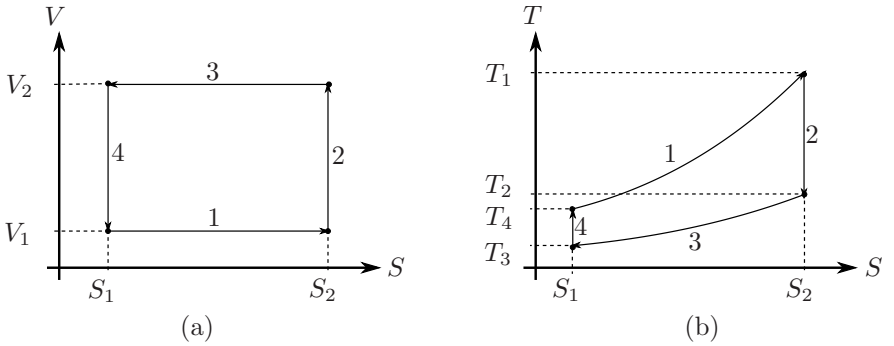


**Figure 5.2:** Classical Otto engine in the (a) $S$-$V$ plane and (b) $S$-$T$ plane. The process consists of two isochores (1,3) and adiabates (2,4).

the statistics of the energy eigenstate occupations (pure decoherence, Alicki [2004]). In this case, the von Neumann entropy of the system changes without a change in energy or statistics of the occupation numbers. Another example is the quantum afterburner proposed by Scully [2002] that makes use of coherence to improve the efficiency of a quantum heat engine beyond the classically achievable one. No violation of the 2nd law is to be expected from that for two reasons: First, the process considered is an Otto process with efficiency well below the Carnot efficiency, and second, the work needed to generate the coherence is probably higher than the excess energy achieved by the use of the coherences.

## 5.2 Quantum thermodynamic Otto process

The Otto process, although in standard thermodynamics not nearly as fundamental as the Carnot process, is often encountered in quantum thermodynamic processes. This is also true for this and the following part where the Otto process is a central theme, and we thus review here the classical Otto process and an example of its quantum counterpart.

The classical Otto process consists of four parts, here shortly given for an ideal gas with internal energy

$$\mathrm{d}U = T\mathrm{d}S - p\mathrm{d}V, \tag{5.10}$$

where $V$ is the volume and $p$ the pressure. We consider the system in the heat engine case:

**step 1 – isochore:** $V = V_1 = \text{const.}$, heat is reversibly consumed from heat baths of increasing temperatures until $T = T_1$ is reached.

**step 2 – adiabate:** $V$ increases from $V_1$ to $V_2$, and work is released. The temperature of the system decreases from $T_1$ to $T_2$.

**step 3 – isochore:** $V = V_2 = \text{const.}$, reversible heat exchange with heat baths until $T = T_3$.

**step 4 – adiabate:** $V$ is changed back to $V_1$, while work is consumed. The temperature changes from $T_3$ to $T_4$.

If the process is performed in the opposite sense, the overall effect is transport of heat from the cold to the hot bath at the expense of work, which is the Otto heat pump case. The efficiency of the engine

$$\eta_{\text{Otto}} = 1 - \left(\frac{V_1}{V_2}\right)^{\gamma-1} \tag{5.11}$$

is independent of the temperature. Here, $\gamma$ is the polytropic exponent $\gamma = c_p/c_V$ with the specific heat capacities at constant pressure ($c_p$) and constant volume ($c_V$).

We address now the quantum Otto process with a single spin as the working medium. The spin splitting $\omega$ takes the place of the work variable $V$ and may be controlled by a variable external magnetic field. Whenever the spin is diagonal in the energy eigenbasis,

$$\hat{\rho} = p_0 \left|0\right\rangle\!\left\langle 0\right| + (1-p_0)\left|1\right\rangle\!\left\langle 1\right| = \begin{pmatrix} p_0 & 0 \\ 0 & 1-p_0 \end{pmatrix}, \tag{5.12}$$

we can associate a temperature

$$\beta(p_0) = -\omega^{-1} \ln\left(\frac{1}{p_0} - 1\right), \quad T(p_0) = -\omega \left[k_B \ln\left(\frac{1}{p_0} - 1\right)\right]^{-1} \tag{5.13}$$

with the state. After the isochoric steps with $\omega = \text{const}$, the spin has the ground state occupation numbers $p_0(\omega_1, T_1)$ and $p_0(\omega_3, T_3)$, respectively, with

$$p_0(\omega, T) = \frac{1}{1 + \exp(-\frac{\omega}{T})}. \tag{5.14}$$

During the isochoric step, we must imagine the spin to be successively coupled to an infinite number of baths with continuous temperature from $T_4$ to $T_1$, and $T_2$ to $T_3$, respectively, in order to render the step quasistatic. If coupled

directly to heat baths with the terminal temperatures, the process would look the same from the spin's point of view, though.

Finally, the quantum Otto process efficiency of the single spin is given by

$$\eta_{\text{Otto}}^{\text{qm}} = 1 - \frac{\omega_1}{\omega_3}. \tag{5.15}$$

This is quite similar to the classical Otto efficiency (5.11) and retains the feature that it depends on the ratio of the values of the mechanical parameter on the two isochore and not on the temperatures of the baths. This similarity comes not as a surprise because the spin is in a diagonal state during the whole cycle and therefore can be considered representing the classical canonical ensemble of a two-level system subject to the Otto process.

The quantum Otto process is particularly simple in terms of control, possible implementation and description. The central element of the process, the spin, is the fundamental building block of quantum information theory and experimental implementations. The spin system itself is very easy to deal with theoretically, but due to the interest in the control and manipulation of qubits in quantum computation, there is also a large number of possible implementations of this process to think of as mentioned in Sec. 5.1.2. Finally, the level of control necessary to implement the quantum Otto process is rather low and limited to being able to change the spin's splitting in some range and to operate the interactions of the spin to two reservoirs. This has lead to a number of publications dealing with spins as quantum heat engines that implement the Otto cycle (Kieu [2004], Kieu [2006], Tonner and Mahler [2005], Janzing [2006], Henrich et al. [2006], Henrich et al. [2007a], Allahverdyan et al. [2008]).

# 6 Models

After the discussion of quantum thermodynamic processes and their properties in general in the previous chapter, we now come to the presentation of two models of quantum thermodynamic machines. The first model (Sec. 6.1) is a fully autonomous model with a quantum work reservoir in the spirit of the first Part of this work. Due to its very general approach to the implementation of the control of the bath couplings it lacks a concrete physical system able to realize this form of control, though. The dynamical three spin machine (D3SM, Sec. 6.2) gives a solution to the problem in terms of bath couplings mediated by filter spins such that due to resonance conditions between the filter spins and the working medium, either one or the other bath is dynamically decoupled from the system. However, the work reservoir in this case is only modeled implicitly by an explicit time-dependent Hamiltonian. We will discuss a model that is the synthesis of those two approaches in the next chapter.

## 6.1 Model of Tonner and Mahler

Tonner and Mahler [2005] presented a quantum system capable of modeling a self-controlled thermodynamic machine. A fairly abstract and general approach allowed them to show that a completely autonomous quantum system can act as a heat engine if the bath couplings are dependent on the state of the system. The model consists of the following parts:

1. a spin as a working medium ("gas"),

2. a harmonic oscillator that acts as work reservoir and control,

3. two heat baths of different temperature.

The core element of the model is exactly the $z$-SOM discussed in Sec. 3.1 although here, the oscillator not only acts as a work reservoir driving the spin's splitting but also as a control for the bath couplings. The time-dependent switching of the bath couplings is necessary in order to implement a thermo-

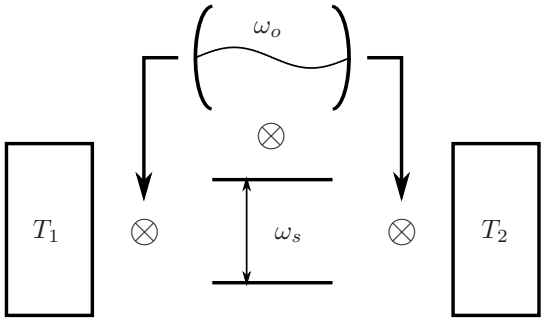


**Figure 6.1:** The model of Tonner and Mahler [2005]: The spin-oscillator system of Sec. 3.1.1 is coupled to two heat baths of different temperatures $T_1$ and $T_2$. The spin acts as the work medium while the oscillator exerts control over interactions of the spin with the baths (arrows) and is the work reservoir of the model at the same time.

dynamic machine. A system constantly coupled to two heat baths of different temperature can only describe transport phenomena[1].

The control of the bath couplings is not explicitly time-dependent, however, as this would clearly violate the constraint of an autonomous system. Instead, the authors introduce special bath-coupling operators that are sensitive to the oscillator state and call them *time-slot operators*. These operators are defined by

$$\hat{\Pi}[f] = \hat{\Pi}[\theta(\tau)\hat{\rho}_o(\tau)] = N_\Pi \int_0^{2\pi/\omega_o} \theta(\tau)\hat{\rho}_o(\tau)\mathrm{d}\tau, \tag{6.1}$$

where $\omega_o$ is the oscillator frequency, $\hat{\rho}_o$ is the oscillator state, $N_\Pi$ is a normalization constant, and $\theta(t)$ is an arbitrary control function. Note that the integration extends over a single period of the oscillator.

In the case of a state with in a part of Fock space uniformly distributed occupation, the matrix elements of $\hat{\Pi}[f]$ in the energy eigenbasis of the oscillator take the form of a Fourier transform

$$\hat{\Pi}_{kl}[f] = \frac{N_\Pi}{n} \int_0^{2\pi/\omega_o} \theta(\tau)\mathrm{e}^{-i\omega_o(k-l)\tau}\mathrm{d}\tau. \tag{6.2}$$

[1] We will see however in the following part that together with selective coupling of baths to a system's transitions, such transport phenomena can exhibit machine-like functionalities, and deserve to be called "pseudomachines".

This explicitly time-independent definition of the time-slot operators leads to an oscillator state dependent interaction strength between the spin and the baths via the Lindblad operators of the form

$$\hat{A}_m = \hat{A}_{\lambda_\pm^{(j)}, f^{(j)}, \pm} = \lambda_\pm^{(j)} \hat{\sigma}_\pm \otimes \Pi^{(j)}[f^{(j)}] \tag{6.3}$$

and the master equation in Lindblad form

$$\dot{\hat{\rho}}(t) = -i[\hat{H}, \hat{\rho}(t)] + \sum_m \left( \hat{A}_m \hat{\rho}(t) \hat{A}_m^\dagger - \frac{1}{2}[\hat{A}_m^\dagger \hat{A}_m, \hat{\rho}(t)]_+ \right). \tag{6.4}$$

The choice of the control functions $\theta(t)$ is motivated by the following procedure. As is seen from Eq. (6.1), the time-slot operators are defined based on some dynamics $\hat{\rho}_o(t)$ of the oscillator, which is taken to be the unitary evolution of the oscillator's initial coherent state. Then, the control functions are chosen such that the spin system is in alternating contact with the hot and the cold bath with periods of complete decoupling in between.

Under these circumstances the system indeed shows cyclic heat engine functionality. The spin-oscillator system as a whole gets energy during the cycles, if the system is in heat engine configuration, or loses it, if the system is designed to be a heat pump. In the heat engine case, the oscillator energy increases over the cycles, while the spin's energy remains constant. The oscillator plays the role of the work reservoir, as already demonstrated in a detailed way in the previous part without taking dissipation into account, though.

The heat baths do not only lead to a increasing coherent excitation of the oscillator, however. Due to the effects of the baths, the initially pure state of the oscillator decoheres over the cycles and part of the energy flux into the oscillator becomes incoherent. Finally, due to the degradation of the phase information in the oscillator by the decoherence, the machine function gets lost and the system reaches a quasistationary transport scenario in the long-time limit with a constant heat flow from the hot to the cold bath.

## 6.2 Dynamical three spin machine

The dynamical three spin machine (D3SM) has been first discussed by Henrich et al. [2006, 2007a,b]. The model's core system is given by the Hamiltonian

$$\hat{H}_S = \sum_{n=1}^{3} \frac{\omega_n}{2} \hat{\sigma}_z(n) + \lambda \sum_{n=1}^{2} \sum_{k=x,y,z} \hat{\sigma}_k(n) \hat{\sigma}_k(n+1) \tag{6.5}$$

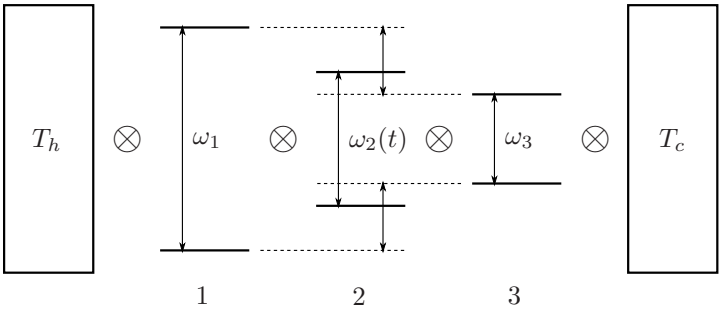


**Figure 6.2:** Dynamical three spin machine: a Heisenberg chain with inhomogeneous splittings between two baths of different temperatures. The center spin is externally driven such that it alternatingly comes into resonance with the two filter spins to the left and right.

and is a linear Heisenberg spin chain with three spins with splittings $\omega_n$ and interaction strength $\lambda$. The left and right spin are detuned by $\delta_{13} = (\omega_1 - \omega_3)/2 > 0$, and the middle spin's splitting is taken to be explicitly time-dependent with

$$\omega_2(t) = \delta_{13} \sin(\Omega t) + \overline{\omega_{13}}, \tag{6.6}$$

where we have defined $\overline{\omega_{13}} = (\omega_1 + \omega_3)/2$ such that its splitting oscillates between $\omega_1$ and $\omega_3$. The first and the last spin are then coupled to separate baths with temperatures $T_h$ and $T_c$. After projecting out the baths and performing a Born-Markov approximation, one is left with a master equation for the system of the form derived by Saito et al. [2000] as

$$\frac{\mathrm{d}}{\mathrm{d}t}\hat{\rho}(t) = -i[\hat{H}(t), \hat{\rho}(t)] + \mathcal{L}_h[\hat{\rho}(t)] + \mathcal{L}_c[\hat{\rho}(t)]. \tag{6.7}$$

The dissipators $\mathcal{L}_k[\hat{\rho}(t)], k = h, c$ (for hot and cold bath) are given by

$$\mathcal{L}_k[\hat{\rho}(t)] = -\pi\kappa^2 \left( [\hat{X}_k, \hat{R}_k \hat{\rho}(t)] + \text{h.c.} \right) \tag{6.8}$$

if the system-bath interaction is of the form $\kappa \hat{X}_k \sum_m g_m(\hat{a}_m^\dagger + \hat{a}_m)$. The operator $\hat{R}_k$ is then given in the energy eigenbasis $\{|\phi_l\rangle\}$ of $\hat{H}_S$ with the eigenvalues $\epsilon_l$ as

$$(\hat{R}_k)_{mn} = \langle \phi_m | \hat{R}_k | \phi_n \rangle = \langle \phi_m | \hat{X}_k | \phi_n \rangle \frac{I(\epsilon_m - \epsilon_n) - I(\epsilon_n - \epsilon_m)}{\exp[\beta_k(\epsilon_m - \epsilon_n)] - 1} \tag{6.9}$$

with the spectral density

$$I(\omega) = I_0 \omega^\nu \theta(\omega) \tag{6.10}$$

[$\theta(x) = 1$ for $x \geq 1$, $= 0$ else]. The interaction operators for the baths are selective to spin 1 or 3, respectively, and are given as

$$\hat{X}_h = \hat{\sigma}_x(1) \otimes \hat{1}(2) \otimes \hat{1}(3) \tag{6.11}$$

$$\hat{X}_c = \hat{1}(1) \otimes \hat{1}(2) \otimes \hat{\sigma}_x(3) \tag{6.12}$$

such that the hot (cold) bath only directly interacts with spin 1 (3). The resulting master equation is not of Lindblad form because the secular approximation usually necessary to arrive at a Lindblad master equation has proven to make it impossible to correctly model transport scenarios (cf. Wichterich et al. [2007]). A more detailed discussion of this problem is given in Sec. 9.4.1.

Due to the strong dependence of the energy exchange rate between adjacent spins on the detuning, the energy flux between spin 1 and 2 is almost completely suppressed when spin 2 has reached its minimum splitting and is in resonance with spin 3, and vice-versa. Through this mechanism, a phase dependent switching of the bath couplings is implemented. This mechanism can be understood as a practical realization of the rather abstract implementation in the autonomous model of the previous section via the time-slot operators.

The authors then choose the driving frequency $\Omega \ll \delta_1, \delta_3$, such that spin 2 is long enough in resonance with spin 1 or 3 for the respective bath to be able to thermalize spin 2 to the respective temperature $T_h$ or $T_c$. In this scenario, spin 2 acts as a working medium and the external field driving its splitting is the work reservoir. Spins 1 and 3 act as filters or valves and make sure that the effective interaction of spin 3 with the two bathes is alternating. If the splitting of spin 2 is held constant, the system shows diffusive heat transport through the spin chain from the hot to the cold bath. Thus, no quasistatic limit of the machine exists because of the non-vanishing leakage current $J_L$, which is also present in the driven case, though.

The authors have shown that the temperature difference $\Delta T$ controls the functionality of the spin chain: For $\Delta T$ below a critical value $\Delta T^*$, the system pumps heat from the cold to the hot bath with approximately constant efficiency with respect to $\Delta T$, which is close to the Otto efficiency until $\Delta T$ approaches $\Delta T^*$ from below. Then, due to the leakage current becoming more and more dominant, the heat pump efficiency degrades until the leakage takes over and the system becomes a transport scenario very close to $\Delta T^*$. Above this value, however, the system operates as a heat engine, with an efficiency that first increases with $\Delta T$ and asymptotically reaches the Otto engine efficiency.

In contrast to the model of the previous section, where the work performed or extracted per cycle changed the oscillators energy expectation value, in the present model, the driving field is not modeled explicitly and thus it cannot be directly observed how much energy has been exchanged. Instead, the work $W$ exchanged per cycle is defined with the help of the first law $\mathrm{d}U = đW + đQ_h + đQ_c$ and the fact, that after one cycle, the spin system's internal energy has not changed:

$$\oint \mathrm{d}U = W + \oint J_c(t)\mathrm{d}t + \oint J_h(t)\mathrm{d}t = 0 \tag{6.13}$$

and thus

$$W = -\oint J_c(t)\mathrm{d}t - \oint J_h(t)\mathrm{d}t \tag{6.14}$$

The two heat fluxes to the cold and the hot bath, $J_c(t)$ and $J_h(t)$ can be readily determined by $\mathrm{Tr}\{\hat{H}_S(t)\mathcal{L}_k(t)\}, k = h, c$. Also, for a closed cycle, the r.h.s. of Eq. (6.14) can also be replaced by the area enclosed by the cycle of the driven spin in the $S$-$T$ plane such that

$$W = -\oint T\mathrm{d}S. \tag{6.15}$$

The reason why this yields correct results is found in a special property of the dynamics of the system: Although time dependent, the local spin states are diagonal all the time due to the decoherence from the baths, which destroys all off-diagonal terms of the local states. Thus, each spin is in a local equilibrium at any time and the work is given by the above formulas.

# 7 Autonomous dynamical three spin machine

The autonomous dynamical three spin machine (AD3SM) presented in this chapter is a certain combination of the two models discussed previously in Chapter 6. It takes its basic structure from the D3SM from Chapter 6.2, but implements the driving medium as in the autonomous quantum thermodynamic machine from Chapter 6.1. It therefore is the link between those two models and can be either understood as a concrete realization of the ideas of Tonner and Mahler [2005] or an autonomous version of the model of Henrich et al. [2007a].

In this chapter, we discuss the definition of the model, its properties, and analytical as well as numerical results. In addition, we compare the results of the AD3SM model to the its two precursors.

## 7.1 Model

The model consists of an open quantum system coupled selectively to two heat baths. The core system is the same spin chain as in Henrich et al. [2007a] (Sec. 6.2) but with no classical external driver. Instead, an additional harmonic oscillator interacts with the center spin. The Hamiltonian of the system reads:

$$\hat{H} = \sum_{n=1}^{3} \hat{H}_n + \lambda_{ss}\hat{H}_{ss} + \lambda_{so}\hat{H}_{so} + \hat{H}_o \tag{7.1}$$

with the single spin Hamilton operators

$$\hat{H}_n = \frac{\omega_n}{2}\hat{\sigma}_z(n), \tag{7.2}$$

the oscillator/field mode Hamiltonian

$$\hat{H}_o = \omega_o \left(\hat{a}^\dagger \hat{a} + \frac{1}{2}\right), \tag{7.3}$$

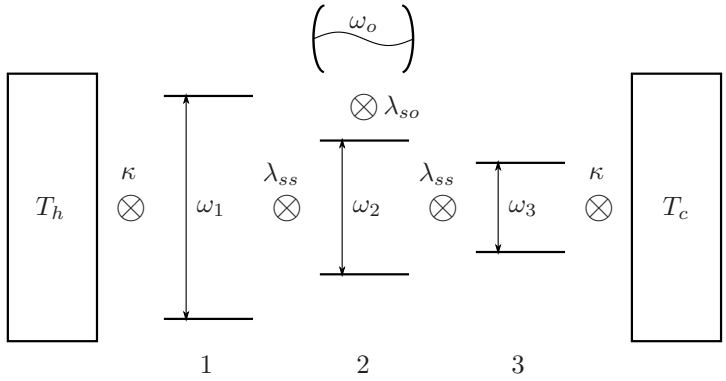


**Figure 7.1:** Autonomous dynamical three spin machine: a Heisenberg chain with inhomogeneous splittings between two baths of different temperatures. The center spin is coupled to a quantum harmonic oscillator (here depicted as a single field mode), which induces effective local time-dependent dynamics such that the spin alternatingly comes in resonance with the two filter spins to the left and right and thus with the bath $T_h$ and $T_c$, respectively.

the Heisenberg next-neighbor coupling

$$\hat{H}_{ss} = \sum_{n=1}^{2} \sum_{k=x,y,z} \hat{\sigma}_k(n)\hat{\sigma}_k(n+1) \tag{7.4}$$

of the spin chain, and the $z$-SOM interaction (cf. Sec. 3.1)

$$\hat{H}_{so} = \hat{\sigma}_z(2)\hat{x} \tag{7.5}$$

between the center spin and the oscillator.

As in the model of Henrich et al. [2007a], we couple the system to two heat baths of the Saito type (Saito et al. [2000]) via the interaction operators $\hat{X}_k \otimes \hat{1}_o$ [(6.11) and (6.12)], which leads to dissipators $\mathcal{L}_h$, $\mathcal{L}_c$ of the form (6.8). The explicit form of the dissipators differ from those of Henrich et al. [2007a], however, because they depend on the eigenbasis of $\hat{H}$, which is obviously not the same here. Eventually, the dynamics of the full model is given by the master equation

$$\frac{\mathrm{d}}{\mathrm{d}t}\hat{\rho}(t) = -i[\hat{H}, \hat{\rho}(t)] + \mathcal{L}_h[\hat{\rho}(t)] + \mathcal{L}_c[\hat{\rho}(t)]. \tag{7.6}$$

In order to have the model operate as a quantum thermodynamic machine, we first need to ensure that the effective dynamics of the central spin are

such that it is alternatively in resonance with the filter spins to the left and right, respectively. Hence, we recall the equation of the effective splitting peak-to-peak amplitude of the SOM from Sec. 3.2, Eq. (3.41):

$$\Delta\omega_2^{\text{eff}} = 2\lambda_{so}\sqrt{\frac{2}{m_o\omega_o}}|\alpha+\gamma| \tag{7.7}$$

with

$$\gamma = \sqrt{\frac{\lambda_{so}^2}{2m_o\omega_o^3}}(1-2c) = \sqrt{\frac{\xi}{2}}(1-2c), \tag{7.8}$$

where $c$ is the ground state occupation of spin 2. We have replaced the quantities of Eq. (3.41) by the corresponding ones from the current model where applicable. Note that the $\gamma$ part of $\Delta\omega_2^{\text{eff}}$ is due to the back-action of the spin on the oscillator [cf. Eq. (3.32)]. We usually want this contribution to be negligible since it is hard to control due to its dependency on the spin state $\hat{\rho}_2(t)$.

In order to have perfect resonance at the reversal points of the effective splitting dynamics, the condition

$$\Delta\omega_2^{\text{eff}} = 2\delta_{13} = \omega_1 - \omega_3 \tag{7.9}$$

has to be met. We note here two problems with using this formula in the context of the AD3SM: First, $\gamma$ depends on the current ground state occupation of the spin, $c$, and second, Eq. (7.7) holds only in this form if the factorization approximation is exact (see the derivation in Sec. 3.2). If, however, $\xi \ll 1$ [cf. Eq. (3.21)] is given, $\gamma$ can be neglected whenever $\alpha$ is at least of the order of unity. This condition implies $\lambda_{so} \ll \sqrt{m_o\omega_o^3}$, and since $\omega_o$ has to be chosen small enough to make sure that the center spin will equilibrate at its reversal points, this condition enforces a weak-coupling limit.

Even if we could take into account analytically how the presence of the filter spins and baths alters $\gamma$, a strong contribution from $\gamma$ would make it difficult to control $\Delta\omega_2^{\text{eff}}$ to the desired degree by adjusting system parameters alone since the center spin's ground state occupation is expected to change significantly when it comes in resonance with one of the filter spins. Thus, we opt for the weak-coupling limit for the AD3SM.

There are two more arguments to do so: First, we do want to keep the decoherence effects due to the presence of the baths on the oscillator small because if the oscillator loses too much purity not only the FA and possibly our prediction about the real $\Delta\omega_2^{\text{eff}}$ become invalid but the driving effect itself is threatened to vanish since a completely decohered oscillator state in the energy eigenbasis has vanishing position expectation.

The second argument is related to the machine function of the model itself: If we chose the strong coupling limit of the SOM, we also would have to choose a high frequency for the oscillator in order to ensure the FA validity. However, the center spin needs to be in resonance with the filter spins at the reversal point of its effective dynamics for as long as possible in order to allow for a good thermalization with the heat baths. Thus, the oscillator frequency should fulfill the condition $\omega_o < \lambda_{ss}$, which is impossible to achieve for moderate spin-spin coupling if we aim for the strong spin-oscillator coupling regime.

Typically, we will choose values for $\lambda_{so}$ of the order of $10^{-2}$ and $\alpha$ so as to be able to neglect the effect of $\gamma$ to Eq. (7.7). Then, the question of the validity of this equation boils down to whether or not the oscillator state in the presence of the baths can support the same amplitude of its position oscillation like in a coherent state $|\alpha\rangle$. We will see in Sec. 7.2 that this is the case for a reasonable amount of time, indeed.

We have yet to consider two aspects of the master equation Eq. (7.6) concerning its validity and the feasibility of the numerical treatment before we can delve into the results and their interpretation. The derivation of the master equation in Saito et al. [2000] makes use of a perturbative ansatz of the dynamics in second order of the system-bath interaction, in this case $\kappa$. This is only valid if the interaction strength is small compared to the smallest transition frequency of the system Hamiltonian $\hat{H}$. By an appropriate choice of the parameters of the system (and possibly choosing the spin-spin couplings independently from each other), all degeneracies in $\hat{H}$ can be avoided and thus, there will always be a choice such that

$$0 < |\kappa| \ll \min_{i,j} |\omega_{ij}| \quad \text{for all } i \neq j,\ i,j \in \mathbb{N} \tag{7.10}$$

where $i, j$ enumerate the eigenstates of $\hat{H}$, and $\omega_{ij}$ are the transition frequencies.

For the numerical results presented in this chapter, we could only ensure that this condition is met to some degree, however, since $\kappa$ would have been so small that the already numerically quite demanding computation of the dynamics of the system would have become infeasible to carry out in a reasonable amount of time. To mitigate that, we back up the validity by checking the consistency of the results, which we establish via three measures: The trace of the system state $\hat{\rho}(t)$, the deviation of the system state $\hat{\rho}(t)$ from $[\hat{\rho}(t) + \hat{\rho}^\dagger(t)]/2$ (that is, whether or not the state stays Hermitian), and the comparison of the present results to the results of the semiclassical counterpart of the models, where the oscillator is replaced by a time-dependent driving.

The second aspect relevant for the numerics is the structure of the matrix elements of the operator $\hat{R}_k$ $(k = h, c)$, that appears in the definition of the

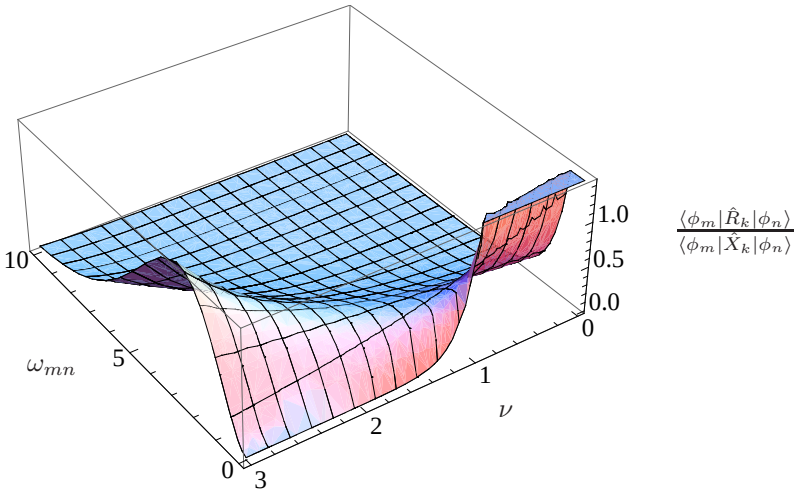


**Figure 7.2:** Behavior of the transition frequency $\omega_{mn}$ dependent part of the matrix elements $(\hat{R}_k)_{mn}$ for $\beta = 1$: The matrix elements diverge for spectral density exponent $\nu < 1$ and $\omega_{mn} \to 0$ if $(\hat{X}_k)_{mn} \neq 0$ at all.

dissipators

$$\mathcal{L}_k[\hat{\rho}(t)] = -\pi\kappa^2 \left( [\hat{X}_k, \hat{R}_k \hat{\rho}(t)] + \text{h.c.} \right). \tag{7.11}$$

This structure is

$$(\hat{R}_k)_{mn} = \langle\phi_m| \hat{R}_k |\phi_n\rangle = \langle\phi_m| \hat{X}_k |\phi_n\rangle \frac{I(\omega_{mn}) - I(\omega_{nm})}{\exp(\beta_k \omega_{mn}) - 1} \tag{7.12}$$

with the energy eigenstates $|\phi_n\rangle$ and eigenenergies $\epsilon_n$ of $\hat{H}$, and the spectral density

$$I(\omega) = I_0 \omega^\nu \theta(\omega). \tag{7.13}$$

Henrich et al. [2007a] used $\nu = 0$ for the spectral density exponent. However, one can easily see that for a system with nearly degenerate states, that is $\omega_{mn} \to 0$ for some combinations of $m \neq n$, the matrix elements associated with these transitions diverge whenever $\nu < 1$ (see Fig. 7.2). The extreme differences in the absolute values of the matrix elements of $\hat{R}_k$ for nearly degenerate transitions and $\nu < 1$ leads to very bad convergence behavior of numerical ODE solver routines and even wrong results. Instead of choosing

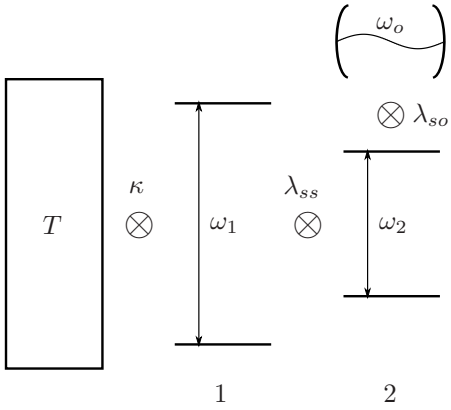


**Figure 7.3:** Filter scenario model: As in the AD3SM model, the spins are Heisenberg coupled and the bath only interacts locally with spin 1 (cf. Fig. 7.1).

$\nu = 0$ like Henrich et al. [2007a], we thus use $\nu = 1$, the smallest value of $\nu$ that exhibits no divergence for $\omega_{mn} \to 0$.

Finally, we briefly comment on how we obtain our numerical results: The simulation is written in *C++* and uses the *Boost.uBLAS* library[1] (version $\geq$ 1.36.0) for all high-level linear algebra [outer matrix products, (partial) traces, system operators, and so on] and some other mathematical functions. For the diagonalization of Hermitian matrices we use the *zheev()*-function from the *LAPACK* library[2]. *zgemm()* is employed for the multiplication of complex matrices wherever performance matters. For the computations that require highest performance, we use the *Intel Math Kernel Library 10.0.3*[3] versions of *zheev()* and *zgemm()*. The time evolution of the system is calculated using the *CVODE* ordinary differential equation solver from the *SUNDIALS* differential equation solver suite[4] with Adams-Moulton formulas of order varying between 1 and 12.

## 7.2 Filter scenario

The crucial feature of the D3SM that leads to its machine behavior is the driving of the spin combined with the resonance effects of the heat flux because

[1] `http://www.boost.org/doc/libs/1_43_0/libs/numeric/ublas/doc/index.htm`
[2] `http://www.netlib.org/lapack/`
[3] `http://software.intel.com/en-us/intel-mkl/`
[4] `https://computation.llnl.gov/casc/sundials/main.html`

of the filter spins. The presence of this mechanism is easily tested for by considering the model with fixed center spin splitting $\omega_2$ and equal filter spin splittings $\omega_1 = \omega_3$. When evaluating the steady state heat flux from the hot to the cold bath as a function of $\omega_2$, one realizes that the flux is maximal for $\omega_2 = \omega_1 = \omega_2$ and rapidly decreases for increasing detuning of the center spin (Henrich et al. [2007a]).

Unfortunately, this approach cannot be used for the AD3SM to test whether the control of the center spin splitting by the quantum oscillator is as good as in the classical case because we would need to examine the model in the limit of $\omega_o \to 0$. This limit implies $\lambda_{so} \to 0$ to keep the FA valid. In order to have a non-vanishing $\Delta\omega_2^{\text{eff}}$ in this case, $\alpha$ would have to go to infinity which in turn would require to consider an infinite number of levels in the oscillator. Even for finite values of $\omega_o$ and $\lambda_{so}$, the dimension of the problem gets so large that it becomes untreatable by numerical methods.

Instead, we discuss the results for only a part of the full model in order to verify the driving and resonance mechanism by comparison of the results with the semiclassical result. The part we are going to consider is depicted in Fig. 7.3 and consists of the left bath, spins 1 and 2, and the oscillator:

$$\hat{H} = \sum_{n=1}^{2} \frac{\omega_n}{2} \hat{\sigma}_z(n) + \lambda_{ss} \sum_{k=x,y,z} \hat{\sigma}_k(1)\hat{\sigma}_k(2) + \lambda_{so}\hat{H}_{so} + \hat{H}_o \tag{7.14}$$

with the oscillator Hamiltonian as of Eq. (7.3) and the spin-oscillator interaction operator from Eq. (7.5). The equation of motion of the filter scenario then reads

$$\frac{\mathrm{d}}{\mathrm{d}t}\hat{\rho}(t) = -i[\hat{H}, \hat{\rho}(t)] + \mathcal{L}[\hat{\rho}(t)]. \tag{7.15}$$

The bath-system coupling operator $\hat{X} = \hat{\sigma}_x(1) \otimes \hat{1}(2) \otimes \hat{1}(o)$ is local to spin 1. The corresponding semiclassical model is given by

$$\hat{H}_{\text{sc}}(t) = \frac{\omega_1}{2}\hat{\sigma}_z(1) + \lambda_{ss} \sum_{k=x,y,z} \hat{\sigma}_k(1)\hat{\sigma}_k(2) + \frac{\omega_2(t)}{2}\hat{\sigma}_z(2) \tag{7.16}$$

with the master equation

$$\frac{\mathrm{d}}{\mathrm{d}t}\hat{\rho}(t) = -i[\hat{H}_{\text{sc}}(t), \hat{\rho}(t)] + \mathcal{L}(t)[\hat{\rho}(t)]. \tag{7.17}$$

Note that the dissipator of Eq. (7.15) has been replaced by a time-dependent dissipator $\mathcal{L}(t)$ that must be calculated for each time-step from the momentary

| Parameters | | | |
|---|---|---|---|
| $\omega_o$ | 0.1 | $\alpha = 5\sqrt{5} \approx$ | 11.180 |
| $\omega_1$ | 1.0 | $T$ | 1.0 |
| $\omega_2$ | 2.0 | $\nu$ | 1.0 |
| $\lambda_{ss}$ | 0.1 | $m_o$ | 1.0 |
| $\lambda_{so}$ | 0.01 | $d_o$ | 212 |
| $\kappa$ | 0.1 | | |

**Table 7.1:** Autonomous filter scenario simulation parameters.

eigenbasis of $\hat{H}_{\rm sc}(t)$. The time dependency of the splitting of spin 2 is chosen to be sinusoidal

$$\omega_2(t) = \delta_2 \cos(\omega_o t) + \overline{\omega_2}. \tag{7.18}$$

We consider here results for the filter scenario with the parameters given in Tab. 7.1. The initial state of the system is of the form

$$\hat{\rho}(0) = \hat{\rho}_1^{\rm can}(T) \otimes \hat{\rho}_2^{\rm can}(T_2) \otimes |\alpha\rangle\langle\alpha| \,, \tag{7.19}$$

where $|\alpha\rangle$ is a coherent state. Note that $m_0$ in Tab. 7.1 is the mass of the oscillator and $d_o$ denotes the high-level cut-off of the oscillator spectrum. $T$ is the bath temperature of the single bath coupled to the system. Spin 1 is initially in equilibrium with the bath, while the second spin starts out at a temperature that is not too far away from the temperature it will be seen to have at the beginning of each cycle. The parameters $\alpha$, $\lambda_{so}$, $\omega_o$, and $m_o$ are chosen such that $\Delta\omega_2^{\rm eff} = 2$ according to Eq. (7.7) if $\gamma$ may be neglected. We compare the results of the quantum model with the semiclassical model with the same parameters, that is, $\overline{\omega_2} = \omega_2$ and $\delta_2 = 1$.

First, as the most important quantity for the machine function, we discuss the result for the heat flux $\dot{Q}(t)$ from the bath into the system, given by either $\mathrm{Tr}\{\hat{H}\mathcal{L}[\hat{\rho}(t)]\}$ or $\mathrm{Tr}\{\hat{H}_{\rm sc}\mathcal{L}(t)[\hat{\rho}_(t)]\}$. In Fig. 7.4 we see that the heat currents in both cases are very much the same. Note how the heat current spikes whenever the two spins come in resonance (cf. Fig. 7.4 and Fig. 7.5). Obviously, the emergent driving almost exactly corresponds to its semiclassical counterpart, and it is thus verified that the model features the mechanism essential for the machine operation of the AD3SM. This is also another supportive point for taking the effective local dynamics together with the FA seriously as it clearly has the same dynamical effect as a classical driver.

Comparing other important properties like the effective splitting of spin 2 to the time-dependent splitting in the semiclassical case (Fig. 7.5), the ground

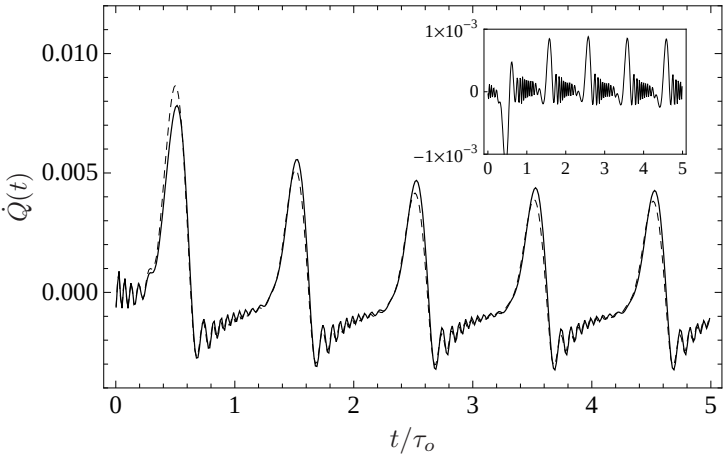


**Figure 7.4:** Heat flux $\dot{Q}(t)$ from the bath into the system for the quantum (solid) and the semiclassical (dashed) filter scenario. The parameters of the semiclassical model are chosen such that they correspond to what is expected from Eq. (7.7) for the effective splitting dynamics. $\tau_o = 2\pi/\omega_o$ is the oscillator period time. The inset shows the difference of the both results.

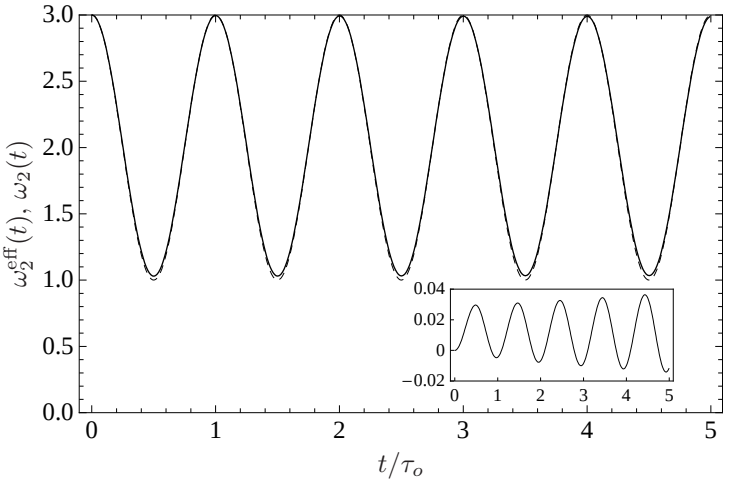


**Figure 7.5:** Filter model effective splitting of spin 2, $\omega_2^{\rm eff}(t)$, in the quantum case (solid) and its splitting $\omega_2(t)$ in the semiclassical case (dashed). $\tau_o = 2\pi/\omega_o$ is the oscillator period time. The inset shows the difference.

state occupation of spin 2, and its inverse temperature (Fig. 7.6) we realize that the dynamics of the quantum model indeed is in almost perfect agreement with the semiclassical result. The small deviations that are present can be attributed to the back-action of the spin on the oscillator as of Eqs. (3.31) and (3.32).

However, if we look at the purity dynamics of the oscillator in Fig. 7.7, we get a surprise. Although we have chosen the parameters carefully such that the FA is fulfilled, the oscillator purity rapidly decreases due to the decoherence induced by the bath. This in itself is not so surprising as the fact that this rather strong decoherence seems not to impede the driving effect noticeably. We will see that this phenomenon carries over to the full AD3SM model discussed in the next section, where we will also attempt an explanation.

## 7.3 Heat engine

This section is dedicated to the discussion of the results for the complete AD3SM in a parameter set that is seen to lead to heat engine functionality. The parameters that were used to produce these results are given in Tab. 7.2. We first discuss constraints that the parameters of the model have to meet

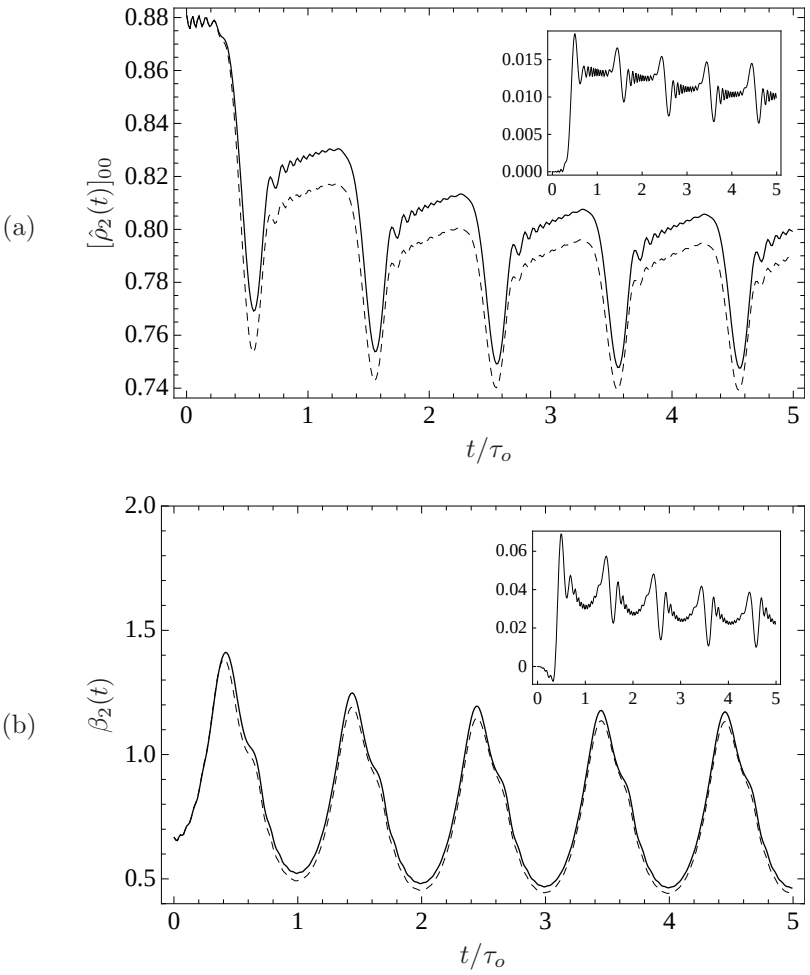


**Figure 7.6:** (a) Ground state occupations and (b) inverse temperatures of spin 2 in the quantum (solid) and the semiclassical case (dashed). $\tau_o = 2\pi/\omega_o$ is the oscillator period time, and for each figure the inset shows the difference of the quantum and semiclassical result.

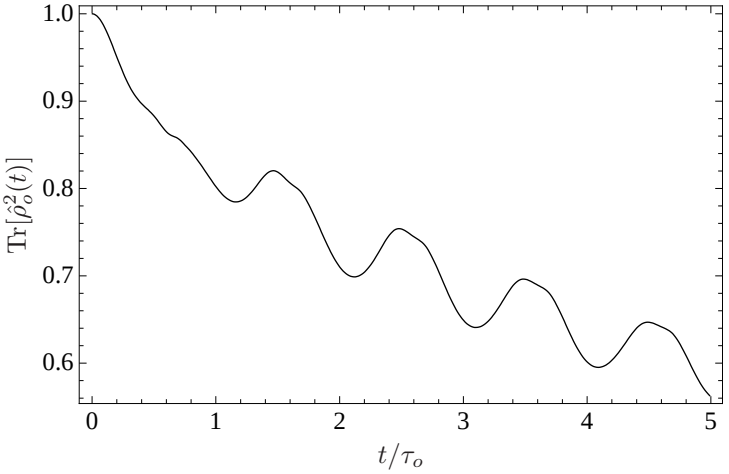


**Figure 7.7:** Filter scenario model: oscillator purity dynamics. $\tau_o = 2\pi/\omega_o$ is the period time of the oscillator.

| Parameters | | | |
|---|---|---|---|
| $\omega_o = \sqrt{5}/16 \approx$ | 0.140 | $\alpha$ | 4.0 |
| $\omega_1$ | 3.0 | $T_h$ | 1.0 |
| $\omega_2$ | 2.5 | $T_c$ | 0.5 |
| $\omega_3$ | 2.0 | $\nu$ | 1.0 |
| $\lambda_{ss}$ | 0.1 | $m_o$ | 1.0 |
| $\lambda_{so} = \sqrt{\omega_o}/(16\sqrt{2}) \approx$ | $1.65 \cdot 10^{-2}$ | $d_o$ | 50 |
| $\kappa$ | 0.1 | | |

**Table 7.2:** Parameters for the AD3SM in heat engine mode.

in order to be able to get the desired functionality at all. Then, we discuss the model with the help of standard quantities like energies and energy flows, oscillator position, and the $S$-$T$-diagram of the driven center spin, before we finally evaluate the results for the LEMBAS heat and work. It is seen that both approaches lead to the same results, namely, that the model with the chosen parameters is a heat engine, indeed, with the quantum harmonic oscillator acting as its work reservoir.

We start by pointing out that there is a condition for the filter spin splittings $\omega_1$, $\omega_3$ and the temperatures of the baths that controls whether or not the model can act as a heat engine or not. Since the Otto efficiency is not temperature dependent, there have to be temperature ranges for the baths such that the Otto engine efficiency is higher than the Carnot efficiency. The reason why despite that the Otto cycle does not violate the 2nd law is that it does no longer implement heat engine functionality for temperatures of the baths that would lead to a higher efficiency than Carnot, but instead becomes a heat pump (cf. Henrich et al. [2007a]). Hence, in order to allow for heat engine functionality, the model needs to meet the condition

$$\eta_{\text{Carnot}} = 1 - \frac{T_c}{T_h} > 1 - \frac{\omega_3}{\omega_1} = \eta_{\text{Otto}}^{\text{qm}}. \tag{7.20}$$

It follows that

$$\frac{\omega_3}{\omega_1} > \frac{T_c}{T_h}, \tag{7.21}$$

or in terms of the temperature gradient $\Delta T = T_h - T_c$ and the splitting difference $\Delta\omega = \omega_1 - \omega_3$,

$$\frac{\Delta T}{T_h} > \frac{\Delta\omega}{\omega_1}. \tag{7.22}$$

Because the driven spin has to be in resonance at the reversal points of its splitting dynamics, the stroke of the effective spin splitting, $\Delta\omega_2^{\text{eff}}$ has to equal $\Delta\omega$. The chosen parameters fulfill both conditions.

Another constraint for the parameters of the model is related to the decoherence induced by the baths. In the D3SM, the temperatures of the baths are rather arbitrary except for the condition (7.22). This is no longer the case in the AD3SM because of decoherence effects of the oscillator, which seem to be stronger for higher temperatures of the baths. This effect can be so strong that the thermodynamic functionality of the spin-oscillator network is buried under heat fluxes caused by this decoherence. We therefore choose the temperatures of the baths small enough as to avoid this problem.

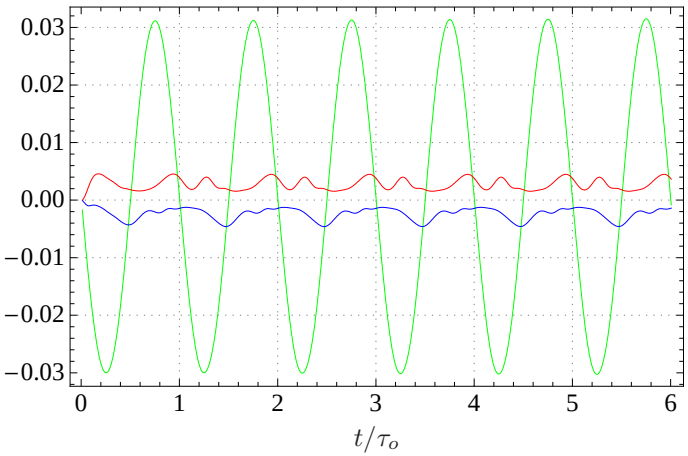


**Figure 7.8:** Energy fluxes in the AD3SM with the parameters of Tab. 7.2 (heat engine): Heat flux $\dot{Q}_h(t)$ from the hot bath (red), heat flux $\dot{Q}_c(t)$ from the cold bath (blue), energy flux $\dot{E}_o(t)$ to the oscillator (green).

We start by trying to assess the functionality of the model from general properties of the dynamics, and focus first on the energy fluxes of the model. In Fig. 7.8, the heat fluxes $\dot{Q}_h(t)$ and $\dot{Q}_c(t)$ from the baths into the system, and the energy flux into the oscillator $\dot{E}_o(t)$ are depicted. It can be seen that after the first transient cycle, the fluxes are periodic with the period time of the oscillator

$$\tau_o = \frac{2\pi}{\omega_o} \approx 44.959. \tag{7.23}$$

Moreover, $\dot{Q}_h(t) > 0$ and $\dot{Q}_c(t) < 0$ during the whole time interval, which means that heat is overall flowing from the hot bath into the system and at least part of it is released to the cold bath. The oscillator energy flux oscillates strongly but is periodic as well. This is the typical energy flux pattern of a heat engine. However, it needs to be verified that the oscillator indeed gains energy during the process and that his gain of energy is work in order to make sure that the model really implements a heat engine.

To strengthen the argument that the model is a heat engine, we first note that the oscillator in fact gains energy over the cycles (cf. Fig. 7.9) in an approximately linear way. Moreover, the oscillator position amplitude increases linearly as well, although only slightly, as is obvious from Fig. 7.10. The position amplitude, however, can only increase with the help of coherent ex-

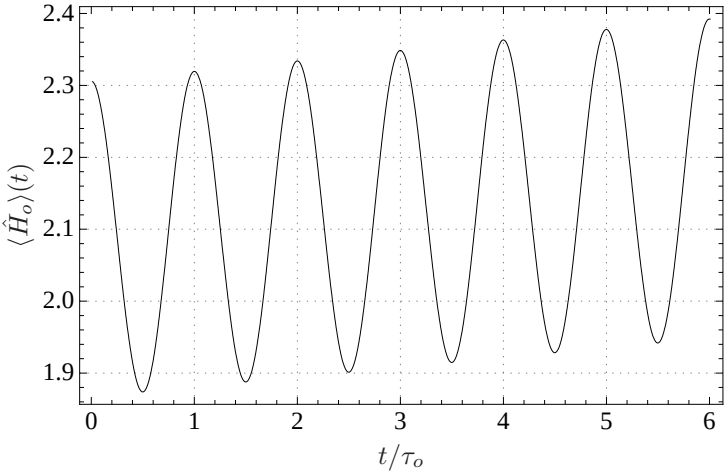


**Figure 7.9:** Oscillator energy time evolution in the AD3SM with the parameters of Tab. 7.2 (heat engine).

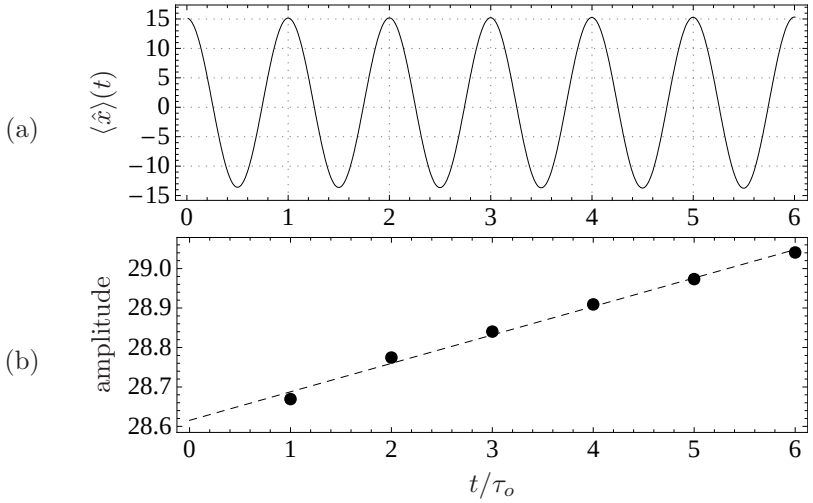


**Figure 7.10:** (a) Oscillator position expectation, and (b) oscillator position peak-to-peak amplitude for each cycle of the AD3SM (parameters as of Tab. 7.2, heat engine).

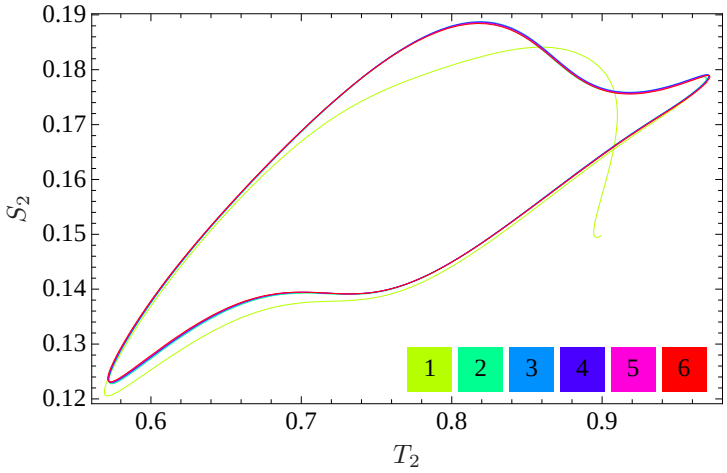


**Figure 7.11:** $S$-$T$-diagram of the driven center spin of the AD3SM (parameters as of Tab. 7.2). The entropy and temperature of the spin are defined for any instant for the spin is always in a diagonal state. The cycles are color coded as shown in the legend.

citation, indicating that at least part of the energy increase of the oscillator is due to work.

Yet another indicator that the model is a heat engine for the given parameters is given by the $S$-$T$-diagram of the driven spin, Fig. 7.11, which can be used here because the driven spin is always in a diagonal state. The temperature of the spin has been calculated by use of the formula

$$T_2(t) = -\omega_2^{\text{eff}}(t) \left[ \ln \left( \frac{1}{[\hat{\rho}_2(t)]_{00}} - 1 \right) \right]^{-1} \tag{7.24}$$

with the effective spin splitting $\omega_2^{\text{eff}}(t)$ and the ground state occupation $[\hat{\rho}_2(t)]_{00}$. Note that the von Neumann entropy $S_2$ in this case coincides with the thermodynamic entropy of the canonical ensemble represented by this single spin as already discussed in Sec. 5.1.1. Although this process is not quasistatic, the spin is in a canonical equilibrium state at all times. This property has already been used by Henrich et al. [2007a] to determine the machine function and work performed over one cycle (cf. Sec. 6.2).

We will do the same and first consider the operation mode that is indicated by the sense in which the cycles are run through. In our case, this sense is counter-clockwise as becomes clear from Fig. 7.11 when considering the

first cycle (green) and its orientation. Such a counter-clockwise orientation is associated with the heat engine cycle, further supporting the interpretation of this model as a heat engine.

Note that the cycles 2 through 6 are almost identical in Fig. 7.11, and this also holds true for the energy flows $\dot{Q}_h(t), \dot{Q}_c(t), \dot{E}_o(t)$, all properties of the driven spin, and the LEMBAS quantities discussed below. We will therefore no longer consider all cycles but the average cycle of the cycles 2 through 6. The first cycle is omitted due to the transient dynamics it exhibits.

The integrated heats $Q_h$ and $Q_c$ over the average cycle from the hot and the cold bath, respectively, are found to be

$$\Delta Q_h \approx 1.197 \cdot 10^{-1}, \qquad \text{and} \tag{7.25}$$

$$\Delta Q_c \approx -1.065 \cdot 10^{-1}, \tag{7.26}$$

while the total energy increase of the oscillator over this average cycle is

$$\Delta E_o \approx 1.393 \cdot 10^{-2} \approx -\Delta Q_h - \Delta Q_c. \tag{7.27}$$

The deviation of the l.h.s. from the r.h.s. is of the order of $10^{-4}$, two orders of magnitude less than the energy change of the oscillator per cycle. Thus, in good approximation, the total energy change of the system is due to the increasing energy of the oscillator.

We can now calculate the work performed by the driven spin according to the thermodynamical formula

$$\Delta W_o^{\mathrm{td}} = -\oint T_2 \mathrm{d}S_2 \approx 9.316 \cdot 10^{-3}, \tag{7.28}$$

which has also been used by Henrich et al. [2007a] to calculate the work performed on the semiclassical driver. This is less than $\Delta E_o$ but of the same order of magnitude. If one accepts that the work performed by the spin has to be performed on the oscillator because it is the source of the spins driving, approximately two third of the oscillator energy gain is recognized as work, and thus, the model really is a heat engine.

We compare now the results obtained so far by use of standard quantities and methods to the LEMBAS results for this model. We use the energy eigenbasis of $\hat{H}_o$ as the measurement basis, thus leading to the usual LEMBAS formulas Eq. (2.31) and (2.32). However, $\hat{H}_{o,a}^{\mathrm{eff}}(t) = 0$ because the complete effective Hamiltonian for the oscillator is

$$\hat{H}_o^{\mathrm{eff}}(t) = \lambda_{so} \mathrm{Tr}_2\{[\hat{\rho}_2(t) \otimes \hat{1}_o]\hat{H}_{so}\} = \lambda_{so}\hat{x}\langle\hat{\sigma}_z(2)\rangle(t), \tag{7.29}$$

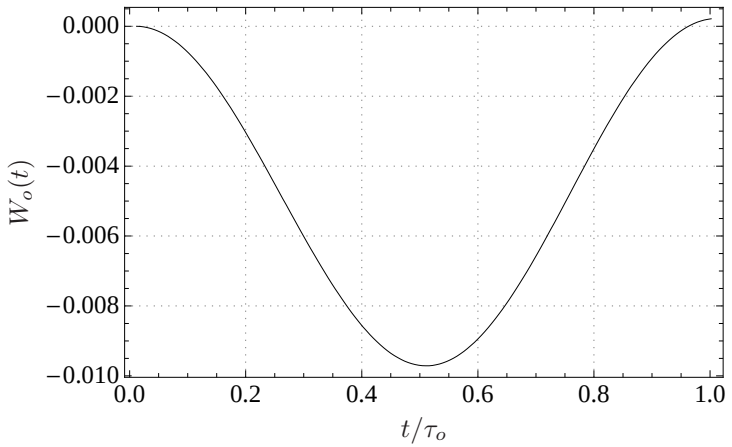


**Figure 7.12:** Integrated work performed on the oscillator according to LEMBAS for the average cycle of the AD3SM with parameters from Tab. 7.2. At the end of the cycle, there remains a small surplus of work.

where $\hat{\rho}_2(t)$ is the reduced state of spin 2 and $\mathrm{Tr}_2$ denotes the partial trace over its Hilbert space, and this effective Hamiltonian has only zero diagonal elements. Therefore, $\hat{H}'_o = \hat{H}_o$, and the LEMBAS heat and work flows $\dot{Q}_o(t)$ and $\dot{W}_o(t)$, respectively, together account for the oscillator energy change

$$\frac{\mathrm{d}}{\mathrm{d}t}\langle \hat{H}_o \rangle(t) = \dot{W}_o(t) + \dot{Q}_o(t). \tag{7.30}$$

If we now focus on the integrated work over the average cycle, we find according to LEMBAS that at the end of the average cycle, there is a small surplus of work that has been performed on the oscillator, which is

$$\Delta W_o \approx 9.571 \cdot 10^{-3}, \tag{7.31}$$

and is almost the same as $\Delta W_o^{\mathrm{td}}$ [cf. Eq. (7.28)]. The deviation is probably due to the errors induced by the averaging. Thus, the LEMBAS result perfectly agrees with our previous assessment of the model functionality, and can be seen again to give correct results. Note that our numerical result shows that no such agreement between the LEMBAS result and the thermodynamic approach can be obtained when choosing the measurement basis such that

$$\hat{H}''_o(t) = \hat{H}_o + \hat{H}_o^{\mathrm{eff}}(t). \tag{7.32}$$

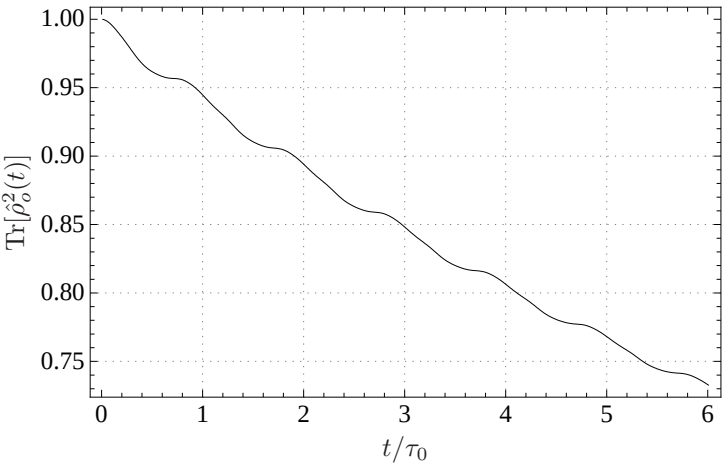


**Figure 7.13:** Oscillator purity dynamics for the AD3SM in the heat engine case (parameters as of Tab. 7.2).

Finally, we note that in this case again, the purity of the oscillator drops quite a bit, although not as fast as in the filter scenario case. This obvious decoherence effect seems not to impede the work source functionality of the oscillator too much. This can be understand as follows. The strength of the work effect exerted by the oscillator over the spin depends mainly on two factors: First, there needs to be dynamics of the oscillator at all, and second, the observable by which the oscillator is coupled to the spin needs to have significant dynamics. In the present case, this observable is the oscillator position. Since the position amplitude of the oscillator is clearly increasing although the purity of the oscillator decreases, the position expectation can obviously be quite high even for somewhat mixed states. This effect has already been noted and discussed by Tonner and Mahler [2005]. This result shows again that a high purity is not the crucial point of quantum work reservoirs, as has also turned out in our discussion of the work source quality measures in Sec. 2.5 and Sec. 3.3. Instead, the reservoir functionality is determined by the relative strength of the effects by $\hat{H}^{\mathrm{eff}}$ and $\mathcal{L}^{\mathrm{eff}}$.

| Parameters | | | |
|---|---|---|---|
| $\omega_o = \sqrt{5}/16 \approx$ | 0.140 | $\alpha$ | 4.0 |
| $\omega_1$ | 3.0 | $T_h$ | 1.5 |
| $\omega_2$ | 2.5 | $T_c$ | 1.49 |
| $\omega_3$ | 2.0 | $\nu$ | 1.0 |
| $\lambda_{ss}$ | 0.1 | $m_o$ | 1.0 |
| $\lambda_{so} = \sqrt{\omega_o}/(16\sqrt{2}) \approx$ | $1.65 \cdot 10^{-2}$ | $d_o$ | 50 |
| $\kappa$ | 0.1 | | |

**Table 7.3:** Parameters for the AD3SM in heat pump mode. They are identical to the heat engine parameters of Tab. 7.2 apart from the heat bath temperatures $T_h$ and $T_c$.

## 7.4 Heat pump

We briefly review in this section the AD3SM configured as a heat pump along the lines of the previous section. First, let us take a look at the parameters in Tab. 7.3 chosen for the present case, and note that they are identical to the previously used parameters except for the heat bath temperatures $T_h$ and $T_c$. The temperatures are chosen such that the efficiency condition (7.20) is violated. This forces the Otto engine in the pump mode as discussed in the previous section. Additionally, we have chosen a very small temperature gradient of $\Delta T = 0.01$ in order to minimize the leakage current through the system (cf. Henrich et al. [2007a]). If this leakage current is too large, it may override the heat pump functionality.

We first discuss the results of the energy flows in Fig. 7.14. Again, one sees that the first cycle shows transient behavior but after that, the fluxes are almost perfectly periodic over the cycles. In contrast to the heat engine case, now both heat bath fluxes have zero-crossings. The phase separation of the fluxes due to the resonance effects of the effective spin splitting with the filter spins is easy to observe here. Whenever the absolute heat flux of one bath is large, the heat flux of the other one is close to zero.

If we consider the integrated heat imparted by the baths over the average cycle, $\Delta Q_h$ and $\Delta Q_c$, we find the following result:

$$\Delta Q_h \approx -2.709 \cdot 10^{-2} \tag{7.33}$$

$$\Delta Q_c \approx 2.407 \cdot 10^{-2}. \tag{7.34}$$

Clearly, heat is pumped from the cold bath to the hot bath by the driving of the oscillator. This pumping is associated with a decrease of the coherent

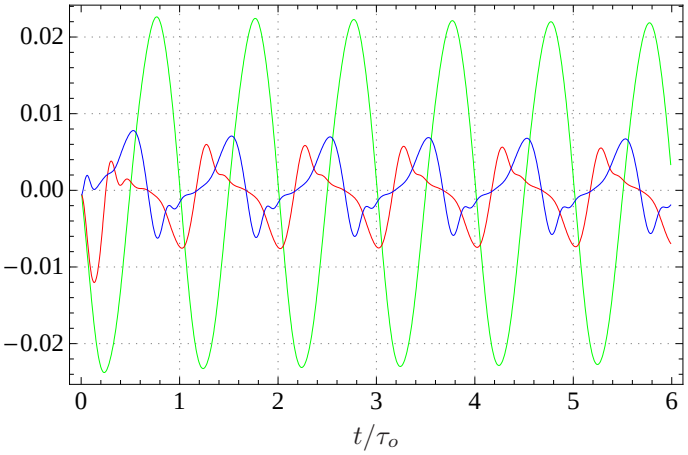


**Figure 7.14:** Energy fluxes in the AD3SM with the parameters of Tab. 7.3 (heat pump): Heat flux $\dot{Q}_h(t)$ from the hot bath (red), heat flux $\dot{Q}_c(t)$ from the cold bath (blue), energy flux $\dot{E}_o(t)$ to the oscillator (green).

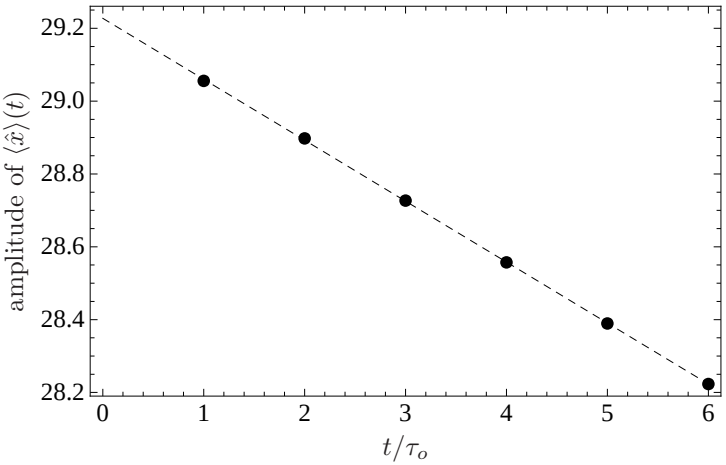


**Figure 7.15:** Oscillator position peak-to-peak amplitude for each cycle of the AD3SM in heat pump configuration (parameters as of Tab. 7.3).

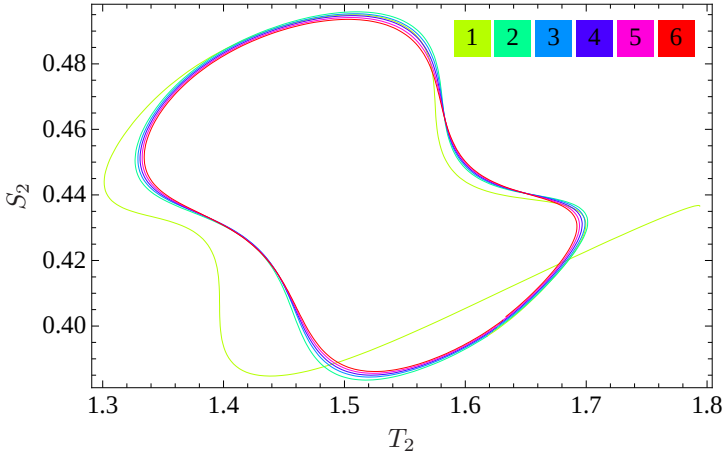


**Figure 7.16:** $S$-$T$-diagram of the driven center spin of the AD3SM in heat pump configuration (parameters as of Tab. 7.3). The entropy and temperature of the spin are defined for any instant for the spin is always in a diagonal state. The cycles are color coded as shown in the legend.

excitation of the oscillator expressed by the fact that the oscillator position amplitude is reduced over the cycles as seen in Fig. 7.15.

The pumping functionality can be assessed also from the $S$-$T$-diagram of the driven spin as in the previous section. Fig. 7.16 clearly shows that the center spin performs clockwise heat pump cycles. Comparing the work performed on the oscillator by integration of the average spin 2 $T$-$S$-diagram, $\Delta W_o^{\mathrm{td}}$, and the work $\Delta W_o$ calculated with the LEMBAS formula, we find

$$\Delta W_o^{\mathrm{td}} \approx -2.220 \cdot 10^{-2} \tag{7.35}$$

$$\Delta W_o \approx -2.468 \cdot 10^{-2}. \tag{7.36}$$

This agreement is not as good as it was in the previous section, but it is still satisfactory. The deviation most probably is due to the averaging over the cycles and the fact that the error made by the averaging is different for different quantities.

Still, it seems justified to call this model a heat pump, especially because we see that the pump functionality consumes coherent excitation of the oscillator (decreasing position amplitude), and because the $S$-$T$-diagram of the spin clearly shows a heat pump cycle.

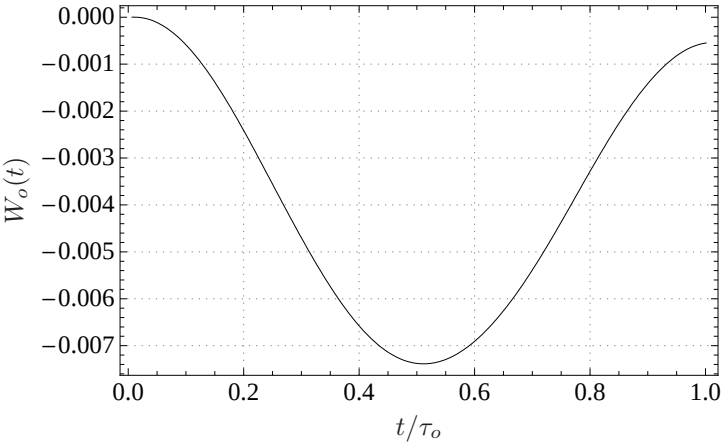


**Figure 7.17:** Integrated work performed on the oscillator according to LEMBAS for the average cycle of the heat pump AD3SM. Over the cycle, the oscillator releases work.

## 7.5 Conclusion

In this chapter we have introduced the autonomous dynamical three spin machine (AD3SM) consisting of a three-spin Heisenberg chain, an oscillator coupled to the center spin of the chain introducing effective splitting dynamics via the $z$-SOM mechanic (Sec. 3.1.1), and two baths coupled locally to the left and right spin of the chain, respectively. We have first discussed some general properties of the resulting master equation and have seen that a spectral density exponent for the baths smaller than 1 makes the problem hard or impossible to solve numerically because of nearly degenerate eigenstates of the model Hamiltonian. We also have pointed out that we could fulfill the condition for the validity of the second-order perturbative ansatz of the master equation only to some degree but verified by comparison of the results to the semiclassical model that no unphysical results were produced.

The evaluation of the filter scenario in the second section of this chapter supported this conclusions, together with showing that the dynamics produced by the quantum mechanical implementation of the classical driver yields almost the same results as the semiclassical one. In particular, the resonance dynamics of the driven spin and the associated phase dependency of the heat flux agree almost perfectly with the semiclassical case.

In Sec. 7.3, we found that the model for the set of parameters used there

exhibits all features of a thermodynamic heat engine: heat flux from hot to cold and increasing mechanical energy of the work reservoir, here the quantum oscillator. Moreover, examination of the $T$-$S$-diagram of the driven spin with the temperature calculated by use of the effective spin splitting showed that this spin indeed performs engine cycles with positive work output over a cycle. This output of work has been shown to be assessed accurately by the LEMBAS work integrated over one cycle giving another argument in favor of the usefulness and validity of the LEMBAS method, particularly since it turns out that one has to use the measurement basis proposed in Weimer et al. [2008] in order to recover the correct result.

Finally, we have presented a set of parameters such that the AD3SM operates as a heat pump in Sec. 7.4. Again, we verified the functionality by the methods of Sec. 7.3 and found an approximate agreement of the work over one cycle calculated by the thermodynamical formula and by the LEMBAS method.

We conclude from the results presented in this chapter that the oscillator can operate as a quantum work source, indeed, as discussed in the previous part, and that this functionality is also recovered when sources of decoherence act on the system, if the model is carefully designed. We have shown that this quantum work source can undoubtedly produce the thermodynamic functions known from classical work sources (classical drivers). Moreover, we established that assessing the work by the LEMBAS method gives the result expected from a thermodynamical analysis of the cycles performed on the effectively driven spin to high accuracy. However, we also notice that setting up the model and choosing the parameters is subject to quite a number of constraints in order to achieve the desired thermodynamic functionality. In this sense, the quantum thermodynamic nanomachine presented here is not as robust as its classical counterparts.

# Part III

# Quantum thermodynamic pseudomachines

# 8 Laser as a thermodynamic process

## 8.1 Why "pseudomachines"?

The previous two parts were concerned with the realization of thermodynamic cycles and work functionality in quantum systems that as a whole are subject to a time-independent Hamiltonian. Thus, the emergence and proper definition of the concept of work on quantum grounds has been clarified, and environments that implement said emergent work cycle behavior have been extensively discussed. The core of the presented quantum work concept is the analogy of work to classical driving by the effective time-dependence of the local dynamics due to the parts of dynamics that are governed by the factorization approximation.

In the present part of this work, we will encounter models that have no effective time-dependency of the local Hamiltonians but still exhibit machine-like features and behavior within certain limits. It turns out that these models in the end are heat transport models but engineered in an elaborate way, which we therefore call *thermodynamic pseudomachines*. The increased functionality over classical transport models is allowed for by an increased control of the couplings of the parts of the system, namely, heat baths that are coupled selectively to single transitions of a quantum system. We note here that as discussed already in Sec. 5.1.2, such detailed spectral control is a feature of quantum thermodynamic processes and may lead to novel thermodynamic behavior.

The chapter at hand is dedicated to the presentation of three models of thermodynamic pseudomachines. All these models are inspired by the thermodynamic description of the lasing (masing) process and bring in an increasing amount of quantumness by explicitly modeling more and more parts of the basic model of Scovil and Schulz-DuBois [1959] (Sec. 8.2) by quantum systems until in Sec. 8.4, the model is completely quantum. In Sec. 8.3, we present the *extended dissipative Jaynes-Cummings model (ED JCM)* by Boukobza and Tannor [2006b] in some detail as we will use this model to clarify the properties and proper interpretation of pseudomachine models in the following chapter,

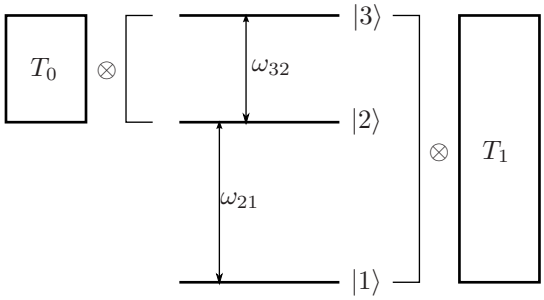


**Figure 8.1:** The three-level maser system considered by Scovil and Schulz-DuBois [1959]. The two baths at temperatures $T_0$ and $T_1$ are selectively coupled to the transitions $|2\rangle\leftrightarrow|3\rangle$ and $|1\rangle\leftrightarrow|3\rangle$, respectively.

where we apply the concepts from Part I – in particular the LEMBAS method (Sec. 2.3) – to the ED JCM.

## 8.2 Maser model of Scovil and Schulz-DuBois [1959]

The first work known to us that deals with the concept of lasing/masing as a thermodynamic process is Scovil and Schulz-DuBois [1959]. They introduce a three-level quantum system system with transitions $|2\rangle\leftrightarrow|3\rangle$ and $|1\rangle\leftrightarrow|3\rangle$ selectively coupled to heat baths at temperatures $T_0$ and $T_1$, respectively, with $T_0 < T_1$. The transition $|1\rangle\leftrightarrow|3\rangle$ is taken to be coupled to the microwave mode (not explicitly modeled here). The authors describe an experimental realization of the model where the three-level system is implemented by gadolinium atoms in a crystal coupled to a spin-bath at temperature $T_0$ provided by cerium atoms in the same crystal. The high-temperature bath can be thought of being a discharge tube coupled via a waveguide acting as a high-pass filter to the gadolinium atoms.

The authors find for the maser efficiency

$$\eta_{\mathrm{M}} = \frac{\omega_{21}}{\omega_{31}}, \tag{8.1}$$

which we can identify with the spin quantum Otto efficiency $\eta_{\mathrm{Otto}}^{\mathrm{qm}}$ of Eq. (5.15) by substituting $\omega_{21} = \omega_{31} - \omega_{32}$

$$\eta_{\mathrm{M}} = 1 - \frac{\omega_{32}}{\omega_{31}} = \eta_{\mathrm{Otto}}^{\mathrm{qm}}. \tag{8.2}$$

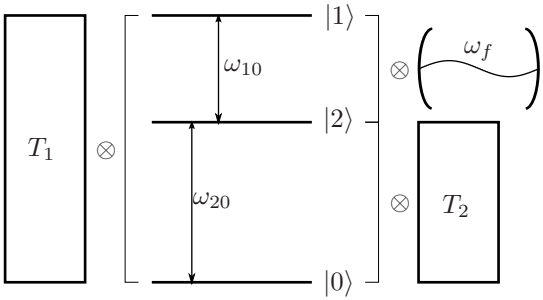


**Figure 8.2:** The extended dissipative Jaynes-Cummings model (ED JCM).

As we will see in the following sections this result seems to indicate a general property of quantum thermodynamic pseudomachines.

## 8.3 Extended dissipative Jaynes-Cummings model

The *extended dissipative Jaynes-Cummings model* (ED JCM) has been proposed and described in a series of papers by Boukobza and Tannor [2006a, 2007, 2008, 2006b]. The model is similar to the model of Scovil and Schulz-DuBois discussed in the previous section but the authors now explicitly model the lasing mode as a quantum harmonic oscillator. Additionally, the authors explicitly formulate a master equation for the model and present the properties and solutions of it. This model gives a much more detailed insight in how the maser model of Scovil and Schulz-DuBois [1959] works, especially with respect to the properties and role of the masing mode and its state. A much related work is that of Youssef et al. [2009], dealing with a model that only slightly differs from the model discussed by Boukobza and Tannor. Most of what we will discuss here for the model of Boukobza and Tannor is the same or at least analogous to the model discussed by Youssef et al.

The ED JCM consists of a three-level system whose upper transition is coupled to a cavity mode via the well-known Jaynes-Cummings coupling Hamiltonian. This interaction Hamiltonian derives from the general interaction between matter and electromagnetic field in non-relativistic quantum theory by the application of both, dipole and rotating-wave approximation. The cavity mode is given as a single harmonic oscillator as usual. The Hamiltonian

of the system thus reads

$$\begin{aligned}\hat{H} &= \hat{H}_m + \hat{H}_{mf} + \hat{H}_f \\ &= \sum_{j=1}^{3} (\omega_j |j\rangle\langle j|) + \lambda_{mf} \left(\hat{\sigma}_{01}\hat{a}^\dagger + \hat{\sigma}_{01}^\dagger \hat{a}\right) + \omega_f \left(\hat{a}^\dagger \hat{a} + \frac{1}{2}\right)\end{aligned} \tag{8.3}$$

with the matter system eigenenergies $\omega_j$, the field mode's frequency $\omega_f$, and the matter-field interaction strength $\lambda_{mf}$. Here, the transition operators $\hat{\sigma}_{ij}$ are defined in analogy to the $\hat{\sigma}_+, \hat{\sigma}_-$ spin operators as

$$\hat{\sigma}_{ij} = |i\rangle\langle j|\,, \tag{8.4}$$

and the model is examined under the case of matter-field resonance $\omega_1 - \omega_2 = \omega_f$. Also, the authors chose $\omega_1 > \omega_2$.

Two baths of temperatures $T_1$ and $T_2$ are selectively coupled to the transitions to the three-level system: The bath with $T_1$ couples to the $|0\rangle \leftrightarrow |1\rangle$ transition, the other to $|0\rangle \leftrightarrow |2\rangle$. Hence, the coupling operators are $\hat{\sigma}_{01}, \hat{\sigma}_{01}^\dagger$ and $\hat{\sigma}_{02}, \hat{\sigma}_{02}^\dagger$, respectively. The master equation is derived from a microscopic model (cf. Sec. 9.4.1), and the dissipators $\mathcal{L}_1, \mathcal{L}_2$ are in Lindblad form:

$$\begin{aligned}\mathcal{L}_{ij}[\hat{\rho}_{mf}] =& \Gamma_{ij} \Big[(n_{ij}+1)([\hat{\sigma}_{ij}\hat{\rho}_{mf}, \hat{\sigma}_{ij}^\dagger] + [\hat{\sigma}_{ij}, \hat{\rho}_{mf}\hat{\sigma}_{ij}^\dagger]) \\ &+ n_{ij}([\hat{\sigma}_{ij}^\dagger \hat{\rho}_{mf}, \hat{\sigma}_{ij}] + [\hat{\sigma}_{ij}^\dagger, \hat{\rho}_{mf}\hat{\sigma}_{ij}])\Big]\,,\end{aligned} \tag{8.5}$$

where we introduced the short-hand notation $\mathcal{L}_1 = \mathcal{L}_{01}$ and $\mathcal{L}_2 = \mathcal{L}_{02}$. $\Gamma_{ij}$ is the Weisskopf-Wigner decay constant associated with the corresponding bath, and $n_{ij}$ is the number of thermal photons in the respective reservoir. The associated reservoir temperature is then given by

$$T_{ij} = \frac{\omega_{ji}}{\ln\left(\frac{1}{n_{ij}} + 1\right)} \tag{8.6}$$

with $\omega_{ji} = \omega_j - \omega_i$. The complete master equation for the model reads

$$\dot{\hat{\rho}}_{mf}(t) = -\,i[\hat{H}, \hat{\rho}_{mf}(t)] + \mathcal{L}_1[\hat{\rho}_{mf}(t)] + \mathcal{L}_2[\hat{\rho}_{mf}(t)]. \tag{8.7}$$

The authors compute the time-dependent dynamics of the model numerically for $\Gamma = \Gamma_{ij} = 0.001$ and $\lambda_{mf} = 1$.

Boukobza and Tannor distinguish two major types of realizations of the model by the comparison of $n_{01}$ and $n_{02}$: The first case, $n_{01} > n_{02}$ is described in Boukobza and Tannor [2006b] and is called *light amplification* mode by the authors. In Boukobza and Tannor [2008] the *light purification* mode is described, which constitutes the second case with $n_{01} < n_{02}$.

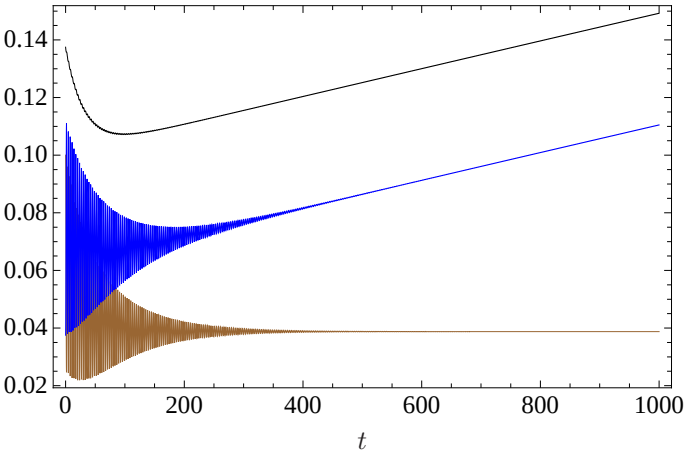


**Figure 8.3:** Energy dynamics of the ED JCM in the light amplification configuration: $\langle \hat{H} \rangle(t)$ (black), $\langle \hat{H}_m \rangle(t)$ (brown), $\langle \hat{H}_f \rangle(t)$ (blue). (The figure shows the results of our own reproduction of the data of Boukobza and Tannor [2006b].)

### 8.3.1 Light amplification dynamics

The authors compute the dynamics of the model for $n_{01} = 10$, $n_{02} = 0.1$, and $\omega_0 = 0$, $\omega_1 = 0.1$, and $\omega_2 = 0.025$. The main features of the dynamics are easily extracted from Fig. 8.3. Initially, there are strong oscillations of the local energies $\langle \hat{H}_f \rangle$ and $\langle \hat{H}_m \rangle$, that die down with an effective decay constant $\Gamma^{\text{eff}} = \Gamma(n_{01} + n_{02})/2$. Moreover, at short times, the collapse and revival phenomenas well known for the JCM (Eberly et al. [1980], Gea-Banacloche [1990]) can be observed.

After the transient dynamics, the three-level matter system exhibits a constant energy and is in a steady state. The whole matter-field system reaches no steady state, though. Instead, the field mode energy increases linearly with time and its state is asymptotically diagonal with a Poissonian distribution for the diagonal elements,

$$\hat{\rho}_f^{\text{asymp}}(t) = \mathrm{e}^{-\langle n \rangle(t)} \sum_{k=0}^{\infty} \frac{\langle n \rangle^k(t)}{k!} |k\rangle\langle k| \,, \tag{8.8}$$

with $\langle n \rangle(t) \propto t$. This state exhibits the same diagonal entries like a coherent

state

$$|\alpha\rangle = \mathrm{e}^{-\frac{|\alpha|^2}{2}} \sum_{k=0}^{\infty} \frac{\alpha^k}{k!} |\alpha\rangle \tag{8.9}$$

but has lost all phase information present in a coherent state, and thus is called *phase-diffused coherent state* by virtue of

$$\hat{\rho}_{\mathrm{PDC}} \propto \int_0^{2\pi} \mathrm{d}\phi \, ||\alpha| \, \mathrm{e}^{i\phi}\rangle\langle|\alpha| \, \mathrm{e}^{i\phi}| \tag{8.10}$$

(Scully and Lamb [1967]). Obviously, in this operation mode, the system leads to a constant and in principle unlimited amplification of the field. The authors compute the amplification efficiency numerically to

$$\eta = \frac{\omega_{12}}{\omega_{20}}, \tag{8.11}$$

which agrees perfectly with the result of Scovil and Schulz-DuBois [1959], Eq. (8.1), and which we have, in turn, identified with the quantum Otto efficiency [Eq. (5.15)]

$$\eta = 1 - \frac{\omega_{20}}{\omega_{10}}. \tag{8.12}$$

### 8.3.2 Light purification dynamics

For $n_{01} < n_{02}$, the system can be shown analytically to relax to an equilibrium state. Clearly, all energy exchange of the system with the baths vanishes. The equilibrium state is characterized by a diagonal state for the three-level system

$$\hat{\rho}_m^{\infty} \propto \begin{pmatrix} r_{02} & & \\ & r_{12} & \\ & & 1 \end{pmatrix} \tag{8.13}$$

with $r_{ij} := (\hat{\rho}_m^{\infty})_{ii}/(\hat{\rho}_m^{\infty})_{jj}$.

The equilibrium state of the field mode is thermal as well, which the authors conclude from the Husimi-Kano function $w$ of the field,

$$w(\hat{\rho}; \mathrm{Re}\,\alpha, \mathrm{Im}\,\alpha) = \frac{1}{\pi} \langle\alpha| \, \hat{\rho} \, |\alpha\rangle \,, \tag{8.14}$$

which is

$$w(\hat{\rho}_f^{\infty}; \mathrm{Re}\,\alpha, \mathrm{Im}\,\alpha) = \frac{1 - r_{12}}{\pi} \exp\left[-(1 - r_{12}) \, |\alpha|^2\right]. \tag{8.15}$$

Comparing this to the Husimi-Kano function of a canonical field state with average photon number $\langle n\rangle = 1/[\exp(\beta\omega_f) - 1]$,

$$w(\hat{\rho}^{\mathrm{can}}; \mathrm{Re}\,\alpha, \mathrm{Im}\,\alpha) = \frac{1}{\pi(\langle n\rangle + 1)} \exp\left(-\frac{|\alpha|^2}{\langle n\rangle + 1}\right), \tag{8.16}$$

the final average photon number of the field mode is found to be $\langle n\rangle_\infty = 1 - r_{12}$.

There are, however, two ways for the field mode to reach its initial state depending on the initial energy content $\langle \hat{H}_f\rangle(0)$ of the field mode. Clearly, when the initial state has more energy than the equilibrium state, $\mathrm{Tr}(\hat{H}_f\hat{\rho}_f^\infty)$, the field excitation will decay until the equilibrium state is reached (light purification). On the other hand, if the initial energy was lower, the field mode's light is amplified but only until it (asymptotically) reaches the equilibrium state. This effect is called by the authors *saturated light amplification*.

### 8.3.3 Thermodynamic interpretation

The authors discuss the ED JCM and the results they found with respect to thermodynamics. They do so by firstly discussing thermodynamics of quantum systems, especially for bipartite quantum systems in Boukobza and Tannor [2006a].

To this end they introduce generalized definitions of work and heat for quantum systems. In particular, they consider a bipartite quantum system with a time-independent Hamilton operator $\hat{H} = \hat{H}_1 \otimes \hat{1}_2 + \hat{H}_{12} + \hat{1}_1 \otimes \hat{H}_2$. The authors assume that the system is coupled to an external heat bath modeled by a dissipative Lindblad super operator $\mathcal{L}$. The action of the Lindblad operator is restricted to system 1.

In order to distinguish between heat and work in this system, they refer to and generalize the heat and work definitions by Alicki [1979]. Alicki considered in his work a single quantum system subject to a time-dependent Hamiltonian $\hat{H}(t)$ and a dissipator in Lindblad form $\mathcal{L}$, thus a system evolving according to the master equation

$$\dot{\hat{\rho}}(t) = -i\left[\hat{H}(t), \hat{\rho}(t)\right] + \mathcal{L}[\hat{\rho}(t)]. \tag{8.17}$$

Alicki identified work $W(t)$ and heat $Q(t)$ as

$$\begin{aligned} W(t) &= \int_0^t \mathrm{d}\tau \,\mathrm{Tr}\left[\left.\frac{\mathrm{d}\hat{H}(t)}{\mathrm{d}t}\right|_{t=\tau} \hat{\rho}(\tau)\right] \\ Q(t) &= \int_0^t \mathrm{d}\tau \,\mathrm{Tr}\left\{\mathcal{L}[\hat{\rho}(\tau)]\hat{\rho}(\tau)\right\}. \end{aligned} \tag{8.18}$$

This definition is justified by proving that it is compatible with the 2nd law and the Carnot efficiency in particular: For any process $\hat{H}(t)$ and any number of baths the quantum system is coupled to, the maximum possible efficiency is Carnot.

The main point of the generalization of the definitions Eq. (8.18) introduced by Boukobza and Tannor [2006a] refers to the definition of work and heat in the bipartite quantum system mentioned above. First, the authors define the local energies of the parts of the system as $U_k = \langle H_k \rangle$. They then consider the change of internal energy of system 1, which is found to be

$$\dot{U}_1(t) = -i\mathrm{Tr}\left(\hat{\rho}(t)[\hat{H}_1, \hat{H}_{12}]\right) + \mathrm{Tr}\left(\mathcal{L}[\hat{\rho}(t)]\hat{H}_1\right). \tag{8.19}$$

The essential step the authors then take is to identify the second term with heat flux by virtue of similarity to Eq. (8.18) and the complete first term as work, defining the work flux $\dot{W}_1$ and heat flux $\dot{Q}_1$ to system 1 as

$$\begin{aligned} \dot{W}_1(t) =& -i\mathrm{Tr}\left(\hat{\rho}(t)[\hat{H}_1, \hat{H}_{12}]\right) \\ \dot{Q}_1(t) =& \mathrm{Tr}\left(\mathcal{L}[\hat{\rho}(t)]\hat{H}_1\right). \end{aligned} \tag{8.20}$$

Consequently, they find for the system 2 only work:

$$\begin{aligned} \dot{W}_2(t) =& -i\mathrm{Tr}\left(\hat{\rho}(t)[\hat{H}_2, \hat{H}_{12}]\right) \\ \dot{Q}_2(t) =& 0. \end{aligned} \tag{8.21}$$

This result can easily be generalized to arbitrary networks of quantum systems coupled to heat baths locally or globally. It can be concluded that the authors implicitly make the following assumptions about heat and work in quantum systems:

1. No heat is exchanged between quantum systems.
2. Heat is only exchanged for systems coupled to heat baths, recognized by their action through dissipative (Lindblad) super operators.

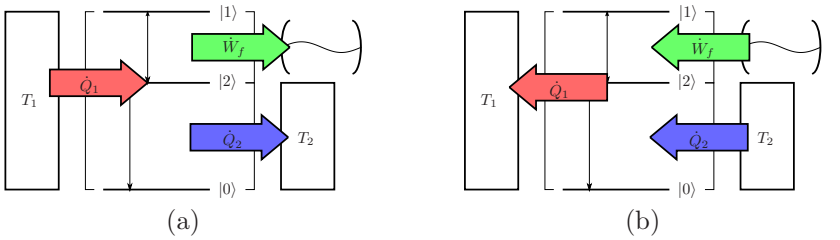


**Figure 8.4:** Operation modes and their heat and work fluxes according to Boukobza and Tannor [2006b] for the two cases of (a) a heat engine for light amplification and (b) a heat pump in the light purification case. The conditions are given in the text. Heat exchanged with the hot bath (red), with the cold bath (blue), and exchanged work (green).

3. Time-dependent Hamiltonians perform work.

If one applies those definitions of heat and work to the ED JCM, the energy exchanged with the field mode is identified as work, while energy exchanged with the heat baths is heat. Thus, whenever the light mode gains energy and the hot bath releases energy, the authors identify the model as a heat engine. This is for example the case in the light amplification case of Sec. 8.3.1 with heat flux $\dot{Q}_1(t)$ coming from the hot bath, being partially converted to work $\dot{W}_f(t)$ and the remainder of the energy being released to the cold bath as heat flux $\dot{Q}_2(t)$. The light purification case is then the opposite, if the field mode relaxes from a high energy state to a energetically lower thermal state, and is therefore considered to be a heat pump. Its effect is to consume work $\dot{W}_f(t)$ from the field mode to take heat $\dot{Q}_2(t)$ from the hot bath $\mathcal{L}_2$ and create a flow $\dot{Q}_1(t) = -\dot{Q}_2(t) - \dot{W}_f(t)$, thus, transferring heat $|\dot{Q}_1(t)|$ to the hot bath $\mathcal{L}_1$ (see Fig. 8.4 for a schematic of the two operation modes).

This interpretation is consistent with the second law since, as noted in Sec. 8.3.1, the efficiency of the light amplification is equal to the quantum Otto efficiency and thus always lower than the Carnot efficiency, and we will see in Sec. 9.1.2 that the efficiency of the light purification equals the efficiency of an Otto heat pump.

## 8.4 Quantum thermodynamic laser model

Waldherr proposed a full quantum model of lasing in analogy to the ED JCM in Waldherr [2009] and Waldherr and Mahler [2010]. The model consists of an interfacing spin (spin 1) resonantly coupled to a quantum harmonic oscillator

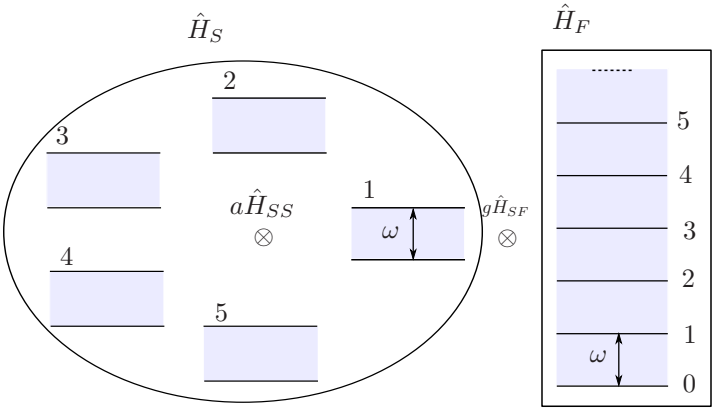


**Figure 8.5:** The full quantum laser model of Waldherr and Mahler [2010]: an interfacing spin coupled to the laser mode is embedded in a finite spin bath. (Figure from Waldherr [2009], with permission of the author.)

representing the lasing field mode. In addition, the spin is coupled to a finite spin bath that models the effect of the two baths in Boukobza and Tannor [2006a] in accordance with the results of quantum thermodynamics for thermodynamically embedded quantum systems (cf. Sec. 1.2). The Hamiltonian of the complete model reads then

$$\hat{H} = \hat{H}_S + \hat{H}_F + a\hat{H}_{SS} + g\hat{H}_{SF} \tag{8.22}$$

with the spin network and field mode Hamiltonians

$$\hat{H}_S = \sum_{j=1}^{N_S} \frac{\omega}{2}\hat{\sigma}_z^{(j)} + \frac{\omega N_S}{2}, \tag{8.23}$$

$$\hat{H}_F = \omega\hat{n} = \omega\hat{a}^\dagger\hat{a}, \tag{8.24}$$

the interaction $\hat{H}_{SF}$ between interfacing spin and field, and the interaction $\hat{H}_{SS}$ between the interfacing spin and its spin environment. $a, g$ are the respective interaction strengths, which are considered to be weak: $a, g \ll 1$.

The spin-field interaction $\hat{H}_{SF}$ is as usual chosen to be the Jaynes-Cummings interaction

$$\hat{H}_{SF} = \hat{a}^\dagger\hat{\sigma}_-^{(1)} + \hat{a}\hat{\sigma}_+^{(1)}, \tag{8.25}$$

while the interaction between the interfacing spin and the spin bath is a random Hermitian matrix drawn from the Gaussian unitary ensemble. The Hamiltonian and its parts fulfill certain commutation relations due to the structure of the Jaynes-Cummings interaction, namely

$$\left[\hat{H}_S + \hat{H}_F, \hat{H}_{SF}\right] = 0 \tag{8.26}$$

$$\left[\hat{H}_F, \hat{H}_{SS}\right] = 0 \tag{8.27}$$

$$\left[\hat{H}_S, \hat{H}_{SS}\right] = 0, \tag{8.28}$$

thus rendering the sum of the energies of the two parts of the system $\hat{H}_S + \hat{H}_F$ a constant of motion. The authors choose an initial state that factorizes for all spins and the field mode. The spins are all taken to start in the excited state, whereas the field mode is initially in its ground state.

According to the findings of quantum thermodynamics, the field subsystem in contact with an environment of spins is expected to relax to an equilibrium state (that is not thermal, however; see below). Due to the structuring of the interaction this equilibration may be inhibited, though, depending on the ratio $a/g$ and the system size $N_S$. This effect has been discussed in Schmidt and Mahler [2005] for spin star and spin ring-star embeddings of a single spin. For a certain parameter range of $a/g$ and $N_S$, Waldherr and Mahler [2010] find that the field mode relaxes to the expected equilibrium state. This equilibrium state has the following local state properties: All spins are found to be in the microcanonical equilibrium state

$$\hat{\rho}^{\infty}_{(j)} = \begin{pmatrix} \frac{1}{2} & \\ & \frac{1}{2} \end{pmatrix}, \tag{8.29}$$

and the field mode's state shows a binomial occupation distribution in the Fock basis

$$P_F(n) \propto \begin{pmatrix} N_S \\ N_S - n \end{pmatrix} \tag{8.30}$$

with a mean photon number $\langle \hat{n} \rangle = N_S/2$. That the field does not relax to a thermal state is merely a result of the small size of the spin environment and the fact that it starts in the state with maximum inversion.

The actual laser operation of the system takes place during the relaxation of the system to its equilibrium state. The author finds that the intermediate states of the field mode are approximately phase-diffused coherent states with increasing average photon number $\langle \hat{n} \rangle(t)$ in nice agreement with the results

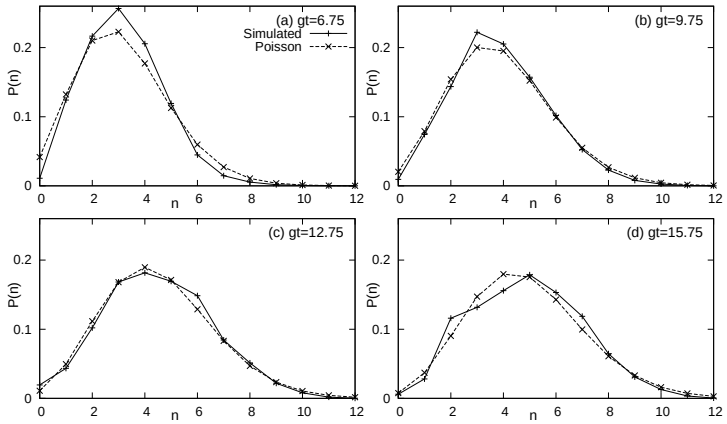


**Figure 8.6:** Field mode occupation numbers at intermediate times of the relaxation process for the initial state with excited spins and field mode in ground state. During the relaxation, the field mode state is nicely approximated by a Poisson distribution for the diagonal. (Figure from Waldherr [2009] with permission of the author.)

of Boukobza and Tannor [2006a], before the field mode eventually blends in with the equilibrium state after the spin network's energy has been depleted as it reaches its own equilibrium state. In Fig. 8.6, the results of Waldherr and Mahler [2010] are depicted.

## 8.5 Laser light and phase-diffused coherent states

In both the previous models, the resulting light mode state is a phased-diffused coherent state characterized by Poisson distributed diagonal elements and vanishing off-diagonal elements in Fock space representation. It might come as a surprise that contrary to what is frequently assumed the laser output state is found to be incoherent, even though "coherence" is actually what is known to distinguish laser light from conventional light sources.

To clarify this seeming contradiction, we must first clearly discriminate between optical coherence and Fock space coherence. Optical coherence means constant phase relations between two modes with different wave vectors $\vec{k}_1$ and $\vec{k}_2$. Fock space coherence on the other hand is a property of a single field mode as in the presented models and refers to the existence of definite

phase relations between the Fock states of this mode and as such is a purely quantum concept.

Scully and Lamb [1967] presented a thorough discussion of a laser model that explicitly models the atoms and the field mode quantum mechanically, and treats the excitation of the atoms and the dissipation of the field mode with a master equation ansatz. It turns out that although the laser field retains its Poissonian distribution for the number of photons in the cavity, the off-diagonal terms decay with a decay constant related to the line width of the laser. Mølmer [1996] triggered a discussion that seems to be going on until today concerning two questions: 1. whether Fock space coherence is necessary to explain quantum optical experiments, and 2. whether laser light should be expected to be Fock space coherent.

Mølmer argues with respect to the first question that all that can or at least usually is measured in quantum optics are mean values of the field operators and their products, that is correlation functions. He is then able to show for the method of heterodyne detection that no Fock state coherence needs to be present in order to derive the expected oscillations of the signal if the measurement process and its effects are taken into account. As the measured quantities in all quantum optical experiments are of the same basic structure as in the heterodyne measurement scheme, he concludes from this result that there is no experimental evidence to expect coherent output states for a large class of typical lasers (although he discusses light generation processes under which the resulting field is expected to show Fock space coherence). On the other hand, by reversing the argument he concludes that it does not "hurt" to assume coherent states for the lasing mode as the results for quantum optical experiments are not changed. To stress this finding, Mølmer calls Fock space coherence a "convenient fiction".

In a quite general analysis of typical laser light generation processes, he then maintains that the excitation of the electromagnetic field by its typically near-resonant interaction with an usually incoherently pumped medium leads 1. to entanglement between field and matter and 2. to vanishing Fock state coherence due to the entanglement and the incoherence of the medium excitation processes. Thus, he concludes that typically laser light will be optically coherent but not Fock space coherent in agreement with Scully and Lamb [1967].

The results of the models presented in this section support this idea, and we take the results of Mølmer [1996] as an indication that we really can and should consider the asymptotic state found in the ED JCM light amplification case and its analogue in the full quantum model of Waldherr and Mahler [2010] laser light. As laser light is usually understood to be useful and able to drive other systems, the result of Sec. 8.3.3 that the field mode is a work reservoir is

supported. However, we will see that this interpretation is neither compulsory nor consistent with the LEMBAS results.

# 9 ED JCM and LEMBAS

In this chapter, we discuss the results found when the LEMBAS method (Sec. 2.3) is applied to the model of Boukobza and Tannor (Sec. 8.3). We start this discussion by some additional analysis of the ED JCM and its properties in the first section of this chapter, introducing the concept of an effective inverse absolute temperature $\beta_{\text{eff}}$ of the transition the field mode of the ED JCM is coupled to and its relation to the operation modes appearing in the model. We then proceed to show that there are fundamental problems with the assumptions of Boukobza and Tannor [2006a], from which the generalized heat and work definitions and the thermodynamic classification of the operation modes of Sec. 8.3.3 are derived. Consequently, in Sec. 9.3 we then apply the LEMBAS method to the ED JCM and will be faced with the completely opposite result to what Boukobza and Tannor found. Finally, in the last section of this chapter, a resolution of the contradictions is attempted.

## 9.1 Effective temperature

We argue in this section that the dynamics and especially the thermodynamics of the ED JCM can be understand more thoroughly by the introduction of an effective inverse temperature parameter

$$\beta_{\text{eff}} = \frac{\beta_1(\omega_1 - \omega_0) - \beta_2(\omega_2 - \omega_0)}{\omega_1 - \omega_2}, \tag{9.1}$$

where $\beta_j$ are the inverse temperatures of the two heat baths connected to the matter system. The average thermal photon number $n_{ij}$ of a heat bath coupled to the transition $|i\rangle\leftrightarrow|j\rangle$ is related to the inverse temperature of the bath by virtue of Eq. (8.6),

$$\beta_{ij} = \frac{\ln\left(\frac{1}{n_{ij}} + 1\right)}{\omega_{ji}}. \tag{9.2}$$

One can always shift the matter system energy levels such that $\omega_0 = 0$ by adding a constant energy term $-\omega_0 \hat{1}_m$ to the matter field Hamiltonian without

changing the model dynamics, and we will therefore assume $\omega_0 = 0$ throughout the following. This leads to the simpler form

$$\beta_{\text{eff}} = \frac{\beta_1\omega_1 - \beta_2\omega_2}{\omega_1 - \omega_2}. \tag{9.3}$$

### 9.1.1 Physical significance

To make the connection of this parameter to the model, we note that $\beta_{\text{eff}}$ is exactly the effective temperature obtained by

$$\frac{(\hat{\rho}_m)_{11}}{(\hat{\rho}_m)_{22}} = \exp\left(-\omega_{12}\beta_{\text{eff}}\right), \tag{9.4}$$

assuming that

$$\frac{(\hat{\rho}_m)_{jj}}{(\hat{\rho}_m)_{00}} = \exp\left(-\omega_{j0}\beta_j\right) \tag{9.5}$$

for $j = 1, 2$ and all other matrix elements of $\hat{\rho}_m$ are zero. Thus, $\beta_{\text{eff}}$ is the effective temperature of the transition $|1\rangle \leftrightarrow |2\rangle$, if the matter system has reached a state where the occupation numbers of state $|1\rangle$ and $|2\rangle$ are in equilibrium with the inverse temperatures of the baths.

But the connection is in fact deeper. In Boukobza and Tannor [2008], the authors derive the equilibrium state of the complete matter-field system analytically, and the part of the state pertaining to the three-level matter system reads [Eq. (8.13)]

$$\hat{\rho}_m^{\infty} \propto \begin{pmatrix} r_{02} & & \\ & r_{12} & \\ & & 1 \end{pmatrix} \tag{9.6}$$

with $r_{ij} := (\hat{\rho}_m^{\infty})_{ii}/(\hat{\rho}_m^{\infty})_{jj}$. The authors find that

$$r_{12} = \exp\left(\beta_2\omega_2 - \beta_1\omega_1\right) \tag{9.7}$$

in the equilibrium state and equating this with Eq. (9.4), we readily find Eq. (9.3). Moreover, the comparison of the Husimi-Kano function of the thermal equilibrium field mode state with the Husimi-Kano function of a thermal state [Eqs. (8.15) and (8.16)] reveals that the average photon number $\langle n\rangle$ of this equilibrium state is

$$\langle n\rangle = \text{Tr}[\hat{n}\hat{\rho}_f^{\text{can}}(\beta_{\text{eff}})], \tag{9.8}$$

and thus the field mode state is a thermal state with exactly the inverse temperature $\beta_{\text{eff}}$.

We can thus conclude that $\beta_{\text{eff}}$ is not a mere formal parameter but, rather, strongly related to the properties of the equilibrium state of the system in the light purification scheme. It is safe to say that the combined effect of the matter system plus heat baths – the environment of the field mode – is that of a heat bath with inverse temperature $\beta_{\text{eff}}$, and it seems highly suggestive that this role of $\beta_{\text{eff}}$ is the same in the amplification case albeit the field mode no longer can reach its designated equilibrium state due to its unbound spectrum.

### 9.1.2 Operation modes and energy flows

The special structure of the interaction and the resonance condition lead to

$$[\hat{H}_m + \hat{H}_f, \hat{H}_{mf}] = 0 \tag{9.9}$$

and thus,

$$\mathrm{d}\langle \hat{H}_m \rangle + \mathrm{d}\langle \hat{H}_f \rangle = 0 \tag{9.10}$$

for the closed system governed by the Hamiltonian of Eq. (8.3) alone. Energy changes in the field, therefore, require corresponding energy changes in the three-level system. So, the change of state $|k\rangle$ in the oscillator to state $|k-1\rangle$ ($|k+1\rangle$) can only happen if the three-level system starts in state $|2\rangle$ ($|1\rangle$) and ends up in state $|1\rangle$ ($|2\rangle$). If the effect from the baths is taken into account, the situation is more complicated. However, one sees from the numerical results that Eq. (9.10) is fulfilled for the considered cases in Boukobza and Tannor [2006b] and Boukobza and Tannor [2008].

This property has a significant effect on the energy fluxes between the matter system and the baths: When the oscillator releases energy to the three-level system, the occupation number of matter state $|2\rangle$ decreases, while that of $|1\rangle$ increases, and vice versa. Since the matter system is found to be in a steady state after the transient oscillations, the baths need to restore the steady state occupation numbers by corresponding energy transfers with the matter system. Hence, if the oscillator releases energy, bath 2 does the same. The sum of the energy flowing from the oscillator and bath 2 into the matter system then necessarily is transferred to bath 1. If the oscillator increases its energy, the energy fluxes are simply reversed.

Obviously, the correlation of the energy flows due to the conservation of the interaction energy allows only for these two different operation modes. We recall here Fig. 8.4, which shows the discussed energy flux patterns, although in

this section we do not yet say anything about the thermodynamic classification of the operation modes.

We have seen in the previous section that the environment of the field mode appears as a heat bath of inverse temperature $\beta_{\text{eff}}$. It is thus expected that the effective temperature will have a significant influence on the operation mode realized by a certain set of system parameters $\omega_1, \omega_2, \beta_1, \beta_2$. For $\beta_{\text{eff}} > 0$, the ED JCM clearly leads to a relaxation of the field mode to a thermal state with the same temperature. For $\beta_{\text{eff}} < 0$, relaxation takes place similarly but due to the unbound spectrum of the field mode instead of reaching an equilibrium state, the average photon number is amplified.

However, not only the effective temperature but also the initial energy content

$$\langle \hat{H}_f \rangle_0 := \text{Tr}[\hat{H}_f \hat{\rho}_f(0)] \tag{9.11}$$

of the field mode plays a role in determining the dynamics of the system. Considering the possible operation modes for the case $\beta_{\text{eff}} > 0$ with respect to the energy fluxes, we have to distinguish whether

$$\langle \hat{H}_f \rangle_0 > \langle \hat{H}_f \rangle_{\beta_{\text{eff}}}, \tag{9.12}$$

where we have defined $\langle \hat{H}_f \rangle_{\beta_{\text{eff}}} := \text{Tr}[\hat{H}_f \hat{\rho}_f^{\text{can}}(\beta_{\text{eff}})]$ as the energy expectation of the field mode in the thermal state with inverse temperature $\beta_{\text{eff}}$. If Eq. (9.12) holds, the field mode relaxes to the equilibrium state defined by $\beta_{\text{eff}}$, releasing energy to the matter system, whereas for the opposite case, $\langle \hat{H}_f \rangle_0 < \langle \hat{H}_f \rangle_{\beta_{\text{eff}}}$, the energy flux is reversed and corresponds to the situation in the light amplification case. Thus, we can distinguish the following two sets of conditions for the occurrence of the two different operation modes depending on $\beta_{\text{eff}}$ and $\langle \hat{H}_f \rangle_0$:

(a) $\beta_{\text{eff}} < 0$, or $\beta_{\text{eff}} > 0 \wedge \langle \hat{H}_m \rangle(0) < \text{Tr}[\hat{H}_m \hat{\rho}_m^{\text{can}}(\beta_{\text{eff}})]$: The field mode gains energy, heat is released by bath 1 and absorbed by bath 2.

(b) $\beta_{\text{eff}} > 0 \wedge \langle \hat{H}_m \rangle(0) > \text{Tr}[\hat{H}_m \hat{\rho}_m^{\text{can}}(\beta_{\text{eff}})]$: The field mode releases energy with reversed heat flux pointing from bath 2 to bath 1.

Whether the system in one of those two operation modes is to be considered a heat engine or heat pump according to the thermodynamic interpretation of Sec. 8.3.3, additionally depends on the temperatures of the baths.

### 9.1.3 Combining operation modes

We note here a peculiarity of the thermodynamics of the ED JCM when considering a combination of two realizations of the model operating in different

modes. To illustrate this, let us first consider the model in the heat engine mode with $\beta_{\text{eff}} < 0$ after the transient behavior. Then, the field mode's excitation will be amplified linearly. After some time $\tau$, which we assume to be much larger than the transient time, the system thus will be in a phase-diffused coherent state with a certain mean photon number $\langle n \rangle(\tau)$.

One could now consider another instance of the ED JCM, but now with $\beta'_{\text{eff}} > 0$. Let us assume that the energy of the oscillator with $\hat{\rho}_f(\tau) = \hat{\rho}_{\text{PDC}}[\langle n \rangle(\tau)]$ be larger than the energy of the canonical state $\hat{\rho}_f = \hat{\rho}_f^{\text{can}}(\beta'_{\text{eff}})$ with inverse temperature $\beta'_{\text{eff}}$. If we now use the field mode of the first instance as the field mode of the second one, according to what we have discussed in the previous paragraphs, the second instance of the system now would run as a heat pump, consuming the energy of the field to maintain a heat flow from the cold to the hot bath. It therefore seems as if the field mode indeed acts as a work source to drive the heat pump. Moreover, as Youssef et al. [2009] have shown with help of their similar model, it really doesn't matter in what state the field mode is in order to get the heat pump running if only $\langle \hat{H}_f \rangle_0$ is higher than the energy of the thermal state with inverse temperature $\beta_{\text{eff}}$.

This gedanken experiment still supports the thermodynamic interpretation of Boukobza and Tannor [2006a]. Nonetheless, we proceed to show in the following section that the approach of the authors is fundamentally flawed. An alternative interpretation based on the LEMBAS method is then discussed in the subsequent sections.

## 9.2 Problems of the thermodynamic definitions

In this section, we point out that the approach of the definition of heat and work of Boukobza and Tannor [2006a] is inconsistent. We start by recalling the basic assumptions of the heat and work definitions by the authors:

1. No heat is exchanged between quantum systems.

2. Heat is only exchanged for systems coupled to heat baths, recognized by their action through dissipative (Lindblad) super operators.

3. Time-dependent Hamiltonians perform work.

The first problem of the approach is that assumption 2 in fact is a tautology: Heat flux is identified by the presence of a heat bath. But how to define a heat bath? Usually, one identifies it by the heat flux it generates, and here the cat eats its tail. Even worse, assumption 1 readily leads to the unphysical result that there exists no heat at all.

To demonstrate this, let us consider a microscopic model of a system coupled to a heat bath that might for example consist of a large number of harmonic oscillators as considered in Breuer and Petruccione [2002], Sec. 3.4, or Saito et al. [2000]. The Hamiltonian of the complete model would then be simply given by $\hat{H} = \hat{H}_S + \hat{H}_{SB} + \hat{H}_B$. Now, according to Boukobza and Tannor [2006a], if we derive the reduced dynamics of the system of interest, we find a master equation

$$\dot{\hat{\rho}}_S = -i[\hat{H}_S, \hat{\rho}_S(t)] + \mathcal{L}[\hat{\rho}_S(t)] \tag{9.13}$$

with a dissipator $\mathcal{L}$ acting on the system state (again, see Breuer and Petruccione [2002], Sec. 3.4, or Saito et al. [2000] for a derivation). Since the system itself is only in contact with the oscillators from the heat bath and the heat bath has been integrated out to give the dissipator, all energy flowing to or from the system is exchanged with the heat bath:

$$\frac{\mathrm{d}U_S}{\mathrm{d}t} = \frac{\mathrm{d}\langle \hat{H}_S \rangle}{\mathrm{d}t} = \mathrm{Tr}\{\hat{H}_S \mathcal{L}[\hat{\rho}_S(t)]\} \tag{9.14}$$

On the other hand, we might alternatively decide not to trace over the degrees of freedoms of the heat bath but consider the complete system as a single closed bipartite quantum system with no external couplings described by the Hamiltonian $\hat{H} = \hat{H}_S + \hat{H}_{SB} + \hat{H}_B$. Hence, we find for the change of internal energy

$$\dot{U}_S(t) = -i\mathrm{Tr}\{\hat{\rho}(t)[\hat{H}_S, \hat{H}_{SB}]\}, \tag{9.15}$$

which, by comparison to the definitions Eq. (8.20), has to be considered pure work if we want to follow the argumentation of the authors. In the end, however, every heat bath is a quantum system, only a very (infinitely) large one with time-independent interactions to the system of interest. By consequence of the present argument, no heat bath could ever exchange heat, which is an awkward contradiction at least.

In the light of Part I, it is obvious where the misapprehension of Boukobza and Tannor [2006a] lies: By identifying the term

$$-i\mathrm{Tr}(\hat{\rho}(t)[\hat{H}_1, \hat{H}_{12}]) \tag{9.16}$$

in Eq. (8.20) completely with work flux, they disregard the possibility of incoherent dynamics introduced by the presence of the second system, as is seen Sec. 2.3, particularly Eq. (2.39). Thus, they cannot account for any heat exchange between quantum systems at all (as shown with the help of the microscopic heat bath model).

We conclude that the assumptions made in Boukobza and Tannor [2006a] for the derivation of heat and work in bipartite quantum systems are inconsistent, despite their seemingly consistent results discussed in the previous section and Sec. 8.3.3. To solve this puzzle, we now apply the LEMBAS method to the ED JCM in the following section, and elaborate on the correct thermodynamic interpretation in the subsequent sections.

## 9.3 Thermodynamics of the ED JCM with LEMBAS

The matter-field system of the ED JCM evolves according to the master equation (8.7). If we want to apply the LEMBAS principle, we have to introduce a partitioning into system and environment first. Since we are interested in the thermodynamic role of the field mode, we will divide the system into the field mode and its surroundings, that is the three-level matter system together with the baths. The effective local equation of the field mode is then given by

$$\dot{\hat{\rho}}_f(t) = -i[\hat{H}_f + \hat{H}_f^{\text{eff}}(t), \hat{\rho}_f(t)] + \mathcal{L}_f^{\text{eff}}[\hat{\rho}_{mf}(t)], \tag{9.17}$$

where $\hat{H}_f^{\text{eff}} = \text{Tr}_m\{[\hat{\rho}_m(t) \otimes \hat{1}_f]\hat{H}_{mf}\}$ as usual. We know from Boukobza and Tannor [2006b] and Boukobza and Tannor [2008] that for both operation modes of the model, the matter system reaches a diagonal state in the energy eigenbasis after the transient behavior. Both terms of the interaction Hamiltonian $\hat{H}_{mf}$ have only non-vanishing off-diagonal terms [cf. Eq. (8.3)], though, and by consequence, $(\hat{\rho}_m \otimes \hat{1}_f)\hat{H}_{mf}$ has only off-diagonal terms, too. Thus, its trace is zero and $\hat{H}_f^{\text{eff}}$ vanishes for all times after the transient regime. It follows that the dynamics of the field mode for both operation modes, laser and heat pump, is completely governed by $\mathcal{L}_f^{\text{eff}}$. Only incoherent dynamics take place.

By consequence, according to LEMBAS, the field mode is a pure heat reservoir because of

$$đW_f = 0, \tag{9.18}$$

$$đQ_f = \text{d}U_f. \tag{9.19}$$

This is not only the exact opposite result to that of Boukobza and Tannor [2006a] but seems also to contradict our intuition: Lasers are usually considered to provide "useful" energy, in the sense that one can drive other systems coherently, a feature we would clearly attribute to work reservoirs. Moreover, the LEMBAS result seems to be outright unacceptable in the light of what

has been said in Sec. 8.3.3. We have seen there that we can first load up the field mode in the lasing operation mode and then plug it to another instance of the baths-matter part of the system and use the energy in the field mode to drive a heat pump.

On the other hand, the fact that the local effective dynamics of the field mode are completely described by the incoherent dissipator $\mathcal{L}_f^{\text{eff}}$ is an indicator – even from the viewpoint of Boukobza and Tannor [2006a], if one takes the local effective dynamics into account – that we cannot simply dismiss the LEMBAS result as wrong. We discuss four different approaches in the following section to solve this conflict and bring forth arguments, why the LEMBAS result is in agreement with thermodynamics and in so far correct.

## 9.4 Resolution of the contradictions

### 9.4.1 Validity of the master equation

We will first turn to the question of the validity of the master equation derived in Boukobza and Tannor [2006b]. The master equation is indeed in Lindblad form and it is well known that it is therefore an element of the dynamical semigroup of quantum Markov processes (see Sec. 1.3.1) describing physical reality (to some accuracy). However, an arbitrary Lindblad master equation conversely may be hard to realize physically and is not necessarily the physically correct description of a given open quantum system. This has been discussed especially for the situation of baths only coupling locally to the system of interest and for transport scenarios, where two or more baths are in contact with the system (see Wichterich et al. [2007] and Saito et al. [2000]). The ED JCM actually has both mentioned properties, and therefore it seems at least possible that – although in Lindblad form and in principle sensible – the actual result is "unphysical."

We first address the effects of local couplings: Consider a bipartite system $\hat{H} = \hat{H}_1 + \lambda_{12}\hat{H}_{12} + \hat{H}_2$ which is coupled via a local interaction operator $\hat{X} = \hat{x} \otimes \hat{1}_2$ to a bath of oscillators, where $\hat{x}$ is some Hermitian operator acting on system 1's Hilbert space only. Let $\mathcal{L}_{\lambda_{12}}$ be the dissipator that is found according to the derivation of a Lindblad master equation for a bosonic bath in the weak system-bath coupling limit as presented in Breuer and Petruccione [2002], Sec. 3.3.1. Because of the local coupling of the bath to the system, one could be tempted to assume that it would be as well possible to derive the master equation by first ignoring system 2, that is, assuming that $\lambda_{12} = 0$, then deriving the dissipator $\mathcal{L}_0$ and then calculate the dynamics of the system with this dissipator. We call this procedure *trivial local-coupling Lindblad*. It

is found, however, that usually $\mathcal{L}_{\lambda_{12}} \neq \mathcal{L}_0$, even for weak coupling $\lambda_{12}$, when the systems 1 and 2 are not homogeneous.

The dissipators in the ED JCM are exactly of this trivial local-coupling Lindblad form in contradiction to the fact that the authors assume strong matter-field interaction ($\lambda_{mf} = 1$ while $\omega_j, \omega_f \approx 10^{-1}$). However, the authors derive the master equation from a microscopic model analogously to the derivation of Saito et al. [2000], and the surprising result can be traced back to the JCM type interaction between matter and field.

With respect to transport scenarios and Lindblad dissipators, the results of Wichterich et al. [2007] are as follows. In order to obtain a Lindblad dissipator from a microscopic model, two approximations have to be made (cf. Sec. 1.3.2): The first one is the Born-Markov approximation and essentially states that the bath correlation time is much smaller than the relaxation time. The second approximation – and this is the problematic one in the context of transport scenarios – is the secular approximation that omits rapidly oscillating terms in the dissipator essentially replacing the generator of the interaction picture master equation by its time average, and is justified for a single bath if the time scale set by the Bohr frequencies of the system is short compared to the relaxation time.

Wichterich et al. [2007] show that the secular approximation leads to unphysical situations for transport scenarios, namely, the steady state exhibits vanishing currents in a chain of identical systems locally coupled to heat baths of different temperatures at both ends. This special property is common to all master equations with Lindblad dissipators obtained through the secular approximation, and is even present in the weak-coupling limit. Moreover, they show that a transport master equation can only be brought into Lindblad form by a non-standard approximation not related to the secular approximation.

However, the authors of Boukobza and Tannor [2006a] numerically established that the steady state of the complete matter-field system in the laser case has non-vanishing off-diagonal terms. Those coherence terms indeed correspond to a current between matter and field, which supports the validity of the ED JCM master equation from the viewpoint of Wichterich et al. [2007]. In addition, the authors performed a microscopic derivation similar to Saito et al. [2000] without explicitly performing a secular approximation, which is another reason to trust its results.

Yet another point in favor of the validity of the ED JCM master equation are the works of Youssef et al. [2009] and Waldherr and Mahler [2010]. In the first work, the interaction is much weaker ($\lambda_{mf} = 0.1$ compared to $\omega_j$ of the order of 1). This model shows the same qualitative behavior as the ED JCM, though, which rules out the possibility that due to the strong coupling and an

implicit unjustified secular approximation the ED JCM does yield erroneous results.

Still, Youssef et al. [2009] use a master equation which necessarily is afflicted by some approximations. This is not the case for the fully quantum model of Waldherr and Mahler [2010], and if the approximations made to derive the master equation of Boukobza and Tannor [2006b] caused any unphysical results or were responsible for vanishing coherences in the matter or field state, those effects should surface in the comparison of the results of this model with the master equation results. However, the energy flow from the spin network to the oscillator is found to be completely heat according to LEMBAS, in agreement with the results found for the ED JCM and Youssef et al. [2009]. Thus, the vanishing of the off-diagonal terms of $\hat{\rho}_m$, that could give rise to a work term through a non-zero $\hat{H}_f^{\text{eff}}$, is confirmed in a fully quantum model.

We conclude from the considerations here that there is no reason to doubt the validity of the ED JCM master equation.

### 9.4.2 Consequences of negative effective temperature

In Sec. 9.1.2, we showed that the laser operation mode is bound to the condition $\beta_{\text{eff}} < 0$. Moreover, the analysis of the local effective dynamics in Sec. 9.3 has shown that the surroundings of the field mode given by the combined system consisting of the matter system and the baths indeed act as a pure dissipative system. We have established the physical significance of $\beta_{\text{eff}}$ in Sec. 9.1.1 and if one takes the result seriously, we should consider the environment of the field mode as a heat bath with negative absolute temperature.

It is known in the literature that negative absolute temperature systems exhibit counterintuitive thermodynamic features. Ramsey [1956] and Landsberg [1977] have discussed the consequences of negative temperatures for fundamental thermodynamic relations and heat engines in particular. A first important conclusion of the authors is that negative temperatures are hotter than positive temperatures, such that one should consider a system to be maximally cold at $T = 0$ ($\beta = \infty$), then go over $T = +\infty$ ($\beta = +0$) and $T = -\infty$ ($\beta = -0$) finally to the maximally hot case $T = -0$ ($\beta = -\infty$), if constantly fed with energy.

Additionally, the authors show that although the Clausius and the entropy formulation of the 2nd law hold also for heat engines operating at negative temperatures, the Kelvin-Planck formulation has to be reformulated as

> "It is impossible to construct an engine that will operate in a closed cycle and produce no effect other than (1) the extraction of heat from a positive temperature reservoir with the performance

> of an equivalent amount of work, or (2) the rejection of heat into a negative-temperature reservoir with the corresponding work being done on the engine."

(cf. Ramsey [1956]). The most important conclusion of this is given by Landsberg [1977] as the modified Kelvin-Planck statement:

> "Heat can be completely converted into work by a heat engine which takes a medium through a cyclic process, if and only if that heat is withdrawn from a negative-temperature reservoir."

Thus, if we consider the fact that the field mode surroundings appear as a negative temperature heat bath, we conclude that it is absolutely possible that a field mode loaded with heat during the lasing operation can have this heat completely converted into work, when coupled to the light purification system, and thus drive a heat engine.

We can even think of a model similar to the one considered in Sec. 9.1.3, where the field mode of a ED JCM in lasing mode is directly coupled to another matter-baths system configured for light purification (see Fig. 9.1). Then, the model is expected to lead to a constant heat flow from the cold to the hot bath in the second system. This seems to support the thermodynamic definitions of Boukobza and Tannor [2006b] as the heat engine is expected to consume work for its operation. However, since the energy is taken from an effective negative temperature bath, there is no longer a contradiction to interpreting the energy as heat since, according to the results of Landsberg [1977], the heat can be completely converted to work.

Although this result seems to merge both of the viewpoints, LEMBAS and Boukobza and Tannor [2006b], it is clear from results of Youssef et al. [2009] and Boukobza and Tannor [2008] that this is not the case: It simply does not matter what state the field mode is in to drive the light purification scenario as long as $\langle \hat{H}_f \rangle$ is larger than the mean energy of the equilibrium state. Thus, not only phase-diffused coherent states that are the result of the field mode being in contact with an effective negative absolute temperature heat bath can drive the heat pump, every state reached by thermalizing the field mode with any other heat bath of positive temperature $\beta_3$ that fulfills $\beta_3 < \beta_{\text{eff}}$ will do the job. This clearly rules out negative temperatures as the resolution of the conflict.

However, if we look at the system as depicted in Fig. 9.1(b) as consisting of three parts, namely an effective bath of negative temperature connected to an effective bath of positive temperature via the field mode, it seems reasonable again to label the energy flow heat. In this picture, the model is a simple transport model with the particularity that we face heat transport between a

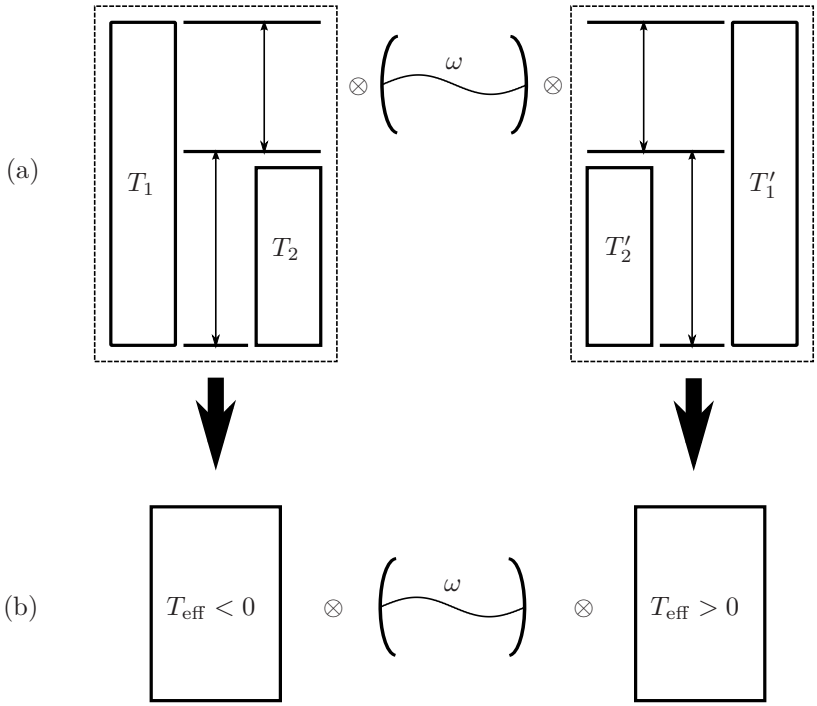


**Figure 9.1:** (a) Combination of two ED JCMs interconnected via a common field mode. The left two-baths-matter part is considered to be configured for light amplification, whereas the right instance is supposed to purify the field mode. (b) Alternative interpretation based on the necessary partitioning introduced by the LEMBAS method: the field mode is considered the system of interest, while the two partial ED JCMs form its surroundings. The two parts of the environment introduce two independent effective dissipators $\mathcal{L}_f^{\text{eff}}$ distinguishable by their exclusive dependence on either the interaction with the left or the right environment.

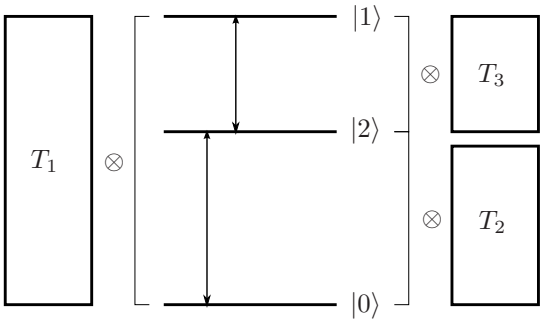


**Figure 9.2:** Analogous model to the ED JCM with the field mode replaced by a third bath. In this case, there is no doubt that the energy flowing to the system is heat.

bath of negative absolute temperature and a "normal" bath. The direction of the heat flux is – as expected from the thermodynamics of negative absolute temperatures – pointing from the hotter negative absolute temperature bath to the colder positive temperature bath. This consideration motivates the approach to the problem taken in the following subsection: replacing the field mode by a third heat bath.

### 9.4.3 Heat pump mode using a third heat bath

A way to clarify whether or not the energy flowing from the field mode to the light purification ED JCM can be heat is to make sure that the matter-bath system is fed by heat only and check whether or not the operation is impeded. We examine this approach by replacing the field mode by a heat bath given by another Lindblad dissipator $\mathcal{L}_3 = \mathcal{L}_{21}$ [cf. Eq. (8.5)].

The master equation for the remaining matter system is then given by

$$\dot{\hat{\rho}}_m(t) = -i[\hat{H}_m, \hat{\rho}_m(t)] + \sum_{j=1}^{3} \mathcal{L}_j[\hat{\rho}_m(t)]. \tag{9.20}$$

In Fig. 9.3, the heat fluxes $\dot{Q}_j$ to the heat baths are displayed for the stationary state dependent on the temperature $T_3$ of the third bath. $\dot{Q}_j$ is thus positive if the bath $j$ gains heat.

Again, we chose the parameters like Boukobza and Tannor [2006b]: $\omega_0 = 0, \omega_1 = 0.1, \omega_2 = 0.025, \Gamma_{01} = \Gamma_{02} = \Gamma_{03} = 0.001, n_{01} = 5, n_{02} = 10$, corresponding to $T_1 \approx 0.55, T_2 \approx 0.26$. Then, $T_{\text{eff}} \approx 0.86 > 0$ and the system

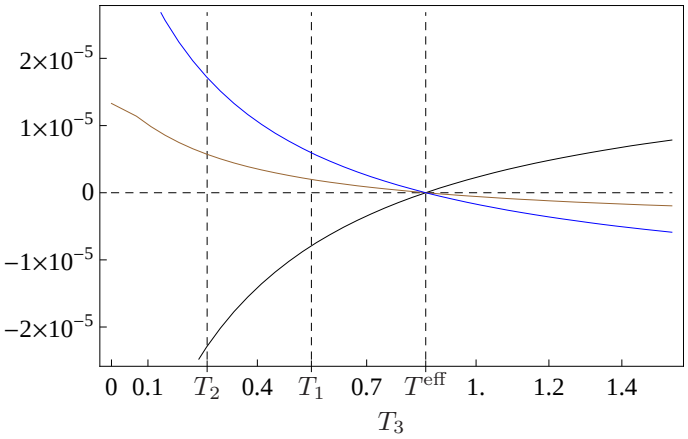


**Figure 9.3:** Stationary state heat fluxes $\dot{Q}_1$ (black, to the hot bath), $\dot{Q}_2$ (brown, to the cold bath), and $\dot{Q}_3$ (blue, to the field mode replacement bath). $\dot{Q}_j$ is positive if the respective bath gains energy.

is in the light purification mode if a field mode were present. The results of Fig. 9.3 show clearly that for $T_3 > T_{\text{eff}}$, heat flows from the cold bath 2 to the hot bath 1, while heat is drawn from the field mode replacement bath. Thus, although the energy coming from the replacement bath is heat for sure, it seems as if this heat were capable to sustain the heat flow from cold to hot. We will see in the following Sec. 9.4.4 that this is not a contradiction to thermodynamics when observing how the effective temperature is determined by the other temperatures in the system.

Let us note here some additional remarkable features of the ED JCM with replacement bath: At $T_3 = T^{\text{eff}}$, all fluxes vanish in the steady state, and below $T^{\text{eff}}$ the operation mode of the model switches back to the lasing mode, where the replacement bath gains energy as well as the cold bath, while the hot bath releases energy (cf. Fig. 9.3). This is again in nice agreement to the properties of ED JCM discussed in Sec. 9.1.2: If the state of the field mode has less energy than the thermal state with $T^{\text{eff}}$, the operation mode switches to lasing (or saturated amplification, as Boukobza and Tannor [2008] call it in the case of the ED JCM).

### 9.4.4 Thermodynamic analysis

In the present section, we will establish that the LEMBAS interpretation is in accord with thermodynamics by fundamental entropic considerations. The core argument will be that for $T_3 > T^{\text{eff}}$ the light purification process is spontaneous and should not be considered a heat pump process.

The key to reach this result is the dependence of the effective temperatures on the other temperatures and the inequalities constraining the possible values of $T^{\text{eff}}$ with respect to $T_1$ and $T_2$. Hence, we first discuss this dependence and to this end, we recall the definition of the effective temperature from Eq. (9.3) in the form for $\omega_0 = 0$

$$\beta_{\text{eff}} = \frac{\beta_1\omega_1 - \beta_2\omega_2}{\omega_1 - \omega_2}. \tag{9.21}$$

Moreover, we assume $\omega_1 > \omega_2$ without loss of generality, since the $\beta_j$ are arbitrary and thus any arrangement of the heat baths and the local coupling can be achieved by choosing the heat bath temperatures appropriately. Let us assume that whenever $\beta_{\text{eff}} > 0$ in the following, the initial field mode energy is greater than the average field mode energy for a thermal state with inverse temperature $\beta_{\text{eff}}$, that is $\langle \hat{H}_f \rangle_0 > \langle \hat{H}_f \rangle_{\beta_{\text{eff}}}$ [cf. Eq. (9.12)], such that saturated light amplification does not take place. Also, let us define

$$\nu := \frac{\omega_2}{\omega_1} < 1 \tag{9.22}$$

and assume $\beta_{1,2} > 0$.

Due to the fact that $\beta_{\text{eff}}$ must be either positive or negative depending on the type of operation mode requested, the possible choices for the other baths are restricted to

$$\frac{\beta_1}{\beta_2} \gtrless \nu < 1, \tag{9.23}$$

where the "less than" sign is for the light amplification case and in this case, $\beta_1 < \beta_2$ for sure. For the light purification case, Eq. (9.21) yields

$$\beta_{\text{eff}}(\beta_1, \beta_2, \nu) = \frac{\beta_1 - \nu\beta_2}{1 - \nu}. \tag{9.24}$$

In the field purification case, even though $\beta_{\text{eff}} > 0$ according to Eq. (9.23), $\beta_1 > \beta_2$ is definitely possible. In this case, however, the bath coupled to the transition $|0\rangle \leftrightarrow |1\rangle$ is colder than the bath coupled to $|0\rangle \leftrightarrow |2\rangle$ and the energy flow from the baths is directed from hot to cold. Since this is no problem with

thermodynamics to happen spontaneously, we will ourselves restrict here to the possibly conflicting case of $\nu\beta_2 < \beta_1 < \beta_2$. Together with the constraint Eq. (9.23) we realize that

$$0 < \beta_{\text{eff}} < \beta_2. \tag{9.25}$$

$\beta_{\text{eff}}$ reaches its maximum $\beta_2$ for the maximum of $\beta_1$, $\beta_1 \to \beta_2$. Eq. (9.24) shows that the slope of $\beta_{\text{eff}}$ as a function of $\beta_1$ is bigger than 1 due to $\nu < 1$ and because of the linearity of $\beta_{\text{eff}}$ in $\beta_1$ we find

$$\beta_{\text{eff}} < \beta_1 \tag{9.26}$$

in the given parameter range. Thus, we know that for the whole class of ED JCMs for which there is a heat flux from the cold to the hot bath sustained by energy flux from the field mode to the matter system, it is

$$T^{\text{eff}} > T_1, T_2. \tag{9.27}$$

Clearly, if the only thermal states of the field mode or replacement baths of temperatures $T_3$ that can sustain the alleged heat pump dynamics are of higher temperature than all other involved baths, it is no longer a surprise that the model can sustain a heat flow from cold to hot.

To make this statement rigorous, we will once again invoke the three bath replacement model of Sec. 9.4.3, Fig. 9.2, and discuss the entropy production of the model in the steady state. For the replacement bath temperature, due to Eq. (9.27) we analogously have to fulfill $T_3 > T_1, T_2$, because obviously $T_3 > T^{\text{eff}}$. In the steady state, the matter systems energy does not change, and thus

$$\frac{\mathrm{d}\langle H_m\rangle}{\mathrm{d}t} = 0 = -\sum_{j=1}^{3} \dot{Q}_j, \tag{9.28}$$

where the $\dot{Q}_j$ are again heat fluxes to the respective baths as in the previous section.

At this point, we need to make use of the extensivity of the entropy in the system in order to be able to give an entropy argument. The derivation of the master equation in Boukobza and Tannor [2006b] implicitly makes use of the assumption that the projection of the total system-baths state $\hat{\rho}$

$$\mathcal{P}\hat{\rho} = \hat{\rho}_{mf} \bigotimes_{j=1}^{3} Z_j^{-1}(\beta_j) \exp\left(-\beta_j \hat{H}_{B,j}\right) \tag{9.29}$$

is a valid approximation for $\hat{\rho}$, where $\hat{H}_{B,j}$ are the respective bath Hamiltonians and $Z_j(\beta_j)$ the partition functions [cf. Sec. 1.3.2, Eq. (1.28), and for more details, Breuer and Petruccione [2002], Sec. 3.3.1 and Sec. 9.1]. This approximation is known as the Born approximation. Hence, by accepting the derivation of the dissipators of the ED JCM, one implicitly also assumes extensivity of entropy.

We can then exactly give the entropy production rate in the steady state (that is vanishing entropy production of the matter system) as

$$\dot{S} = -\sum_{j=1}^{3} \beta_j \dot{Q}_j. \tag{9.30}$$

Together with Eq. (9.28) we can bring this into the form

$$\dot{S} = -\dot{Q}_2(\beta_1 - \beta_2) - \dot{Q}_3(\beta_1 - \beta_3). \tag{9.31}$$

Here, we make use of a special property of a steady state situation that not only the energy of the three-level system is conserved [used to obtain Eq. (9.31)] but the occupation numbers are as well. Thus, if the hot heat bath 1 gets one quantum $\omega_1$ of heat, in order to fulfill the steady state condition, the heat bath 2 and 3 have to feed the matter system with heat quantums $\omega_2$ and $\omega_{12} = \omega_1 - \omega_2$, respectively. If the overall heat flux into bath 1 is given by

$$\dot{Q}_1 = q\omega_1, \qquad q > 0 \quad \text{here}, \tag{9.32}$$

we get the relations

$$\begin{aligned} \dot{Q}_2 &= -q\omega_2, \\ \dot{Q}_3 &= -q(\omega_1 - \omega_2), \end{aligned} \tag{9.33}$$

and the entropy production then is found to be

$$\dot{S} = q\left[\omega_2(\beta_1 - \beta_2) + (\omega_1 - \omega_2)(\beta_1 - \beta_3)\right]. \tag{9.34}$$

Next, we invoke $-\beta_3 > -\beta_{\text{eff}}$ and thus $-(\omega_1 - \omega_2)\beta_3 > -(\omega_1 - \omega_2)\beta_{\text{eff}}$ to eventually end up with

$$\dot{S} > q\left[\omega_2(\beta_1 - \beta_2) + (\omega_1 - \omega_2)(\beta_1 - \beta_{\text{eff}})\right] = 0 \tag{9.35}$$

for the entropy production. The equality on the right-hand side can easily be verified by insertion of $\beta_{\text{eff}}$ from its definition in Eq. (9.21).

We conclude that since the entropy production of the total system is positive, this process is spontaneous and therefore bound to happen by the laws

of thermodynamics even though the system is "driven" by a heat bath. In fact, the light purification mode is therefore no heat pump but a transport scenario with a very special structuring of the heat flows through intricate engineering of the way the heat baths couple to each other leading to strict correlations in the heat flows. Note, that for $\beta_3 = \beta_{\text{eff}}$, the inequality becomes an equality and the three-bath model reaches its quasistatic limit. As usual, for the dynamic model the fluxes vanish in this case as is seen to perfectly agree with the result of the previous section in Fig. 9.3.

## 9.5 Conclusion

In Ch. 8 we have presented a number of thermodynamic models of the lasing process with particular focus on the ED JCM, for which we have thoroughly discussed its pertinent operation modes, mainly light amplification and purification, and their thermodynamic interpretation according to Boukobza and Tannor [2006a]. As a central feature of the operation modes, we highlighted the heat flux from the cold to the hot bath sustained by an additional energy flow from the field mode to the system. The resemblance of the model to a heat pump and the arguments of Boukobza and Tannor [2006a] seemed to support the idea that the field mode in this model is a work source. In addition, we have related the results to the models of Scovil and Schulz-DuBois [1959], Youssef et al. [2009], and the fully quantum model of Waldherr and Mahler [2010], and have shown that the results are qualitatively very much all the same, strengthening the position of ED JCM.

In the present chapter, we first elaborated on a number of new details of the properties of the ED JCM, especially the physical significance of the effective inverse temperature $\beta_{\text{eff}}$ of the $|1\rangle \leftrightarrow |2\rangle$ transition and its relation to the operation modes. We then pointed out that the thermodynamic definitions used by Boukobza and Tannor [2006a] to distinguish work and heat and thus classify the operation modes with respect to their thermodynamic functionality are seriously flawed. We then applied the LEMBAS method to the ED JCM and were faced with the contradiction that according to LEMBAS, all the energy exchanged with the field mode after the transient dynamics of the model should be heat, even though the field energy can be used to sustain a heat transport from cold to hot.

So as to decide this conflict, we have combined four approaches. First, we tried to make sure in Sec. 9.4.1 that the derived master equation of Boukobza and Tannor [2006b] is correct and physically reasonable. We then invoked in Sec. 9.4.2 the concept of negative absolute temperature baths and the consequences for the thermodynamics of systems interacting with them. We showed

there that a light amplification ED JCM sharing its field mode with a light purification ED JCM does not violate the 2nd law and is consistent with the peculiarities of thermodynamics with negative absolute temperatures. However, not only negative temperature states or states reached by the application of heat at negative temperatures were seen to be capable of driving the heat pump. Thus, this explanation falls short as well. In the subsequent Sec. 9.4.3, we replaced the field mode with a heat bath and found that the heat bath can sustain the heat flux from cold to hot the same way as the field mode did in the ED JCM. We thus confirmed that there is no necessity to consider the field energy flux as work on thermodynamic grounds. The resolution of these contradictory findings was finally given in the last section by invoking the entropy production of the three bath model to show the thermodynamic consistency of considering the energy released from the field mode as heat. Based on the properties of the effective temperature $\beta_{\text{eff}}$, we proved that the three bath heat pump situation is in agreement with the 2nd law and thus, the interpretation given by LEMBAS is as well.

We thus conclude from these elaborations that the ED JCM should be correctly be identified as a very special heat transport model justifying the name "pseudomachine" for this and similar models (see, e.g., Linden et al. [2009b]). The surprising conclusion is that the energy provided by a laser should be considered heat. This is in accordance with the results of Scully and Lamb [1967], Mølmer [1996], and others. However, the ED JCM nevertheless provides us with an interesting feature of transition selective heat bath couplings, namely the fact that this increased control over the interaction compared to phenomenological thermodynamics and classical systems is rewarded by an increased usefulness of the heat: The heat taken from the field mode clearly can be used to sustain a "heat pseudopump" that operates with quantum Otto efficiency. No classical transport scenario can be conceived that exhibits such a work-like functionality as provided by the transition selectivity of a quantum thermodynamic model: this type of control is simply not available in a classical world.

# 10 Conclusion and outlook

In this thesis we have focused on two aspects of quantum thermodynamics: First, we noticed that quantum thermodynamics so far did only deal with the question of emergence of thermal equilibrium and the relaxation to it from quantum mechanics. However, thermodynamics is a theory of state changes, and thus processes, that involve not only relaxation and heat exchange but also variation of mechanical parameters. We therefore dealt with the question how mechanical control can emerge from quantum mechanics in Part I. The factorization approximation is an answer to this question in the form of a sufficient condition, namely, that for a system consisting of one pure and one mixed part, the pure part has to stay pure in order to allow for the effective description of the local dynamics of the two parts with effective time-dependent Hamiltonians only. With the SOM we then demonstrated how a system fulfilling this condition could look like, and we showed that there are indeed quantum systems that can act as ideal work sources in some limit.

However, the SOM is a somewhat special model, and we did already see for this tailored system that its work functionality strongly depends on the accuracy of its implementation and preparation. Based on this, one is prone to get the impression that work reservoirs would need careful setup, and work reservoir functionality is neither robust nor typical. This is not true, though, as we all know from everyday life and observation of nature: mechanical effects are absolutely not uncommon or atypical, although they are usually not directed or even cyclic like in artificial mechanical devices. Thus, the question arises how it can be explained that at least in our macroscopic world, mechanical effects are so ubiquitous, a question we did not cover with our considerations here.

Nevertheless, the SOM might give a hint to the answer. We found that the work reservoir functionality is enhanced for weak interaction, high oscillator number, and high oscillator mass, which leads to the situation that the effect of the spin on the oscillator becomes small compared to the bare dynamics of the oscillator. It seems that the existence of a degree of freedom that shows an asymmetry in that it is weakly affected by the interaction with its environment while at the same time strongly affects the dynamics of some part of its surroundings is a necessary premise for mechanical control. Such a degree of freedom would be for example the center of mass variable of a massive

piece of condensed matter in interaction with a fluid. However, also fluids can exhibit such emergent degrees of freedoms, for example a gust of wind that hits a car and alters its trajectory. However, as long as this air portion interacting with the car exhibits a significant mechanical effect, its overall momentum has to show stability versus the interaction with its environment, while at the same moment have a strong effect on it. Obviously, the emergence of such collective degrees of freedom is typical but as we pointed out, it is expected that an asymmetry of the interacting systems in the described sense has to be a crucial element of any attempt to explain the typicality of work effects for the macroscopic regime.

The other part of what we explored in this work has been the question of the relationship of machines and pseudomachines, and thus how new types of control only possible by quantum means might change the thermodynamic functionalities achieved by quantum systems. We have seen in the first and second part that it is possible to recover classical driving and thus classical thermodynamic cycles on the quantum level. We also have seen that implementing such quantum models of classical thermodynamic machines typically seems to require a significant amount of control and accuracy of the setup.

In contrast, we encountered quantum thermodynamical pseudomachines in the last part which did comparatively well in producing machine-like functionalities and seem to be significantly less demanding in maintaining them than cyclic machines. Nonetheless, cyclic quantum thermodynamic machines complete the picture of thermodynamic functional quantum networks, and so far only this type of machines can be conceived of reaching the Carnot efficiency since the isotherms of the Carnot process cannot be implemented in a static spectrum setting. Still, pseudomachines show nicely the link between control and thermodynamic functionality: Heat becomes more "useful" if it is subject to enhanced control, and heat transport models suddenly exhibit machine-like features. Note that this type of control is completely unconceivable in classical thermodynamics and thus this is a genuinely quantum thermodynamic concept. It is an open question what other forms of quantum control can be used to achieve machine-like functionality not known from classical thermodynamics.

# Part IV

# Appendices

# A Inference of the measurement basis $\hat{H}_1'$

In this section, we elaborate on the question of how the measurement basis and local energy definition $\hat{H}_1'$ can be inferred for general situations. Unfortunately, it turns out that this – although intuitive at first glance and supported by the various useful results presented in this thesis – is a complicated problem and we do not succeed to give an obvious or unique explanation for a certain choice of $\hat{H}_1'$.

## A.1 Ambiguity of the decomposition $\hat{H}_{1,a}^{\text{eff}}$ and $\hat{H}_{1,b}^{\text{eff}}$

In Weimer et al. [2008] and Sec. 2.3 we introduced the decomposition of the local effective Hamiltonian $\hat{H}_1^{\text{eff}}$ in two parts, $\hat{H}_{1,a}^{\text{eff}}$ and $\hat{H}_{1,b}^{\text{eff}}$, defined by

$$\hat{H}_1^{\text{eff}} = \hat{H}_{1,a}^{\text{eff}} + \hat{H}_{1,b}^{\text{eff}} \qquad \text{and} \tag{A.1}$$

$$[\hat{H}_{1,a}^{\text{eff}}, \hat{H}_1] = 0 \qquad \text{and} \tag{A.2}$$

$$[\hat{H}_{1,b}^{\text{eff}}, \hat{H}_1] \neq 0 \qquad \forall \hat{H}_{1,b}^{\text{eff}} \neq 0, \tag{A.3}$$

if $\hat{H}_1$ is taken to be the measurement basis. Clearly, those two equations do not uniquely determine the decomposition for given $\hat{H}_1^{\text{eff}}$ and $\hat{H}_1$, as for any operator $\hat{A}$ that fulfills

$$[\hat{A}, \hat{H}_1] = 0, \tag{A.4}$$

we can define a new decomposition $\hat{H}_{1,a}^{\text{eff}} + \hat{A}$, $\hat{H}_{1,b}^{\text{eff}} - \hat{A}$, which still fulfills Eqs. (A.2) and (A.3). Thus, we proposed in Weimer et al. [2008] to make use of the properties of the energy eigenstate transition operator basis $\{|i\rangle\langle j|\}$, where $\{|i\rangle\}$ is the energy eigenbasis of $\hat{H}_1$. To show rigorously, that with respect to this operator basis, the decomposition is unique, we will make use of the following properties of the basis:

$$[|i\rangle\langle j|, |k\rangle\langle l|] = |i\rangle\langle l|\,\delta_{j,k} - |k\rangle\langle j|\,\delta_{i,l} \qquad \text{and} \tag{A.5}$$

$$[|i\rangle\langle j|, \hat{H}_1] = (\epsilon_j - \epsilon_i)\,|i\rangle\langle j| = \omega_{ji}\,|i\rangle\langle j|, \tag{A.6}$$

which hold if we define

$$\hat{H}_1 = \sum_i \epsilon_i \left|i\right\rangle\!\left\langle i\right| . \tag{A.7}$$

For a non-degenerate $\hat{H}_1$, we have additionally that $\omega_{ij} = 0$ if and only if $i = j$.

We define now

$$\hat{H}_{1,a}^{\text{eff}} = \sum_j \left\langle j\right| \hat{H}_1^{\text{eff}} \left|j\right\rangle \left|j\right\rangle\!\left\langle j\right| , \tag{A.8}$$

and consider

$$\hat{H}_{1,b}^{\text{eff}} = \hat{H}_1^{\text{eff}} - \hat{H}_{1,a}^{\text{eff}} = \sum_{i\neq j} \left\langle i\right| \hat{H}_1^{\text{eff}} \left|j\right\rangle \left|i\right\rangle\!\left\langle j\right| . \tag{A.9}$$

According to Eq. (A.6), there is no part $\hat{X}$ of $\hat{H}_{1,b}^{\text{eff}}$ that can produce a zero commutator with $\hat{H}_1$, since the commutator of each summand of $\hat{X}$ is the same apart from multiplication with the non-zero number $\omega_{kj}$. As the transition operators are mutually orthonormal,

$$\text{Tr}\left[(\left|i\right\rangle\!\left\langle j\right|)^\dagger \left|k\right\rangle\!\left\langle l\right|\right] = \delta_{ik}\delta_{jl}, \tag{A.10}$$

and the summands do not vanish by themselves, there is no way that by the prefactors to the summands the sum and thus the operator $\hat{X}$ can vanish.

The situation is slightly different in the case of a degenerate Hamiltonian

$$\hat{H}_1 = \sum_j \sum_{\alpha=1}^{g_j} \epsilon_j \left|j,\alpha\right\rangle\!\left\langle j,\alpha\right| , \tag{A.11}$$

where $g_j$ is the degree of degeneracy of the eigenvalue $\epsilon_j$, and $\{\left|j,\alpha\right\rangle\}$ is an orthonormal basis of $\hat{H}_1$. In this case, relation (A.6) is changed to

$$[\left|i,\alpha\right\rangle\!\left\langle j,\beta\right| , \hat{H}_1] = \omega_{ji} \left|i,\alpha\right\rangle\!\left\langle j,\beta\right| , \tag{A.12}$$

and thus, we have to redefine $\hat{H}_{1,a}^{\text{eff}}$ as the block-diagonal part

$$\hat{H}_{1,a} = \sum_j \sum_{\alpha,\beta=1}^{g_j} \left\langle j,\alpha\right| \hat{H}_1^{\text{eff}} \left|j,\beta\right\rangle \left|j,\alpha\right\rangle\!\left\langle j,\beta\right| . \tag{A.13}$$

Clearly, the commutator of $\hat{H}_{1,a}$ and $\hat{H}_1$ vanishes as before, since each term of the sum commutes by itself with $\hat{H}_1$ as of Eq. (A.12). $\hat{H}_{1,b}^{\text{eff}}$ takes the form

$$\hat{H}_{1,b}^{\text{eff}} = \hat{H}_1^{\text{eff}} - \hat{H}_{1,a}^{\text{eff}} = \sum_{i \neq j} \sum_{\alpha=1}^{g_i} \sum_{\beta=1}^{g_j} \langle i, \alpha | \, \hat{H}_1^{\text{eff}} \, | j, \beta \rangle \, | i, \alpha \rangle \langle j, \beta | \,, \tag{A.14}$$

and we can make use of the same argument as in the non-degenerate case: Any operator $\hat{X}$ that is a sum of any non-zero number of summands of the transition operator basis expansion Eq. (A.14) of $\hat{H}_{1,b}^{\text{eff}}$ cannot commute with $\hat{H}_1$ because the commutator will contain exactly the same summands as $\hat{X}$ multiplied by $\omega_{ji}$ according to Eq. (A.12). Invoking once again the orthonormality of the transition operators, it is proven that $[\hat{H}_1, \hat{X}] \neq 0$ for any $\hat{X}$ that is a part of $\hat{H}_{1,b}^{\text{eff}}$ in the given sense.

However, this splitting of the effective Hamiltonian in the commuting and the non-commuting part is only unique for a given operator basis. We will illustrate this with a simple example. Consider a spin with Hamiltonian

$$\hat{H}_1 = \hat{\sigma}_z \tag{A.15}$$

and a $\hat{H}_1^{\text{eff}}$ of the form

$$\hat{H}_1^{\text{eff}} = \begin{pmatrix} 1 & 1 \\ 1 & 1 \end{pmatrix}, \tag{A.16}$$

and the Pauli operator basis

$$\hat{Q}_j = \frac{1}{\sqrt{2}} \hat{\sigma}_j \tag{A.17}$$

with $\hat{\sigma}_0 = \hat{1}$ and the spin operators $\hat{\sigma}_j$, $j = 1, 2, 3$. The expansion of $\hat{H}_1^{\text{eff}}$ in this basis is

$$\hat{H}_1^{\text{eff}} = \sqrt{2}\hat{1} + \sqrt{2}\hat{\sigma}_x. \tag{A.18}$$

Since $\hat{1}$ commutes with $\hat{\sigma}_z$, we find

$$\hat{H}_{1,a}^{\text{eff}} = \sqrt{2}\hat{1}. \tag{A.19}$$

Let us now turn to a basis $\{\hat{Q}'_j\}$ which is derived from $\{\hat{Q}_j\}$ by a superposition of $\hat{1}$ and $\hat{\sigma}_y$, namely

$$\begin{aligned} \hat{Q}'_0 &= \cos(\phi)\hat{Q}_0 + \sin(\phi)\hat{Q}_2 \\ \hat{Q}'_1 &= \hat{Q}_1 \\ \hat{Q}'_2 &= -\sin(\phi)\hat{Q}_0 + \cos(\phi)\hat{Q}_2 \\ \hat{Q}'_3 &= \hat{Q}_3 \end{aligned} \tag{A.20}$$

with some arbitrary real parameter $\phi$. The expansion of the same $\hat{H}_1^{\text{eff}}$ in this case is

$$\hat{H}_1^{\text{eff}} = \sqrt{2}\cos(\phi)\hat{1} + \sqrt{2}\hat{\sigma}_x - \sqrt{2}\sin(\phi)\hat{\sigma}_y \tag{A.21}$$

and because only $\hat{1}$ commutes with $\hat{\sigma}_z$, now

$$\hat{H}_{1,a}^{\text{eff}} = \sqrt{2}\cos(\phi)\hat{1}. \tag{A.22}$$

We conclude that the decomposition of $\hat{H}_1^{\text{eff}}$ into $\hat{H}_{1,a}^{\text{eff}}$ and $\hat{H}_{1,b}^{\text{eff}}$ is only unique for a given operator basis expansion. Which operator basis is the correct one to choose may depend on the considered experiment.

## A.2 Measurement models based on locally coupled reservoirs

The LEMBAS work and heat measurement, respectively, is inspired by thermodynamics where the distinction of work and heat is made based on what type of reservoirs are coupled to a system and how the energy of these reservoirs changes. Consider for example a container filled with gas and capped by a piston, which itself is connected to a spring in order to sustain a certain pressure on the gas. If this gas is now heated and expands against the pressure of the piston, the work performed during this process may be determined by the energy change of the spring.

In the same sense, the LEMBAS measurements are considered to take place: A system subject to effective local dynamics

$$\dot{\hat{\rho}}(t) = -i[\hat{H} + \hat{H}^{\text{eff}}(t), \hat{\rho}(t)] + \mathcal{L}^{\text{eff}}(t) \tag{A.23}$$

is connected to heat and work reservoirs in order to measure the heat and work flowing into the system. We consider an infinitesimal short process step during which the system exchanges infinitesimal heat $đQ = \dot{Q}(t)\mathrm{d}t$ and infinitesimal work $đW = \dot{W}(t)\mathrm{d}t$ with its surrounding. Then, the outcome of the measurement will be the work and the heat current $\dot{W}(t)$ and $\dot{Q}(t)$, respectively. The measurement reservoirs introduce additional local effects on the local dynamics, denoted as $\hat{H}_M^{\text{eff}}(t)$ and $\mathcal{L}_M^{\text{eff}}(t)$ for the work and heat measurement reservoir, respectively. We thus arrive at the equation of motion for the system under the influence of both, the environment and the measurement reservoirs:

$$\dot{\hat{\tilde{\rho}}}(t) = -i[\hat{H} + \hat{H}^{\text{eff}}(t) + \hat{H}_M^{\text{eff}}(t), \hat{\tilde{\rho}}(t)] + \mathcal{L}^{\text{eff}}(t) + \mathcal{L}_M^{\text{eff}}(t). \tag{A.24}$$

The tilde denotes the dynamics of the system with the measurement reservoir effects taken into account. We distinguish expectation values with respect to the state reached with or without the influence of the measurement reservoirs by $\langle\cdot\rangle_{\hat{\tilde{\rho}}}$ and $\langle\cdot\rangle_{\hat{\rho}}$, respectively.

We present now the results of two so far unsuccessful approaches to the derivation of the LEMBAS formulas from a more detailed measurement scheme based on the ansatz above. We have taken the approach to first try to find a number of plausible assumptions about the measurement model that can reproduce the LEMBAS measurement, which we would then try to justify in a second step.

Without additional constraints, the measurement reservoirs in Eq. (A.24) could exchange arbitrary amounts of work and heat with the system. It is therefore necessary to make some additional assumptions, the first of which is that the measurement reservoirs consume all the energy imparted from other sources, that is

$$\frac{\mathrm{d}}{\mathrm{d}t}\langle\hat{\tilde{H}}\rangle_{\hat{\tilde{\rho}}_t} = 0, \tag{A.25}$$

where

$$\hat{\tilde{H}}(t) = \hat{H} + \hat{H}^{\mathrm{eff}}(t) + \hat{H}_M^{\mathrm{eff}}(t) \tag{A.26}$$

is the complete local effective Hamiltonian including the measurement reservoir effects. So far, heat transferred by the environment to the system could be consumed by the work measurement reservoir. To avoid this, we require additionally

$$\frac{\mathrm{d}}{\mathrm{d}t}\tilde{S}(t) = \frac{\mathrm{d}}{\mathrm{d}t}\mathrm{Tr}[-\hat{\tilde{\rho}}(t)\ln\hat{\tilde{\rho}}(t)] = 0, \tag{A.27}$$

which is the conservation of the local von Neumann entropy. Then, the contribution of $\mathcal{L}_M^{\mathrm{eff}}(t)$ to the total energy flux has to be at least large enough to cancel $\mathcal{L}^{\mathrm{eff}}$. It might be bigger, however, and the surplus may be absorbed by $\hat{H}_M^{\mathrm{eff}}(t)$. Hence, we additionally assume that $\mathcal{L}_M^{\mathrm{eff}}(t)$ is chosen such that the heat flux is minimal under the given constraints.

In the simplest case, that fulfills all assumptions made so far, we require to have

$$\hat{H}_M^{\mathrm{eff}}(t) = -\hat{H}^{\mathrm{eff}}(t), \tag{A.28}$$

$$\mathcal{L}_M^{\mathrm{eff}}(t) = -\mathcal{L}^{\mathrm{eff}}(t). \tag{A.29}$$

The total energy change of the system is then

$$\begin{aligned}\frac{\mathrm{d}}{\mathrm{d}t}\langle\hat{\tilde{H}}(t)\rangle_{\hat{\tilde{\rho}}(t)} =&\mathrm{Tr}\left[\left(\frac{\mathrm{d}}{\mathrm{d}t}\hat{\tilde{H}}(t)\right)\hat{\tilde{\rho}}(t)+\hat{\tilde{H}}(t)\left(\frac{\mathrm{d}}{\mathrm{d}t}\hat{\tilde{\rho}}(t)\right)\right]\\ =&\mathrm{Tr}[\dot{\hat{H}}^{\mathrm{eff}}(t)\hat{\tilde{\rho}}(t)]+\mathrm{Tr}[\dot{\hat{H}}_M^{\mathrm{eff}}(t)\hat{\tilde{\rho}}(t)]\\ &-i\mathrm{Tr}\left[\hat{\tilde{H}}(t)\left([\hat{\tilde{H}}(t),\hat{\tilde{\rho}}(t)]+\mathcal{L}^{\mathrm{eff}}(t)+\mathcal{L}_M^{\mathrm{eff}}(t)\right)\right].\end{aligned} \tag{A.30}$$

The trace over the product of $\hat{\tilde{H}}(t)$ and the commutator vanishes due to the cyclicity of the trace. Since $\hat{\tilde{H}}(t)=\hat{H}$ for the given choice (A.28) and (A.29), we are left with

$$\begin{aligned}\frac{\mathrm{d}}{\mathrm{d}t}\langle\hat{\tilde{H}}(t)\rangle_{\hat{\tilde{\rho}}(t)} =&\mathrm{Tr}[\dot{\hat{H}}^{\mathrm{eff}}(t)\hat{\tilde{\rho}}(t)]+\mathrm{Tr}[\dot{\hat{H}}_M^{\mathrm{eff}}(t)\hat{\tilde{\rho}}(t)]\\ &+\mathrm{Tr}[\hat{H}\mathcal{L}^{\mathrm{eff}}(t)]+\mathrm{Tr}[\hat{H}\mathcal{L}_M^{\mathrm{eff}}(t)].\end{aligned} \tag{A.31}$$

Due to the constraint (A.27), the currents

$$\dot{W}_M(t)=\mathrm{Tr}[\dot{\hat{H}}_M^{\mathrm{eff}}(t)\hat{\tilde{\rho}}(t)] \tag{A.32}$$

and

$$\dot{Q}_M(t)=\mathrm{Tr}[\hat{H}\mathcal{L}_M^{\mathrm{eff}}(t)] \tag{A.33}$$

flowing from the measurement reservoirs into the system independently cancel the fluxes

$$\dot{W}(t)=\mathrm{Tr}[\dot{\hat{H}}^{\mathrm{eff}}(t)\hat{\tilde{\rho}}(t)] \tag{A.34}$$

and

$$\dot{Q}(t)=\mathrm{Tr}[\hat{H}\mathcal{L}^{\mathrm{eff}}(t)], \tag{A.35}$$

and thus

$$\dot{W}_M(t)=-\dot{W}(t) \tag{A.36}$$

$$\dot{Q}_M(t)=-\dot{Q}(t). \tag{A.37}$$

However, the display of the measurement apparatus would exactly due to the negative of the currents provided by the measurement reservoirs, and thus simply $\dot{W}(t)$ and $\dot{Q}(t)$, which are the quantities measured by this setup. Unfortunately, they neither agree with the LEMBAS formulas (2.31) and (2.32),

nor with the formulas expected to result if the whole $\hat{H} + \hat{H}^{\mathrm{eff}}(t)$ is chosen to be the measurement basis [cf. Eqs. (3.53) and (3.54)].

One could conceive that the assumptions above have to be modified in the way that the measurement reservoir effects on the dynamics are not taken into account for the dynamics (this would make the measurement non-invasive), but still calculate the currents that the measurement reservoirs would read. Skipping the derivation here, this leads to a work definition of the form

$$\dot{W}(t) = \mathrm{Tr}\left(\dot{\hat{H}}^{\mathrm{eff}}(t)\hat{\rho}(t) - i[\hat{H}_b^{\mathrm{eff}}(t), \hat{H}]\hat{\rho}(t)\right), \tag{A.38}$$

where $\hat{H}_b^{\mathrm{eff}}(t)$ is the non-commuting part of $\hat{H}^{\mathrm{eff}}(t)$ in the transition operator basis as of Eq. (2.27). Though, this looks similar to the LEMBAS formula, it can be shown to be never the same. Thus, the stringent derivation of the LEMBAS definitions of heat and work form an appropriate measurement model is still an open issue.

## A.3 Local projective measurements

As mentioned already in Sec. 2.4.5, when considering measuring a system subject to effective dynamics, additional questions arise due to co-jump effects under projective measurements. In the end, if one wants to measure anything, one has to perform projective measurements in the LEMBAS measurement scheme as well, and due to quantum correlations of the system being measured with its environment, the environment might also change its state.

To make this statement precise, we consider a bipartite quantum system

$$\hat{H} = \hat{H}_1 + \hat{H}_{12} + \hat{H}_2 \tag{A.39}$$

in a state

$$\hat{\rho} = \hat{\rho}_1 \otimes \hat{\rho}_2 + \hat{C}_{12}, \tag{A.40}$$

where $\hat{\rho}_j$ are the reduced density matrices of the system parts. Clearly, $\hat{C}_{12}$ has the property that its trace as well as the partial traces over the subsystem Hilbert spaces $\mathcal{H}_j$ vanish.

Consider now an observable $\hat{X}$ which is going to be measured by ideal projective measurements. The eigenbasis of $\hat{X}$ is denoted by $\{|k\rangle\}$, and the corresponding eigenvalues by $x_k$. If the $k$th eigenvalue has been measured in one measurement, the state of the total system is given by

$$\hat{\rho}'_k = \frac{1}{q_k} |k\rangle\langle k| \, \hat{\rho} \, |k\rangle\langle k| = |k\rangle\langle k| \otimes \hat{\rho}_2 + \frac{1}{q_k} |k\rangle\langle k| \, \hat{C}_{12} \, |k\rangle\langle k| \tag{A.41}$$

where

$$q_k = \mathrm{Tr}(|k\rangle\langle k|\,\hat{\rho}) = \langle k|\,\hat{\rho}_1\,|k\rangle \tag{A.42}$$

is the probability for this measurement outcome. With

$$|k\rangle\langle k|\,\hat{C}_{12}\,|k\rangle\langle k| = |k\rangle\langle k| \otimes \langle k|\,\hat{C}_{12}\,|k\rangle\,, \tag{A.43}$$

which can be shown by use of the expansion

$$\sum_{ijkl} (\hat{C}_{12})_{ijkl}\,|i\rangle\langle j| \otimes |k\rangle\langle l|\,, \tag{A.44}$$

we arrive at

$$\hat{\rho}_k' = |k\rangle\langle k| \otimes \left(\hat{\rho}_2 + \frac{1}{q_k}\,\langle k|\,\hat{C}_{12}\,|k\rangle\right) \tag{A.45}$$

for the state after the projection. Clearly, the reduced state of the second subsystem has changed from $\hat{\rho}_2$ to

$$\hat{\rho}_{2,k}' = \hat{\rho}_2 + \frac{1}{q_k}\,\langle k|\,\hat{C}_{12}\,|k\rangle\,. \tag{A.46}$$

The additional summand on the r.h.s. is exactly what we call the *co-jump effect*.

The open question here is how to deal with this co-jump effect in the LEMBAS method. It is clear that if we want to measure for example energy changes of attached work reservoirs to determine the work flux, we need to do it by projections. However, due to the co-jumps the state of the environment of a measured system is altered, and so is the effective Hamiltonian and the effective dissipator (since $\hat{C}_{12}' = 0$ after the measurement). It is not impossible that this should be taken into account in some way when interpreting the LEMBAS results. However, the results gained with the LEMBAS method in this thesis are conclusive without dealing with the co-jump effects, which may signify that they can be safely neglected.

# B Partial trace relations

We make use of the following partial trace relations:

$$\mathrm{Tr}_1\left[\hat{A}\otimes\hat{1}_2,\hat{C}\right]=0 \tag{B.1}$$

$$\mathrm{Tr}_1\left[\hat{1}_1\otimes\hat{A},\hat{C}\right]=\left[\hat{A},\mathrm{Tr}_1\hat{C}\right]. \tag{B.2}$$

To prove them, we employ the expansion of the operators in arbitrary operator bases $\{\hat{Q}_i\}$ and $\{\hat{\tilde{Q}}_i\}$ of the two participating Hilbert spaces leading to

$$\hat{A}=\sum_i a_i\hat{Q}_i, \tag{B.3}$$

$$\hat{B}=\sum_i b_i\hat{\tilde{Q}}_i, \tag{B.4}$$

$$\hat{C}=\sum_{ij} c_{ij}\hat{Q}_i\otimes\hat{\tilde{Q}}_j. \tag{B.5}$$

Inserting Eq. (B.5) in Eq. (B.1), we get

$$\begin{aligned}\mathrm{Tr}_1\left[\hat{A}\otimes\hat{1}_2,\hat{C}\right]&=\sum_{ij}c_{ij}\mathrm{Tr}_1\left([\hat{A}\otimes\hat{1},\hat{Q}_i\otimes\hat{\tilde{Q}}_j]\right)\\&=\sum_{ij}c_{ij}\mathrm{Tr}_1\left([\hat{A},\hat{Q}_i]\otimes\hat{\tilde{Q}}_j\right)\\&=\sum_{ij}c_{ij}\hat{\tilde{Q}}_j\mathrm{Tr}\left([\hat{A},\hat{Q}_i]\right)\\&=0\end{aligned}$$ q.e.d.

because of the self-similarity of the trace, the trace over a commutator vanishes always.

For the proof of Eq. (B.2) we first consider the partial trace relation

$$\begin{aligned}
\mathrm{Tr}_1[(\hat{A}\otimes\hat{B})\hat{C}] &= \sum_{ij} c_{ij}\mathrm{Tr}_1[(\hat{A}\otimes\hat{B})(\hat{Q}_i\otimes\hat{\tilde{Q}}_j)] \\
&= \sum_{ij} c_{ij}\mathrm{Tr}_1[(\hat{A}\hat{Q}_i)\otimes(\hat{B}\hat{\tilde{Q}}_j)] \\
&= \sum_{ij} c_{ij}(\hat{B}\hat{\tilde{Q}}_j)\mathrm{Tr}(\hat{A}\hat{Q}_i) \\
&= \hat{B}\sum_{ij} c_{ij}\mathrm{Tr}_1[(\hat{A}\otimes\hat{1}_2)(\hat{Q}_i\otimes\hat{\tilde{Q}}_j)] \\
&= \hat{B}\mathrm{Tr}_1[(\hat{A}\otimes\hat{1}_2)\hat{C}]. \qquad \text{(B.6)}
\end{aligned}$$

Thus, we find the special cases

$$\mathrm{Tr}_1[(\hat{1}_1\otimes\hat{B})\hat{C}] = \hat{B}\mathrm{Tr}_1(\hat{C}) \qquad \text{(B.7)}$$

$$\mathrm{Tr}_2[(\hat{A}\otimes\hat{1}_2)\hat{C}] = \hat{A}\mathrm{Tr}_2(\hat{C}), \qquad \text{(B.8)}$$

and from that (B.2) follows immediately.

# C Time-evolution of a coherent state

In this appendix, we prove the relation

$$|\alpha(t)\rangle = \exp(-i\hat{H}_o t)\,|\alpha\rangle = \exp(-i\omega_o t/2)\,|\alpha\exp(-i\omega_o t)\rangle \tag{C.1}$$

with the oscillator Hamiltonian

$$\hat{H}_o = \omega_o\left(\hat{a}^\dagger\hat{a} + \frac{1}{2}\right). \tag{C.2}$$

Inserting the definition of a coherent state [Eq. (8.9)] in the l.h.s. of Eq. (C.1), we get

$$\begin{aligned}|\alpha(t)\rangle &= \exp\left(\frac{|\alpha|^2}{2}\right)\sum_{n=0}^{\infty}\frac{\alpha^n}{\sqrt{n!}}\exp(-i\hat{H}_o t)\,|n\rangle \\ &= \exp\left(\frac{|\alpha|^2}{2}\right)\sum_{n=0}^{\infty}\frac{\alpha^n}{\sqrt{n!}}\exp\left[-i\omega_o\left(n+\frac{1}{2}\right)t\right]|n\rangle \\ &= \exp\left(-\frac{i\omega_o t}{2}\right)\exp\left(\frac{|\alpha|^2}{2}\right)\sum_{n=0}^{\infty}\frac{1}{\sqrt{n!}}\left[\alpha\exp\left(-i\omega_o t\right)\right]^n|n\rangle\,.\end{aligned} \tag{C.3}$$

Because of $|\alpha| = |\alpha\exp(-i\omega_o t)|$,

$$\exp\left(\frac{|\alpha|^2}{2}\right)\sum_{n=0}^{\infty}\frac{1}{\sqrt{n!}}\left[\alpha\exp\left(-i\omega_o t\right)\right]^n|n\rangle = |\alpha\exp(-i\omega_o t)\rangle\,, \tag{C.4}$$

which is a coherent state with coherent parameter $\alpha\exp(-i\omega_o t)$. By that, we readily arrive at Eq. (C.1), q.e.d..

# D Deutsche Zusammenfassung

Der Anwendungsbereich von Thermodynamik erstreckt sich trotz ihrer Entstehung im 16. und 17. Jahrhundert als rein phänomenologische Theorie über fast alle Skalen, vom Kosmos bis zum Molekül, und erweist sich dabei immer wieder als wichtiges Element zur Beschreibung physikalischer Effekte. Im letzten Jahrzehnt wurde von Gemmer et al. [2004] und anderen[1] ein neuer Zugang zur Erklärung der Emergenz der Thermodynamik aus den quantenmechanischen Grundgesetzen der Natur entwickelt, der unsere Vorstellung von Thermodynamik auf den Kopf stellt. Ausgehend von einem autonomen Gesamtsystem in einem reinen Zustand zeigen die Autoren, dass der reduzierte Zustand eines kleinen Subsystems nahezu jederzeit ein Gleichgewichtszustand ist, falls der Rest des Systems schwach mit dem Subsystem wechselwirkt und exponentiell entartet ist, was typischerweise der Fall ist. Darüberhinaus ergibt sich, dass bereits ein Netzwerk aus 10 Spins für einen weiteren Spin als groß gelten kann, und den Spin in hervorragender Näherung im thermodynamischen Gleichgewichtszustand hält. In diesem Sinne weisen selbst endliche und autonome Quantennetzwerke in einem reinen Gesamtzustand thermodynamische Funktionalität auf.

Diese Ergebnisse werfen einige hochinteressante Fragen auf: Wenn die Relaxation zum thermischen Gleichgewicht und somit Wärme eine emergente Funktionalität der Quantenmechanik ist, kann dasselbe für die thermodynamische Arbeit gezeigt werden? Welche Eigenschaften haben Einbettungen, die als Arbeitsreservoire fungieren? Wenn die Konzepte Arbeit und Wärme für endliche Quantennetzwerke existieren, wie können wir die thermodynamischen Definitionen verallgemeinern, um diese Effekte zu quantifizieren? Und welche neuen thermodynamischen Funktionen ergeben sich durch Formen der Kontrolle über Systeme, die nur für quantenmechanische Systeme existieren? Diese Fragen und ihre Antworten sind Inhalt der vorliegenden Arbeit, über deren Ergebnisse wir an dieser Stelle einen Überblick geben.

[1] Tasaki [1998], Gemmer et al. [2001], Borowski et al. [2003], Gemmer et al. [2004], Henrich et al. [2005]

# D.1 Quantenmechanische Arbeitsquellen

## D.1.1 Arbeit und Wärme in quantenmechanischen Systemen

Wir nähern uns dem Problem der Definition der Emergenz von Arbeitsquellen aus der Quantenmechanik mit Hilfe der *verallgemeinerten Faktorisierungsnäherung* (*FN*, siehe Schröder and Mahler [2010]). Diese besagt für zwei wechselwirkende Quantensysteme beschrieben durch den zeitunabhängigen Hamilton-Operator $\hat{H} = \hat{H}_1 + \hat{H}_{12} + \hat{H}_2$ und einem faktorisierenden Anfangszustand der Form

$$\hat{\rho}(0) = \hat{\rho}_1(0) \otimes \rho_2(0) = \hat{\rho}_1(0) \otimes |\Psi_2(0)\rangle\langle\Psi_2(0)|\,, \tag{D.1}$$

dass die Dynamik für die beiden gekoppelten Systeme in guter Näherung gegeben ist durch

$$\dot{\hat{\rho}}_1(t) = -i\left[\hat{H}_1 + \hat{H}_1^{\text{eff}}(t), \hat{\rho}_1(t)\right] \tag{D.2}$$

$$|\dot{\Psi}_2(t)\rangle = -i\left(\hat{H}_2 + \hat{H}_2^{\text{eff}}(t)\right)|\Psi_2(t)\rangle\,, \tag{D.3}$$

solange System 2 nahezu rein bleibt, d.h. für seine Purity $\mathrm{Tr}\{[\hat{\rho}_2(t)]^2\} \approx 1$ gilt. Die zeitabhängigen effektiven lokalen Hamiltonoperatoren $\hat{H}_1^{\text{eff}}(t)$ und $\hat{H}_2^{\text{eff}}(t)$ sind dabei durch

$$\hat{H}_1^{\text{eff}}(t) = \mathrm{Tr}_2\{\hat{H}_{12}[\hat{1} \otimes \hat{\rho}_2(t)]\} \tag{D.4}$$

$$\hat{H}_2^{\text{eff}}(t) = \mathrm{Tr}_1\{\hat{H}_{12}[\hat{\rho}_1(t) \otimes \hat{1}]\} \tag{D.5}$$

gegeben. Die Systeme verhalten sich im Falle gültiger FN wie klassische Treiber zueinander, und tauschen sie unter diesen Bedingungen Energie aus, ist diese thermodynamisch als Arbeit zu identifizieren gemäß der Definition als Energie, die einem System durch die parametrische Änderung der Hamiltonfunktion oder des Hamiltonoperators zugeführt wird.

Betrachten wir nun die allgemeine effektive lokale Dynamik des ersten der beiden Quantensysteme, so erhalten wir

$$\dot{\hat{\rho}}_1(t) = -i\left[\hat{H}_1 + \hat{H}_1^{\text{eff}}(t), \hat{\rho}_1(t)\right] + \mathcal{L}_1^{\text{eff}}[\hat{\rho}(t)], \tag{D.6}$$

mit dem effektiven Hamiltonoperator aus Eq. (D.4) und dem effektiven Dissipator

$$\mathcal{L}_1^{\text{eff}}[\hat{\rho}(t)] = -i\mathrm{Tr}_2[\hat{H}_{12}, \hat{C}_{12}(t)], \tag{D.7}$$

der die von der Verschränkung mit dem anderen System herrührende inkohärente Dynamik beschreibt. Dabei ist in diesem allgemeinen Fall $\hat{\rho}(t) = \hat{\rho}_1(t) \otimes \hat{\rho}_2(t) + \hat{C}_{12}(t)$.

Ausgehend von Gl. (D.6) haben wir in Weimer et al. [2008] verallgemeinerte Definitionen von Arbeit und Wärme formuliert, die für beliebige quantenmechanische Systeme in Kontakt mit einer quantenmechanischen Umgebung definiert sind. Wärme $W$ und Arbeit $Q$ werden dabei anhand ihres Effekts auf die lokale von-Neumann-Entropie $S$ unterschieden. Es ergibt sich, dass die durch $\hat{H}^{\text{eff}}(t)$ hervorgerufene Dynamik $S$ unverändert lässt und daher in Einklang mit dem Ergebnis aus der Betrachtung der FN als Arbeit einzustufen ist, wohingegen der Einfluss von $\mathcal{L}^{\text{eff}}$ zwangsweise zu $\mathrm{d}S \neq 0$ führt und daher mit Wärme assoziiert ist.

Zur tatsächlichen Definition der Flüsse đ$W$ und đ$Q$ muss noch beachtet werden, dass diese Größen wie in der Thermodynamik durch die Ankopplung von Wärmebädern und Arbeitsreservoiren gemessen werden, die durch die an das System gekoppelten Reservoirs gemessene Arbeit und Wärme im Gegensatz zum klassischen Fall jedoch von der Art der Kopplung zwischen den Reservoirs und dem System abhängig ist. Dadurch ergibt sich eine *lokale effektive Messbasis (LEMBAS)* für die Messung von đ$W$ und đ$Q$, die vom betrachteten Experiment abhängt. Wählt man die Energieeigenbasis des Systems als Messbasis, so erhält man $\hat{H}'(t) = \hat{H} + \hat{H}_a^{\text{eff}}(t)$ als den Operator für die lokale interne Energie des Systems. Dabei ist $\hat{H}_a^{\text{eff}}(t)$ der Diagonalanteil von $\hat{H}^{\text{eff}}(t)$, so dass

$$\hat{H}^{\text{eff}}(t) = \hat{H}_a^{\text{eff}}(t) + \hat{H}_b^{\text{eff}}(t) \text{ und} \tag{D.8}$$

$$[\hat{H}_a^{\text{eff}}(t), \hat{H}] = 0, \quad [\hat{H}_b^{\text{eff}}(t), \hat{H}] \neq 0 \tag{D.9}$$

(falls $\hat{H}_b^{\text{eff}}(t) = 0$ muss die letzte Ungleichung nicht erfüllt sein). Aus der zeitlichen Änderung von $\langle \hat{H}'(t) \rangle$ und der Unterscheidung nach Anteilen, die $S$ konstant lassen (Arbeit) oder ändern (Wärme), ergeben sich die Definitionen

$$đW = \mathrm{Tr}\left( \dot{\hat{H}}_a^{\text{eff}}(t)\hat{\rho}_1(t) - i\left[\hat{H}'(t), \hat{H}_b^{\text{eff}}(t)\right]\hat{\rho}(t)\right) \mathrm{d}t \tag{D.10}$$

$$đQ = \mathrm{Tr}\{\hat{H}'(t)\mathcal{L}^{\text{eff}}[\hat{\rho}(t)]\}\mathrm{d}t. \tag{D.11}$$

für die verallgemeinerte Arbeit und Wärme. Diese Definitionen erfüllen für Gleichgewichtsprozesse die Clausius-Relation und liefern für ein durch einen Laser getriebenes Zwei-Niveau-Atom korrekterweise maximalen Arbeitsübertrag für den Resonanzfall im Gegensatz zu der üblicherweise in der Literatur verwendeten quantenmechanischen Arbeitsdefinition (Alicki [1979]). Im thermodynamischen Grenzfall (nahe dem Gleichgewicht und für unendlich große,

unendlich schwach gekoppelte Systeme) gehen diese Definitionen in ihre thermodynamischen Entsprechungen über.

### D.1.2 Funktionalitätsmaße für thermodynamische Reservoirs

Um die thermodynamische Funktion von Quantennetzwerken erfassen zu können, müssen die idealisierten thermodynamischen Definitionen von Arbeits- und Wärmereservoirs ebenfalls verallgemeinert werden, denn endliche Systeme mit nicht verschwindender Wechselwirkung sind fast niemals nur Arbeits- oder Wärmequellen, sondern üblicherweise zu einem gewissen Grad beides zugleich. Zu diesem Zweck führen wir in Schröder and Mahler [2010] zwei verschiedene Maße für die thermodynamische Funktion eines Quantensystems ein.

Zuerst betrachten wir die Purity $P[\hat{\rho}(t)]$ des Systems, die gemäß der FN ein Maß für die Größe von $\mathcal{L}^{\text{eff}}$ ist und damit mit der Größe von $đQ$ zusammenhängt. Allerdings ist dieser Zusammenhang schwierig zu quantifizieren, und es ist unklar, wie Änderungen der Purity für verschiedene Systeme gewichtet werden sollen. Darüberhinaus sagt die Purity nichts über die relative Stärke der Effekte von $\hat{H}^{\text{eff}}$ und $\mathcal{L}^{\text{eff}}$, die jedoch entscheidenden Einfluss auf die Funktionalität des Systems hat.

Deswegen führen wir zusätzlich das Maß

$$R(t_1, t_0) = \frac{\mathcal{W}(t_1, t_0)}{\mathcal{W}(t_1, t_0) + \mathcal{Q}(t_1, t_0)} \tag{D.12}$$

ein, das die Arbeitsreservoirqualität für ein Intervall $[t_o, t_1]$ mit Hilfe des integrierten absoluten Arbeits- und Wärmeflusses, $\mathcal{W}(t_1, t_0)$ und $\mathcal{Q}(t_1, t_0)$, definiert. Dabei ist $R(t_1, t_0) \in [0, 1]$, und für die Extremalwerte gelten die folgenden Interpretationen:

- $R(t_1, t_0) = 1 \Leftrightarrow \dot{Q}(t) = 0$ für alle $t \in [t_0, t_1]$ und $\dot{W}(t) \neq 0$ für einige $t \in [t_0, t_1]$: ideale Arbeitsquelle
- $R(t_1, t_0) = 0 \Leftrightarrow \dot{W}(t) = 0$ für alle $t \in [t_0, t_1]$ und $\dot{Q}(t) \neq 0$ für einige $t \in [t_0, t_1]$: ideale Wärmequelle

Die analoge Definition, die anstelle von $\mathcal{W}$ und $\mathcal{Q}$ die direkt integrierte Wärme und Arbeit verwendet, erweist sich als ungeeignet.

### D.1.3 Spin-Oszillator-Modell (SOM)

Das SOM dient uns als einfaches Modell zur Illustration und zum Test der bisher beschriebenden Konzepte. Insbesondere lässt sich damit zeigen, dass

unter bestimmten Bedingungen ein einzelner quantenmechanischer harmonischer Oszillator als ideales Arbeitsreservoir agieren kann.

Das Modell besteht aus einem Zwei-Niveau-Atom und einem Oszillator,

$$\hat{H} = \frac{\omega_s}{2}\hat{\sigma}_z + \hat{H}_{\text{int}} + \omega_o \left(\hat{a}^\dagger \hat{a} + \frac{1}{2}\right) \tag{D.13}$$

und wird betrachtet für zwei verschiedene Wechselwirkungen

$$\hat{H}_{\text{int}} = \hat{H}_z = \lambda \hat{\sigma}_z \hat{x} \tag{D.14}$$

$$\hat{H}_{\text{int}} = \hat{H}_{xz} = \lambda(\hat{\sigma}_z + \kappa\hat{\sigma}_x)\hat{x} \tag{D.15}$$

($z$-SOM und $xz$-SOM). Der Spin befindet sich anfangs in einem thermischen Zustand, während der Oszilllator einen kohärenten Zustand $|\alpha\rangle$ einnimmt, und der Gesamtzustand faktorisiert. Betrachtet werden soll die thermodynamische Funktion, die der Oszillator auf den Spin ausübt. Dies wird zunächst an Hand der Gültigkeit der FN gemäß dem ersten Funktionalitätsmaß aus Kap. D.1.2 erörtert und – für das $xz$-SOM – zusätzlich mit $R$.

Für das $z$-SOM ergibt sich, dass die minimale Purity des Oszillators ausschließlich von den Systemparametern und nicht von den Parametern des genannten Anfangszustands abhängt. Durch geeignete Wahl der Systemparameter kann demnach die FN beliebig exakt erfüllt werden, und der Oszillator wirkt in diesem Fall wie ein zusätzliches magnetisches Feld, das die Aufspaltung des Spins in Abhängigkeit des Ortserwartungswerts $\langle\hat{x}\rangle(t)$ verändert. Die sich dadurch ergebende Energieänderung des Spins ist Arbeit und der Oszillator ein perfektes Arbeitsreservoir ($R = 1$). Es existieren zwei wichtige Grenzfälle, für die die FN exakt wird und die Amplitude der effektiven Aufspaltung des Spins nicht verschwindet: Einen klassischen, für den die Frequenz des Oszillators und die Wechselwirkung endlich bleiben, seine Masse und die anfängliche kohärente Anregung aber gegen unendlich streben, und einen Quantenlimes mit endlicher Oszillatormasse und Anregung, aber gegen unendlich strebender Frequenz und Wechselwirkungsstärke. In diesem Quantenlimes erscheint der Oszillator des Modells als ideale quantenmechanische Arbeitsquelle im Sinne der Thermodynamik.

Das $xz$-SOM beleuchtet die Situation für den Fall einer nicht perfekten Arbeitsquelle und zeigt die Vor- und Nachteile der beiden Funktionalitätsmaße auf. Der zusätzliche $\hat{\sigma}_x$-Term in der Wechselwirkung steht dabei für eine Störung des Systems durch möglicherweise eingeschränkte experimentelle Kontrolle über die Wechselwirkungseigenschaften des Systems und hängt mit der Robustheit der Arbeitsquellenfunktionalität des Oszillators zusammen.

Die Dynamik des $xz$-SOMs stimmt für den resonanten Fall $\omega_o = \omega_s$ unter der Bedingung $\kappa \lesssim 1$ in guter Näherung mit der Dynamik des *Jaynes-Cummings-Modells* (*JCM*, Jaynes and Cummings [1963]) überein, was sich

mit Hilfe einer *rotating-wave approximation* zeigen lässt. Aus dem Skalenverhalten des JCM bezüglich der Wechselwirkungsstärke $\lambda$ ergibt sich, dass das Minimum der Purity des Oszillators unabhängig von $\kappa$ ist. Da die minimale Purity von 1 weit entfernt ist, ergibt sich, dass die FN in jedem Fall früher ($\kappa$ groß) oder später ($\kappa$ klein) ungültig wird und mit einem zusätzlichen Wärmefluss aus dem Oszillator gerechnet werden muss. Mit Hilfe des Funktionalitätsmaßes $R$ zeigt sich jedoch, dass das Modell für verschiedene Anfangszustände z.T. erhebliche Unterschiede in der Funktionalität aufweist, obwohl das Purity-Verhalten für diese Fälle recht ähnlich ist. Dies bestätigt, dass die Purity nur als Indikator für einen geringen Wärmefluss dienen kann, jedoch keinerlei Aussage über das Verhältnis von Wärme zu Arbeit machen kann, außer im Grenzfall idealer Arbeitsreservoire.

## D.2 Zyklisch arbeitende quantenthermodynamische Maschinen

Der erste Teil der Arbeit befasste sich ausschließlich mit der verallgemeinerten Definition von Arbeit und Wärme in quantenmechanischen Systemen und der Identifizierung quantenmechanischer Arbeitsquellen. Möchte man jedoch die Thermodynamik autonomer Quantennetzwerke behandeln, darf man nicht außer Acht lassen, dass die Thermodynamik eine Theorie von Prozessen ist. Zur Implementierung eines Prozesses benötigt man jedoch beide Arten von thermodynamischer Kontrolle: thermische und mechanische. In diesem Sinne behandelt der zweite Teil der Arbeit autonome Quantennetzwerke, die thermodynamische Zyklen implementieren und dadurch thermodynamische Maschinen-Funktionalität aufweisen. Außerdem wird der Beweis angetreten, dass die effektive Beschreibung aus Gl. (D.6) nicht nur ein mathematischer Kniff ist, sondern die physikalische Wirklichkeit widerspiegelt.

Zu diesem Zweck führen wir das Modell der *autonomen dynamischen Drei-Spin-Maschine* (*AD3SM*,Fig. D.1) ein, welches aus einer Heisenberg-Spin-Kette mit drei inhomogen aufgespaltenen Spins, einem quantenmechanischen Oszillator und zwei Wärmebädern besteht. Der Oszillator wechselwirkt nur mit dem mittleren Spin und bildet mit diesem das $z$-SOM nach. Das warme Bad wechselwirkt ausschließlich mit dem linken Spin der Kette, wohingegen das kalte Bad nur mit dem rechen Spin wechselwirkt. Die Wärmebäder werden mit einer Mastergleichung gemäß Saito et al. [2000] modelliert, die geeignet ist, Wärmetransport in quantenmechanischen Systemen korrekt zu beschreiben (Wichterich et al. [2007]).

Die AD3SM ist eine autonome Version der *dynamischen Drei-Spin-Maschine*

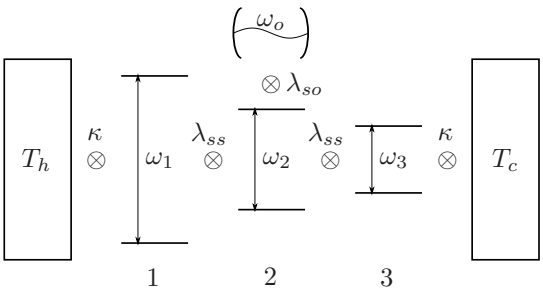


**Abbildung D.1:** Schema der autonomen dynamischen Drei-Spin-Maschine (AD3SM).

*(D3SM)* von Henrich et al. [2007a], bei der der Oszillator fehlt und der mittlere Spin stattdessen klassisch durch eine explizit zeitabhängige Aufspaltung periodisch so getrieben wird, dass er abwechselnd mit dem linken und dem rechten Spin in Resonanz ist und so mit dem linken und rechten Bad in Kontakt steht. Die D3SM kann in Abhängigkeit vom Temperaturgradienten $\Delta T = T_h - T_c$ und der Aufspaltung der Spins den Otto-Prozess als Maschine oder als Wärmepumpe näherungsweise implementieren.

Wir diskutieren die numerischen Ergebnisse für die AD3SM für zwei verschiedene Parametersätze. Die effektive Aufspaltung durch den Oszillator wird in beiden Fällen so gewählt, dass der mittlere Spin an den Umkehrpunkten der effektiven Aufspaltung abwechselnd in Resonanz mit dem linken und rechten Spin kommt. Wir bewerten die Funktionalität des Quantennetzwerks an Hand verschiedener Kriterien, deren Ergebnisse wir miteinander vergleichen, nämlich mit Hilfe der Wärmeflüsse von den Bädern, dem Energiefluss in den Oszillator, der kohärenten Anregung des Oszillators gemessen durch die Amplitude des Ortserwartungswerts, dem $S$-$T$-Diagramm des mittleren Spins und schließlich der LEMBAS-Wärme und -Arbeit über einen Zyklus.

Für den ersten betrachteten Satz an Parametern implementiert die AD3SM eine Wärmekraftmaschine, wie die D3SM für dieselben Parameter, und wie für eine Wärmekraftmaschine erwartet fließt während eines Zyklus' Wärme vom heißen Bad in das System und Wärme vom System in das kalte Bad. Der Energieüberschuss wird dabei an das Arbeitsreservoir abgegeben, hier also an den Oszillator. Dass diese Energie nicht ausschließlich Wärme ist, wird durch die über die Zyklen nahezu exakt linear zunehmende Amplitude des Ortserwartungswerts des Oszillators bestätigt. Da der zentrale Spin zu jedem Zeitpunkt der Dynamik in einem diagonalen und somit kanonischen Zustand ist, lassen sich seine thermodynamische Entropy $S$ und seine Temperatur $T$ zu

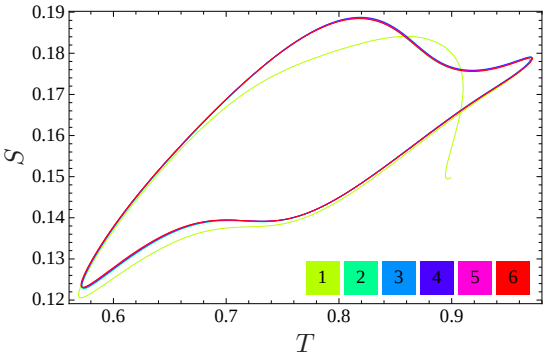


**Abbildung D.2:** $S$-$T$-Diagramm des zentralen Spins der AD3SM für die ersten sechs Zyklen im Wärmekraftmaschinenfall.

jedem Zeitpunkt angeben, wobei die Temperatur bezüglich der effektiven Aufspaltung des Spins berechnet wird. Auch der Umlaufsinn des $S$-$T$-Diagramms (Fig. D.2) kennzeichnet den Prozess als Wärmekraftmaschine. Aus dem Vergleich der nach LEMBAS berechneten, vom Oszillator über einen Zyklus aufgenommenen Arbeit $\Delta W$ mit der Arbeit $\Delta W^{\mathrm{td}}$, die sich durch die Integration der vom Zyklus im $S$-$T$-Diagramm eingeschlossenen Fläche ergibt, ist ersichtlich, dass die beiden Arbeiten im Rahmen der Genauigkeit der numerischen Methode übereinstimmen.

Ganz analog ergibt sich, dass im zweiten betrachteten Fall die AD3SM eine Wärmepumpe implementiert, erneut in Übereinstimmung mit der Erwartung durch Vergleich mit der D3SM. Ebenso stimmt die mit LEMBAS ermittelte und die aus dem $S$-$T$-Diagramm abgeleitete Arbeit im Rahmen der Genauigkeit der Methode überein.

Die Ergebnisse belegen, dass der quantenmechanische Oszillator in der AD3SM in der Tat wie ein klassischer Treiber und damit als Arbeitsreservoir agieren kann, und dass die Vorhersagen über die Dynamik auf Grund der effektiven lokalen Dynamik (D.6) und über die verrichtete Arbeit und Wärme gemäß LEMBAS zutreffend sind.

## D.3 Quantenthermodynamische Pseudomaschinen

Der letzte Teil der Arbeit ist einer besonderen Form von Quantennetzwerken mit thermodynamischer Funktionalität gewidmet, die wir „quantenthermodynamische Pseudomaschinen“ nennen, weil sie weder einen thermodynamischen

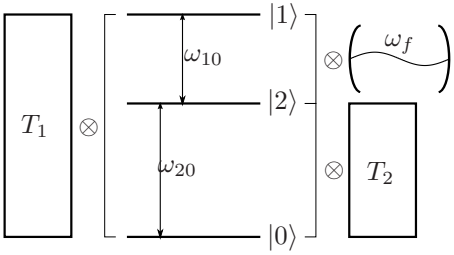


**Abbildung D.3:** Schema des erweiterten dissipativen Jaynes-Cummings-Modells (ED JCM).

Zyklus implementieren noch thermodynamische Maschinen im eigentlichen Sinn darstellen. Ihre Funktionalität ist die Konsequenz einer quantenmechanischen Kontrolle über das System, für die es keinerlei klassische Entsprechung gibt. Konkret äußert sich diese Kontrolle in der selektiven Kopplung von Wärmebädern an bestimmte Übergänge in einem quantenmechanischen System. Insgesamt ist eine Pseudomaschine dadurch ein sehr spezieller Fall eines Transportszenarios. Durch die Korrelation der Wärmeflüsse, die durch die selektive Kopplung erreicht wird, lassen sich mit einem solchen Quantennetzwerk dennoch Funktionen realisieren, die denen thermodynamischer Maschinen gleichen.

Eine zentrale Rolle bei unseren Betrachtungen zu Pseudomaschinen nimmt dabei das *erweiterte dissipative Jaynes-Cummings-Modell (ED JCM)* von Boukobza and Tannor [2006b] ein (Fig. D.3). Es handelt sich dabei um ein Laser-Modell bestehend aus einem Drei-Niveau-Atom, einer einzelnen Mode des elektromagnetischen Felds und zwei Wärmebädern. Wie bereits erwähnt sind die Bäder selektiv an bestimmte Übergänge des Atoms gekoppelt. Die Feldmode ist in Resonanz mit dem verbleibenden Übergang und die Kopplung ist dieselbe wie im JCM üblich. Die Bäder sind durch eine Mastergleichung modelliert und das heiße Bad beschreibt den inkohärenten Pumpprozess beim Laser.

Nach einer kurzen Übergangsdynamik am Anfang weist das ED JCM im wesentlichen zwei Operationsmodi auf, wobei bei beiden auf Grund der Kopplungseigenschaften des Modells die Energieflüsse streng korreliert sind: Entweder fließt Wärme vom heißen Bad ins System und vom System ins kalte Bad, sowie Energie in den Oszillator, oder die Energieflüsse sind genau umgekehrt. Im ersten Fall handelt es sich um ein Laser-Modell, wie durch das lineare Anwachsen der Feldenergie und die Eigenschaften des Feldzustands belegt wird. Im zweiten Fall relaxiert das Feld zu einem thermischen Zustand mit einer Temperatur $T^{\text{eff}}$.

Die Autoren interpretieren auch die Thermodynamik des Modells in Boukobza and Tannor [2006b] und identifizieren den Laser-Fall als Wärmekraftmaschine und den Relaxationsfall als Wärmepumpe. Beide Prozesse arbeiten dabei mit der Effizienz des jeweilig entsprechenden Otto-Prozesses. Das wohl stärkste Argument für diese Interpretation ergibt sich aus der Kombination zweier ED JCMs, die sich ein Feld teilen und, bei der das eine Modell als Laser und das andere als Relaxationsfall konfiguriert ist. In diesem Fall erhält der Energiefluss des Lasermodels in die Feldmode einen Wärmestrom von kalt nach warm in dem anderen Exemplar des Modells aufrecht, wie wir es für eine solche Kombination von Wärmekraftmaschine und Wärmepumpe erwarten würden.

Es ist jedoch leicht zu zeigen, dass die Annahmen, auf denen die thermodynamische Interpretation der Autoren beruht, in sich widersprüchlich sind. Ein konkretes Problem liegt dabei darin, dass die Autoren bei Energieflüssen zwischen Quantensystemen nicht zwischen kohärentem und inkohärentem Energieübertrag unterscheiden, wie in Sec. D.1.1 bei uns geschehen, und somit allen Energieaustausch zwischen Quantensystemen als Arbeit werten. Tatsächlich ergibt sich bei der Anwendung von LEMBAS auf das ED JCM, dass der Energiefluss von und zum Feld reine Wärme ist, da der effektive Hamiltonoperator für alle Zeiten verschwindet. Dieses Ergebnis scheint jedoch im Widerspruch zu der Tatsache zu stehen, dass mit der Energie aus dem Feld im Relaxationsfall für beliebige Feldanfangszustände ausreichender Energie ein Wärmetransport von kalt nach warm aufrechterhalten werden kann.

Dieser scheinbare Widerspruch lässt sich in zwei Schritten auflösen. Der erste besteht darin zu verifizieren, dass sich der Wärmetransport in der Tat durch Zuführung von Wärme aufrechterhalten lässt, und im zweiten Schritt zeigen wir, dass dieses Ergebnis den zweiten Hauptsatz nicht verletzt. Zur Durchführung des ersten Schritts ersetzen wir das Feld im Modell durch ein weiteres Wärmebad mit einer Temperatur $T_3$, die höher ist als die Temperatur $T^{\text{eff}}$, zu der das Feld üblicherweise relaxieren würde. Es zeigt sich, dass so zugeführte Wärme den Wärmetransport von kalt nach warm tatsächlich ermöglicht. Außerdem ergibt sich, dass für die Temperatur $T_3$ des dritten Bads notwendigerweise $T_3 > T^{\text{eff}} > T_1, T_2$ gilt, als $T_3$ immer über den Temperaturen von Bad 1 und 2 liegen muss. Der zweite Schritt wird durch eine Analyse der Entropieproduktion dieses Drei-Bad-Modells ermöglicht und ergibt, dass für den geforderten Operationsmodus $\dot{S} > 0$ immer erfüllt ist, und der Prozess somit mit der Thermodynamik konsistent ist, was wegen $T_3 > T_1, T_2$ nun nicht mehr völlig überraschend ist.

Wir können daraus schließen, dass es sich bei dem beschriebenden Modell und allgemein bei quantenthermodynamischen Pseudomaschinen nicht um thermodynamische Maschinen im eigentlichen Sinne handelt, sondern um

Wärmeleitungsszenarien mit außergewöhnlichen Eigenschaften auf Grund der frequenzselektiven Badkopplungen. Darüberhinaus ist dieses Resultat ein weiterer Beleg für die Tragfähigkeit der mit der LEMBAS-Methode ermittelten Ergebnisse für die thermodynamische Funktionalität eines Quantennetzwerks. Dennoch bestätigt das LEMBAS-Ergebnis damit ein Kuriosum, nämlich dass durch eine erweiterte nicht-klassische Kontrolle von Wärmeströmen maschinenartige thermodynamische Funktionalität erreicht werden kann.

## D.4 Fazit

Quantennetzwerke, ob offen oder geschlossen, zeigen vielfältige Funktionalitäten. In dieser Arbeit haben wir uns mit der Frage nach der Emergenz thermodynamischer Funktionalität aus der Quantenmechanik, ihrer quantitativen Beschreibung durch verallgemeinerte Definitionen von Arbeit und Wärme sowie nach dem Effekt erweiterter quantenmechanischer Kontrolle auf diese Funktionalität beschäftigt und einige Antworten geben können: Wir haben gezeigt, dass einzelne Quantensysteme wie ein harmonischer Oszillator unter geeigneten Bedingungen eine (z.T. ideale) Arbeitsquelle im thermodynamischen Sinn darstellen können und haben diese Eigenschaft genutzt, um in einem autonomen Quantennetzwerk eine thermodynamische Maschine zu implementieren (AD3SM). Darüberhinaus konnten wir belegen, dass die von uns entwickelte verallgemeinerte Definition von Arbeit und Wärme in ganz unterschiedlichen Modellen konsistente Ergebnisse liefert. Schließlich haben wir den Status quantenthermodynamischer Pseudomaschinen klären können und haben dazu beigetragen, ihre thermodynamischen Eigenschaften zu verstehen.

Natürlich bleiben auch offene Fragen. Die stringente Herleitung der Messbasis für die LEMBAS-Methode für allgemeine Experimente ist bisher nicht geglückt. Weiter stellt sich die Frage, ob die „Effizienz“ der Pseudomaschinen auf die Otto-Effizienz limitiert ist, wie es für alle Modelle aus dieser Gruppe der Fall zu sein scheint – oder ob durch Weiterentwicklung dieses Konzepts, eventuell unter Berücksichtigung weiterer Formen rein quantenmechanischer Kontrolle – noch bessere Ausnutzung von Wärmeflüssen erreicht werden kann. Schließlich bleibt auch die Frage unbeantwortet, warum in unserer makroskopischen Alltagswelt mechanische Kontrolle, also Arbeit, so typisch ist, obwohl sie in den von uns betrachteten Modellen erhebliche Ansprüche an Präparation und Kontrolle eines solchen Systems stellt.

# List of symbols and abbreviations

| | |
|---|---|
| 3LS | three-level system |
| AD3SM | autonomous dynamical three spin machine |
| $\beta$ | inverse absolute temperature $1/T$ |
| d | total differential |
| D3SM | dynamical three spin machine |
| đ | partial differential |
| ED JCM | extended dissipative Jaynes-Cummings model, see 8.3 |
| $\epsilon_n$ | energy eigenvalue |
| $\eta_{\mathrm{Otto}}$ | efficiency of the classical Otto process |
| $\eta^{\mathrm{e}}$ | heat engine efficiency |
| $\eta^{\mathrm{p}}$ | heat pump efficiency |
| $\eta_{\mathrm{Otto}}^{\mathrm{qm}}$ | efficiency of the quantum Otto process |
| FA | factorization approximation (see Sec. 2.1) |
| $\hbar$ | Planck constant |
| $\mathcal{H}$ | Hilbert space |
| $\hat{H}^{\mathrm{eff}}$ | time-dependent effective Hamilton operator (see Sec. 2.1) |
| $\hat{H}$ | Hamilton operator |
| JCM | Jaynes-Cummings model |
| $k_B$ | Boltzmann constant |
| l.h.s. | left-hand side |
| $\mathcal{L}^{\mathrm{eff}}$ | local effective incoherent dynamics |
| LEMBAS | local effective measurement basis (principle), Sec. 2.3 |
| $\mu$ | chemical potential |
| $N$ | particle number |
| $\nu$ | spectral density exponent, cf. Eq. (6.10) |
| $P$ | purity |
| $p$ | pressure |
| $Q$ | heat |
| QME | quantum master equation |
| r.h.s. | right-hand side |
| $\hat{\rho}^{\mathrm{asymp}}$ | asymptotically reached state |
| $\hat{\rho}^{\mathrm{can}}$ | canonical density matrix, see Eq. (1.11) |
| $\hat{\rho}_{\mathrm{PDC}}$ | phase-diffused coherent state (PDC), see Eq. (5.14) |
| $\hat{\rho}^{\infty}$ | stationary density matrix |

| | |
|---|---|
| $S$ | von Neumann entropy |
| SOM | spin-oscillator model, Sec. 3.1 |
| $S^{\mathrm{td}}$ | thermodynamic entropy |
| $T$ | absolute temperature in units of $k_B$ |
| TLS | two-level system |
| $U$ | internal energy |
| $\hat{U}$ | unitary time-evolution operator |
| $V$ | volume |
| $\hat{V}$ | dynamical map |
| $W$ | work |
| $Z$ | partition sum |

# Bibliography


R. Alicki. The quantum open system as a model of the heat engine. *J. Phys. A*, **12**, L103 (1979).

R. Alicki. Pure Decoherence in Quantum Systems. *Open Systems & Information Dynamics*, **11**, 53 (2004).

A. E. Allahverdyan, R. S. Johal, and G. Mahler. Work extremum principle: Structure and function of quantum heat engines. *Physical Review E (Statistical, Nonlinear, and Soft Matter Physics)*, **77**, 041118 (2008).

J.-L. Basdevant and J. Dalibard. *The quantum mechanics solver: how to apply quantum theory to modern physics* (Springer, 2000).

M. Baus and C. F. Tejero. *Equilibrium Statistical Physics. Phases of Matter and Phase Transitions* (Springer Berlin Heidelberg, 2008).

A. Blais, J. Gambetta, A. Wallraff, D. I. Schuster, S. M. Girvin, M. H. Devoret, and R. J. Schoelkopf. Quantum-information processing with circuit quantum electrodynamics. *Phys. Rev. A*, **75**, 032329 (2007).

P. Bocchieri and A. Loinger. Ergodic Foundation of Quantum Statistical Mechanics. *Phys. Rev.*, **114**, 948 (1959).

L. Boltzmann. Weitere Studien über das Wärmegleichgewicht unter Gasmolekülen. *Sitzungsberichte der Akademie der Wissenschaften zu Wien, mathematischnaturwissenschaftliche Klasse*, **66**, 275 (1872).

M. Born and V. Fock. Beweis des Adiabatensatzes. *Z. Phys. A*, **51**, 165 (1928).

P. Borowski, J. Gemmer, and G. Mahler. Relaxation to equilibrium under pure Schrödinger-dynamics. *Eur. Phys. J. B*, **35**, 255 (2003).

E. Boukobza and D. J. Tannor. Thermodynamics of bipartite systems: Application to light-matter interactions. *Phys. Rev. A*, **74**, 063823 (2006a).

E. Boukobza and D. J. Tannor. Three-Level Systems as Amplifiers and Attenuators: A Thermodynamic Analysis. *Phys. Rev. Lett.*, **98**, 240601 (2007).

E. Boukobza and D. J. Tannor. Thermodynamic analysis of quantum light purification. *Phys. Rev. A*, **78**, 013825 (2008).

E. Boukobza and J. D. Tannor. Thermodynamic analysis of quantum light amplification. *Phys. Rev. A*, **74**, 063822 (2006b).

H.-P. Breuer and F. Petruccione. *The Theory of Open Quantum Systems* (Oxford University Press, 2002).

J. M. Deutsch. Quantum statistical mechanics in a closed system. *Phys. Rev. A*, **43**, 2046 (1991).

L. DiCarlo, J. M. Chow, J. M. Gambetta, L. S. Bishop, B. R. Johnson, D. I. Schuster, J. Majer, A. Blais, L. Frunzio, S. M. Girvin, and R. J. Schoelkopf. Demonstration of Two-Qubit Algorithms with a Superconducting Quantum Processor. *Nature*, **460**, 240 (2009).

J. H. Eberly, N. B. Narozhny, and J. J. Sanchez-Mondragon. Periodic Spontaneous Collapse and Revival in a Simple Quantum Model. *Phys. Rev. Lett.*, **44**, 1323 (1980).

P. Ehrenfest. Adiabatische Invarianten und Quantentheorie. *Ann. Physik (Leipzig)*, **51**, 327 (1916).

J. Gea-Banacloche. Collapse and revival of the state vector in the Jaynes-Cummings model: An example of state preparation by a quantum apparatus. *Phys. Rev. Lett.*, **65**, 3385 (1990).

J. Gemmer and G. Mahler. Entanglement and the factorization-approximation. *Eur. Phys. J. D*, **17**, 385 (2001).

J. Gemmer, A. Otte, and G. Mahler. Quantum Approach to a Derivation of the Second Law of Thermodynamics. *Phys. Rev. Lett.*, **86**, 1927 (2001).

J. Gemmer, M. Michel, and G. Mahler. *Quantum Thermodynamics* (Springer, 2004).

J. W. Gibbs. *Elementary Principles of in Statistical Mechanics* (Dover Publications, New York, 1960).

S. Goldstein, J. L. Lebowitz, R. Tumulka, and N. Zanghì. Canonical Typicality. *Physical Review Letters*, **96**, 050403 (2006).

P. Hänggi and G.-L. Ingold. Fundamental aspects of quantum Brownian motion. *Chaos*, **15**, 026105 (2005).

M. Hartmann, G. Mahler, and O. Hess. Existence of temperature on the nanoscale. *Phys. Rev. Lett.*, **93** (2004a).

M. Hartmann, G. Mahler, and O. Hess. Local versus global thermal states: Correlations and the existence of local temperatures. *Phys. Rev. E*, **70** (2004b).

M. Henrich, M. Michel, M. Hartmann, G. Mahler, and J. Gemmer. Global and local relaxation of a spin-chain under exact Schrödinger and master equation dynamics. *Phys. Rev. E*, **72** (2005).

M. J. Henrich, M. Michel, and G. Mahler. Small quantum networks operating as quantum thermodynamic machines. *Europhys. Lett.*, **76**, 1057 (2006).

M. J. Henrich, G. Mahler, and M. Michel. Driven spin systems as quantum thermodynamic machines: Fundamental limits. *Phys. Rev. E*, **75**, 051118 (2007a).

M. J. Henrich, F. Rempp, and G. Mahler. Quantum thermodynamic Otto machines: A spin-system approach. *The European Physical Journal - Special Topics*, **151**, 157 (2007b).

P. Hänggi, G.-L. Ingold, and P. Talkner. Finite quantum dissipation: the challenge of obtaining specific heat. *New Journal of Physics*, **10**, 115008 (2008).

D. Janzing. On the Computational Power of Molecular Heat Engines. *Journal of Statistical Physics*, **122**, 531 (2006).

C. Jarzynski. Equilibrium free-energy differences from nonequilibrium measurements: A master-equation approach. *Phys. Rev. E*, **56**, 5018 (1997).

E. Jaynes and F. Cummings. Comparison of quantum and semiclassical radiation theories with application to the beam maser. *Proc. IEEE*, **51**, 89 (1963).

T. D. Kieu. The Second Law, Maxwell's Demon, and Work Derivable from Quantum Heat Engines. *Phys. Rev. Lett.*, **93**, 140403 (2004).

T. D. Kieu. Quantum heat engines, the second law and Maxwell's daemon. *The European Physical Journal D - Atomic, Molecular, Optical and Plasma Physics*, **39**, 115 (2006).

I. Kim and G. Mahler. Quantum Brownian motion and the second law of thermodynamics. *Eur. Phys. J. B*, **54**, 405 (2006).

R. Kosloff and M. A. Ratner. Beyond linear response: Line shapes for coupled spins or oscillators via direct calculation of dissipated power. *J. Chem. Phys.*, **80**, 2352 (1984).

P. T. Landsberg. Heat engines and heat pumps at positive and negative absolute temperatures. *Journal of Physics A: Mathematical and General*, **10**, 1773 (1977).

J. Larson. Dynamics of the Jaynes–Cummings and Rabi models: old wine in new bottles. *Phys. Scr.*, **76**, 146 (2007).

D. Leibfried, R. Blatt, C. Monroe, and D. Wineland. Quantum dynamics of single trapped ions. *Rev. Mod. Phys.*, **75**, 281 (2003).

N. Linden, S. Popescu, A. J. Short, and A. Winter. Quantum mechanical evolution towards thermal equilibrium. *Physical Review E (Statistical, Nonlinear, and Soft Matter Physics)*, **79**, 061103 (2009a).

N. Linden, S. Popescu, and P. Skrzypczyk. How small can thermal machines be? Towards the smallest possible refrigerator (2009b). `http://arxiv.org/abs/0909.4777`.

G. Mahler and V. A. Weberruß. *Quantum Networks – Dynamics of Open Nanostructures*. 2nd edition (Springer, 1998).

A. Messiah. *Quantenmechanik*, volume 2. 3rd ed. edition (Walter de Gruyter, Berlin, 1990).

K. Mølmer. Optical coherence: A convenient fiction. *Phys. Rev. A*, **55**, 3195 (1996).

J. v. Neumann. Beweis des Ergodensatzes und des H-Theorems in der neuen Mechanik. *Z. Phys. A*, **57**, 30 (1929).

P. Neumann, N. Mizuochi, F. Rempp, P. Hemmer, H. Watanabe, S. Yamasaki, V. Jacques, T. Gaebel, F. Jelezko, and J. Wrachtrup. Multipartite Entanglement Among Single Spins in Diamond. *Science*, **320**, 1326 (2008).

P. Neumann, R. Kolesov, B. Naydenov, J. Beck, F. Rempp, M. Steiner, V. Jacques, G. Balasubramanian, M. L. Markham, D. J. Twitchen, S. Pezzagna, J. Meijer, J. Twamley, F. Jelezko, and J. Wrachtrup. Quantum register based on coupled electron spins in a room-temperature solid. *Nat Phys*, **6**, 249 (2010).

M. A. Nielsen and I. L. Chuang. *Quantum Computation and Quantum Information*. 1st edition (Cambridge University Press, Cambridge, New York, Melbourne, Madrid, 2000).

S. Popescu, A. J. Short, and A. Winter. Entanglement and the foundations of statistical mechanics. *Nat. Phys.*, **2**, 754 (2006).

H. T. Quan. Quantum thermodynamic cycles and quantum heat engines. II. *Phys. Rev. E*, **79**, 041129 (2009).

H. T. Quan, Y.-x. Liu, C. P. Sun, and F. Nori. Quantum thermodynamic cycles and quantum heat engines. *Phys. Rev. E*, **76**, 031105 (2007).

N. F. Ramsey. Thermodynamics and Statistical Mechanics at Negative Absolute Temperatures. *Phys. Rev.*, **103**, 20 (1956).

P. Reimann. Typicality for Generalized Microcanonical Ensembles. *Phys. Rev. Lett.*, **99**, 160404 (2007).

P. Reimann. Foundation of Statistical Mechanics under Experimentally Realistic Conditions. *Phys. Rev. Lett.*, **101**, 190403 (2008).

M. Saffman, T. G. Walker, and K. Mølmer. Quantum information with Rydberg atoms. *Rev. Mod. Phys.*, **82**, 2313 (2010).

K. Saito, S. Takesue, and S. Miyashita. Energy transport in the integrable system in contact with various types of phonon reservoirs. *Phys. Rev. E*, **61**, 2397 (2000).

H. Schmidt and G. Mahler. Control of local relaxation behavior in closed bipartite quantum systems. *Phys. Rev. E*, **72**, 016117 (2005).

H. Schröder and G. Mahler. Work exchange between quantum systems: The spin-oscillator model. *Phys. Rev. E*, **81**, 021118 (2010).

F. Schwabl. *Statistische Mechanik*. Springer-Lehrbuch, dritte, aktualisierte auflage edition (Springer Berlin Heidelberg, 2006).

H. E. D. Scovil and E. O. Schulz-DuBois. Three-Level Masers as Heat Engines. *Phys. Rev. Lett.*, **2**, 262 (1959).

M. O. Scully. Quantum Afterburner: Improving the Efficiency of an Ideal Heat Engine. *Phys. Rev. Lett.*, **88**, 050602 (2002).

M. O. Scully and W. E. Lamb. Quantum Theory of an Optical Maser. I. General Theory. *Phys. Rev.*, **159**, 208 (1967).

M. O. Scully and M. S. Zubairy. *Quantum Optics* (Cambridge University Press, 1997).

J. H. Shirley. Solution of the Schrödinger Equation with a Hamiltonian Periodic in Time. *Phys. Rev.*, **138**, B979 (1965).

B. W. Shore and P. L. Knight. The Jaynes-Cummings model. *J. Mod. Opt.*, **40**, 1195 (1993).

M. Srednicki. Chaos and quantum thermalization. *Phys. Rev. E*, **50**, 888 (1994).

P. Talkner, E. Lutz, and P. Hänggi. Fluctuation theorems: Work is not an observable. *Phys. Rev. E*, **75**, 050102(R) (2007).

H. Tasaki. From Quantum Dynamics to the Canonical Distribution: General Picture and a Rigorous Example. *Phys. Rev. Lett.*, **80**, 1373 (1998).

F. Tonner and G. Mahler. Autonomous quantum thermodynamic machines. *Phys. Rev. E*, **72**, 066118 (2005).

F. Tonner and G. Mahler. Quantum limit of the Carnot engine. *Fortschr. Physik*, **54**, 939 (2006).

W. Vogel and D.-G. Welsch. *Quantum Optics*. 3rd edition (Wiley-VCH Verlag GmbH & Co. KGaA., Weinheim, 2006).

G. Waldherr. *On Quantum Thermodynamics of Coupled Light-Matter Systems.* diploma thesis, Universität Stuttgart, 1. Institut für Theoretische Physik, Pfaffenwaldring 57, 70550 Stuttgart, Germany (2009).

G. Waldherr and G. Mahler. Lasing process in a closed bipartite quantum system: A thermodynamical analysis. *Phys. Rev. E*, **81**, 061122 (2010).

H. Weimer, M. J. Henrich, F. Rempp, H. Schröder, and G. Mahler. Local effective dynamics of quantum systems: A generalized approach to work and heat. *EPL (Europhysics Letters)*, **83**, 30008 (2008).

H. Wichterich, M. J. Henrich, H.-P. Breuer, J. Gemmer, and M. Michel. Modeling heat transport through completely positive maps. *Phys. Rev. E*, **76**, 031115 (2007).

C. R. Willis and R. Picard. Time-dependent projection-operator approach to master equations for coupled systems. *Phys. Rev. A*, **9**, 1343 (1974).

M. Youssef, G. Mahler, and A.-S. F. Obada. Quantum optical thermodynamic machines: Lasing as relaxation. *Phys. Rev. E*, **80**, 061129 (2009).